

**Study on Wireless Ad Hoc Network
Considering Hidden Terminal Problem and
Intra-Flow Interference Cancellation**

Jingze Dai

THE UNIVERSITY OF ELECTRO-COMMUNICATIONS
Department of Communication Engineering and Informatics

*A Thesis Submitted in Partial Fulfillment of the Requirements for the
Degree of Doctor of Philosophy
September 2015*

Study on Wireless Ad Hoc Network
Considering Hidden Terminal Problem and
Intra-Flow Interference Cancellation

SUPERVISORY COMMITTEE:

Professor Yasushi Yamao

Professor Yoshio Karasawa

Professor Takeo Fujii

Associate Professor Toshiharu Kojima

Associate Professor Koji Ishibashi

Copyright ©2015

by

Jingze Dai

All rights reserved

概要

CSMA/CA 自律分散無線ネットワークの性能は隠れ端末問題によって大きく低下する。本研究は 4 つのステップでマルチホップ自律分散ネットワークの性能を向上させる手法を提案・検証する。まずフェージングおよびキャプチャ効果を含んだ実際の通信環境を考慮して、CSMA/CA ユニキャスト通信に対する隠れ端末問題の影響を、2次元空間における送信、受信、干渉ノードの位置に依存する確率現象として分析した。さらにこの問題の分析を CSMA/CA マルチホップ通信に拡張し、その伝送特性を正確に評価できる解析法を提案してフロー内干渉の影響を分析した。分析結果から、CSMA/CA を用いた高信頼・高効率なマルチホップ伝送は、隠れ端末の関係にある 2 つのノードからそれぞれ送信された先行パケットと後続パケットのホップ間干渉のために困難であることを明らかにした。そこで、高負荷かつフェージング環境下においても高信頼・高効率にマルチホップ伝送を行えるフロー内干渉キャンセリング (Intra-Flow Interference Canceling) 伝送法を提案した。本提案では先行パケットの情報を用いて適応信号処理によって干渉信号をキャンセルするので、この方法に適したフレームフォーマットを新たに設計した。最後に、フロー内干渉とフロー間干渉の両者が発生する大規模自律分散ネットワークに対する IFIC 伝送法の拡張およびその効果を検討した。

Summary

Performance of CSMA/CA (carrier sense multiple access/collision avoidance) wireless ad hoc network is severely affected by hidden terminal (HT) problem that results in the failure of carrier sense and causes the packet error due to collision. This thesis proposes a method of improving the performance of multi-hop ad hoc network by 4 steps which can be summarized as follows. First, the thesis analyzes HT effect on CSMA/CA unicast communication taking into account actual radio environments including both fading and capture effect. Based on the analysis results, it is predicted that multi-hop transmission is vulnerable to HT problem because of intra-flow interference (IFI). Regarding to this issue, as the second step, a CINR (carrier to interference and noise ratio) -based analysis method is proposed that can precisely estimate the packet delivery probability for CSMA/CA multi-hop transmission suffering from HT-caused IFI under fading environment. The results prove that conventional CSMA/CA media access control cannot achieve efficient multi-hop transmission. Therefore, as the third step, this thesis further proposes IFI-canceling multi-hop transmission (IFIC-MHT) scheme that enables efficient relaying with the highest traffic load for half-duplex multi-hop networks. The interference cancellation (IC) technique employs adaptive signal processing with a normalized least mean square (NLMS) algorithm for channel estimation and has good BER (bit error rate) and PER (packet error rate) performance under a wide range of SNR (signal to noise ratio) and SIR (signal to interference ratio) conditions. A multi-hop packet transmission frame format dedicated to the IFIC is designed. Finally, this thesis studies the effect of IFIC on large-scale ad hoc network where both intra-flow interference and inter-flow interference take place and together affect the multi-hop transmission.

Acknowledgements

I would like to thank my supervisor Prof. Yasushi Yamao. It is very difficult for me to easily complete this paragraph because many moving moments, snapshots, and stories about me and him in my memory keep recalling to my mind. Seven years ago, he accepted me to join his lab when I was an exchange student. He treated me the same as other students giving me enough time to make presentation in seminar and spending plenty of time for reviewing my report. Three years ago, when I had a big trouble in the entrance application of doctor course, he drew a picture of mountains and valleys and told me that there must be difficulties in one's life and there must be ways to get across. During the seven years since 2008, he always stood by my side encouraging me to confront challenges, supporting me to deal with problems, and guiding me to make choices.

I also would like to express my gratitude to other members of supervisory committee: Professor Yoshio Karasawa, Professor Takeo Fujii, Associate Professor Toshiharu Kojima, and Associate Professor Koji Ishibashi. Thank them for their insightful comments and valuable suggestions.

I would like to thank the members of Yamao and Fujii Labs for being supportive and friendly.

I would like to thank the financial support from Japanese Government Scholarship.

Finally, I want to thank my parents for their love and everything that they did and sacrificed for me.

CONTENTS

List of Figures	1
List of Tables	5
Acronyms	6
Chapter 1 Introduction	9
1.1 Wireless Ad Hoc Network	9
1.2 Hidden Terminal Problem	11
1.3 Intra-Flow Interference Caused by Hidden Terminal	12
1.4 Intra-Flow Interference Cancellation	13
1.5 About the Study	15
1.5.1 Scope and Structure	
1.5.2 Contribution of the Study	
Chapter 2 CSMA/CA Unicast Communication Performance with Two-Dimensional Distribution of Hidden Terminal	18
2.1 Analysis	19
2.1.1 Hidden Terminal Model	
2.1.2 Traffic Model	
2.1.3 Analysis Model for Deriving Probability of Successful Communication	
2.2 Analytical Results	31
2.2.1 HT Effect on Probability of Successful Communication	
2.2.1.1 One-Dimensional Node Layout Case	
2.2.1.2 Two-Dimensional Node Layout Case	
2.2.1.2.1 Collision Probability	
2.2.1.2.2 CINR	
2.2.1.2.3 Data Packet Error Probability	
2.2.1.2.4 Probability of Successful Communication	
2.2.2 Comparison with Fading-Free Case	
2.2.3 Hidden Terminal Effect on Communication Efficiency	
2.3 Conclusion of Chapter 2	41

Chapter 3 CSMA/CA Multi-Hop Transmission Performance	
Considering Intra-Flow Interference Caused by Hidden Terminal	43
3.1 Analysis	44
3.1.1 Multi-Hop Network Model	
3.1.2 Traffic Model	
3.1.3 Analysis Model for Deriving Packet Delivery Ratio	
3.1.3.1 Packet Delivery Ratio with G of 1/2	
3.1.3.2 Packet Delivery Ratio with G of 1/3	
3.2 Analytical Results	51
3.2.1 Arrival Probability and Packet Delivery Ratio	
3.2.2 Delay Probability	
3.2.3 Normalized Throughput	
3.3 Performance Limitation in CSMA/CA Multi-Hop Transmission	58
3.4 Conclusion of Chapter 3	60
Chapter 4 Highly Efficient Multi-Hop Packet Transmission Using	
Intra-Flow Interference Cancellation	61
4.1 Modeling for Multi-Hop Transmission	62
4.1.1 Traffic Model	
4.1.2 Antenna Settings	
4.2 Intra-Flow Interference Canceller	63
4.2.1 Mechanism of Cancellation	
4.2.2 Channel Estimation with LMS or NLMS	
4.3 Detailed Design for Intra-Interference Cancellation (IFIC)	66
4.3.1 Packet Format	
4.3.1.1 Payload Identifier	
4.3.1.2 ACK	
4.3.1.3 Comparison of Packet Format with Analog Network Coding	
4.3.2 Relay Process	
4.3.2.1 Scenario 1: Idea Relay without Packet Loss	

4.3.2.2 Scenario 2: Relay Process with Packet Loss and Retransmission	
4.3.3 Receiving Operation	
4.3.3.1 Demodulation Mode 1	
4.3.3.2 Demodulation Mode 2	
4.3.3.3 Demodulation Mode 3	
4.3.4 Buffering Process	
4.4 Analysis	75
4.4.1 Analysis Model for No-Retransmission Case	
4.4.2 Analysis Model Considering Time-Correlated Retransmission	
4.5 Performance Evaluation Settings	82
4.5.1 Simulation Conditions	
4.5.2 Optimizing the Step Size of Equalizer	
4.6 Performance of IFIC Multi-Hop Transmission (IFIC-MHT)	84
4.6.1 Basic Behavior of IFIC	
4.6.2 Further Performance Improvement by Combining IFIC with MRC	
4.6.3 Basic BER/PER Performance of IFIC and IFIC-MRC	
4.6.4 Performance of 5-Hop IFIC-MHT without Retransmission	
4.6.5 Performance of 5-Hop IFIC-MHT with Retransmission	
4.6.5.1 Relationship between Arrival Probability and Retransmission	
4.6.5.2 Relationship between Throughput, Doppler Frequency and Number of Retransmissions	
4.7 Consideration for Multiple IFIs	98
4.7.1 Zigzag Node Layout	
4.7.2 Branch Topologies	
4.8 Intra-Flow Interference Cancellation in Large-Scale Ad Hoc Network	102
4.8.1 Modeling for Large-Scale Ad Hoc Network	
4.8.1.1 Node Layout and Traffic Generation Model	
4.8.1.2 Topology: Random Pair Model	
4.8.2 Implementation of IFIC-MHT for Large-Scale Ad-Hoc Network	
4.8.3 Simulation and Discussion	
4.9 Conclusion of Chapter 4	110

Chapter 5 Conclusion	112
References	114
Publications	119

List of Figures

- Fig. 1-1 Structure of the thesis and the corresponding scope of each chapter.
- Fig. 2-1 Hidden Terminal analysis model.
- Fig. 2-2 Traffic model used in analysis.
- Fig. 2-3 Flow chart for deriving the probability of successful communication.
- Fig. 2-4 Communication sequence for case 1.1.1.
- Fig. 2-5 Analyzed PSC for one-dimensional nodes layout.
- Fig. 2-6 Simulated PSC for one-dimensional nodes layout.
- Fig. 2-7 Probability of collision between data packets for Cases 1.1.1 and 2.1.1.
- Fig. 2-8 Probability $1-p_1$ that CINR is less than CINR threshold Γ_x .
- Fig. 2-9 Joint probability that data packet collision happens and *CINR* is less than the threshold Γ_x (rotated view) for Cases 1.1.1 and 2.1.1.
- Fig. 2-10 PSC, CSL=-76dBm.
- Fig. 2-11 PSC, CSL=-81dBm.
- Fig. 2-12 PSC without fading, CSL=-81dBm.
- Fig. 2-13 PSC(x, 0), with or without fading, CSL=-81dBm.
- Fig. 2-14 Communication efficiency, CSL=-81dBm.
- Fig. 2-15 Communication efficiency vs. communication interval, CSL=-81dBm.
- Fig. 3-1 Multi-hop traffic flows and Intra-flow Interference.
- Fig. 3-2 Potential contending links with G equals to 1/2.
- Fig. 3-3 Arrival probability and PDR, CSL=-81dBm, $G=1/2$.
- Fig. 3-4 Arrival probability and PDR, CSL=-81dBm & -85dBm, $G=1/2$.
- Fig. 3-5 Percentages of P_N , P_E , P_{DN} and P_{DE} to P_A at each transmitting node, 5-hop.

- Fig. 3-6 Simulated arrival probability and PDR, CSL=-81dBm & -85dBm, $G=1/2$.
- Fig. 3-7 Delay probability, CSL=-81dBm & -85dBm, $G=1/2$.
- Fig. 3-8 Arrival probability and PDR, CSL=-81Bm, $G=1/3$.
- Fig. 3-9 Throughputs of CSMA/CA multi-hop network for different number of hops.
- Fig. 3-10 Throughputs of CSMA/CA multi-hop network.
- Fig. 4-1 Ideal multi-hop traffic flows and intra-flow interference.
- Fig. 4-2 Interference cancellation algorithm.
- Fig. 4-3 Overlapping pattern of two packets and the packet formats for IFIC-MHT scheme.
- Fig. 4-4 Difference of packet format between ANC and IFIC-MHT.
- Fig. 4-5 Relay process of 5-hop IFIC-MHT for scenario 1 (without packet loss).
- Fig. 4-6 Relay process of 5-hop IFIC-MHT for scenario 2.
- Fig. 4-7 Flow-chart of the receiving operation.
- Fig. 4-8 Process of IFIC.
- Fig. 4-9 Example that demonstrates the buffering process in IFIC-MHT.
- Fig. 4-10 Three cases for analyzing the STP of hop $i-1$.
- Fig. 4-11 BER performance of IFIC with different step sizes. ($f_D=3\text{Hz}$)
- Fig. 4-12 Relationship between channel gain, LMS estimation error and packet reception error.
- Fig. 4-13 Two-branch IFIC-MRC receiver.
- Fig. 4-14 Two-branch MRC-IFIC receiver.
- Fig. 4-15 Settings of SNR and INR.
- Fig. 4-16 BER/PER performance of IFIC with single-antenna receivers for single-hop scenario.

Fig. 4-17 BER/PER performances of different combinations of IFIC and MRC with 2-antenna receivers for single-hop.

Fig. 4-18 BER/PER performance of IFIC with single antenna for canceling multiple IFIs.

Fig. 4-19 BER/PER performance of IFIC for QAM signals.

Fig. 4-20 Block diagram of OFDM transmitters and receiver with IFIC.

Fig. 4-21 A group of snapshots that record the constellations and spectrums of desired signal at receiver. (16QAM in OFDM subcarrier)

Fig. 4-22 Arrival probabilities of IFIC-MHT and CSMA/CA for 5-hop network.

Fig. 4-23 Occurrence ratios of three demodulation modes to Arrival probabilities.

Fig. 4-24 Throughput for 5-hop IFIC-MHT and CSMA /CA under different traffic loads G .

Fig. 4-25 Arrival probabilities of 5-hop IFIC-MHT with or without retransmission (SNR=23 dB, SIR=0 dB, $G=1/2$).

Fig. 4-26 Throughput of 5-hop IFIC-MHT with a variety of maximum Doppler frequencies and maximum number of retransmissions (SNR=23 dB, SIR=0 dB, $G=1/2$).

Fig. 4-27 Zigzag multi-hop transmission scenarios.

Fig. 4-28 Arrival probabilities of 5-hop IFIC-MHT with zigzag node layout (single retransmission).

Fig. 4-29 IFIs in Branch Topology.

Fig. 4-30 Ad hoc network with nodes (grey and red dots) follow Poisson Point Process. The transmitting nodes (red dots) obey hard-core process.

Fig. 4-31 Node layout, routes and interferences at Node 2.

Fig. 4-32 Data traffic model ($M=3$).

Fig. 4-33 Transmitting and receiving process for implementing intra-flow IC in ad hoc network.

Fig. 4-34 IFIC-MHT with backoff mechanism.

Fig. 4-35 PDRs vs. traffic load with different *CSLs* and numbers of hops.

List of Tables

- TABLE 2-1 Cases that Communications Succeed
- TABLE 2-2 Major parameters for evaluation
- TABLE 3-1 Configuration and fixed parameters
- TABLE 3-2 Normalized Throughput, $CSL=-81\text{dBm}$
- TABLE 4-1 Radio Transmission Parameters
- TABLE 4-2 Simulation Parameters

Acronyms

ACK	Acknowledgement
ANC	Analog Network Coding
AODV	Ad hoc On-demand Distance Vector)
BER	Bit Error Rate
BPSK	Binary Phase-Shift Keying
CBR	Constant Bit Rate
CCK	Complementary Code Keying
CP	Canceling Phase
CSMA/CA	Carrier Sense Multiple Access/Collision Avoidance
CS	Carrier Sense
CSI	Channel state Information
CSL	Carrier Sense Level
CINR	Carrier to Interference and Noise Ratio
DIFS	Distributed Inter-Frame Space
FCS	Frame Check Sequence
FIFO	First In First Out
HT	Hidden Terminal
IC	Interference Cancellation
IEEE	Institute of Electrical and Electronics Engineers
IFI	Intra-Flow Interference
IFIC	Intra-Flow Interference Cancellation
IFIC-MHT	Intra-Flow Interference Canceling Multi-Hop Transmission
LMS	Least Mean Square

MAC	Media Access Control
MMSE	Minimum Mean-Square Error
MRC	Maximal-Ratio Combining
MSE	Mean-Square Error
MSK	Minimum Shift Keying
NLMS	Normalized Least Mean Square
OFDM	Orthogonal Frequency-Division Multiplexing
PDF	Probability Density Function
PDR	Packet Delivery Ratio
PER	Packet Error Rate
PHY	Physical Layer
PI	Payload Identifier
PLCP	Physical Layer Convergence Protocol
PPP	Poisson Point Process
PSC	Probability of Successful Communication
PSD	Power Spectrum Density
QAM	Quadrature Amplitude Modulation
QPSK	Quadrature Phase-Shift Keying
RTS/CTS	Request-To-Send/Clear-To-Send
STP	Successful Transmission Probability
SIFS	Short Inter-Frame Space
SIR	Signal to Interference Ratio
SNR	Signal to Noise Ratio
TS	Training Sequence
TP	Training Phase

TPC	Transmission Power Control
WLAN	Wireless Local Area Networks
WPAN	Wireless Personal Area Networks
V2V	Vehicle-to-Vehicle
ANC	Analog network Coding

Chapter 1

Introduction

1.1 Wireless Ad Hoc Network

Wireless ad hoc network [1] is a kind of decentralized wireless network where nodes have equal status and are able to communicate with any other nodes via temporally built links or multi-hop routes. Since wireless ad hoc network does not rely on preexisting infrastructure or architecture, it is expected to be useful in rural areas or for temporary recovery in emergency where providing a fully covered wired network is infeasible due to time and expense limitation. For example, a mountain fire alarming system consisting of a large number of sensors deep in the mountain can be inter-connected by wireless ad hoc network and relay sensor information to a distant wired network.

The emergence of machine-to-machine (M2M) communications also accelerates the implementation of ad hoc networks because it allows devices to easily establish communications without the aid of a central infrastructure [2]. In recent years, with the diffusion of smart phones, tablets and wearable devices, real-time multimedia services such as high-definition video streaming, high-quality music streaming become the major applications over wireless networks. Cisco has reported that wireless traffic occupies 61% of global internet traffic in 2014 and the figure will climb to 81% by 2019 [3]. The reports also indicate that the number of M2M connections will triple over next few years. Therefore, video traffic for M2M communications such as connected cars and health monitors will increase, which need to be conveyed through wireless ad hoc network.

The growth of real-time multimedia applications as well as the expansion of M2M communications drives us to review the capability of current wireless multi-hop ad hoc network: Is it capable of support high data rate multi-hop transmission? The frequent change of network topology, node mobility, fading, shadowing, low efficient routing,

unpredictable interferences make the conventional ad hoc network not adequate for high bit rate low delay multi-hop transmission [4] [5]. To find the solution, numeric researches have been done, which includes performance analysis for conventional ad hoc network [6], cross layer design [4][5], and dynamic routing algorithm [7] [8]. Authors in [6] proved that it is necessary to use multi-hop ad hoc transmission to obtain wider coverage and higher throughput for video streaming rather than traditional AP (access point) infrastructure model. Authors in [7] presented a modified AODV (ad hoc on-demand distance vector) routing protocol which exploits the cooperative diversity from neighboring nodes for routing and transmission so that the network is more robust to the node mobility and has more steady throughput performance. Authors in [8] proposed a SINR (signal to interference plus noise ratio) based routing protocol that enables the network dynamically adjust multi-hop routes according to a short-term propagation change caused by fading. Reference [9] discussed the combination between multi-stream coding with multipath transport. The results show that path diversity is an effective way to alleviate the transmission error in ad hoc networks.

At the same time, many researchers focus on the media access control (MAC) of ad hoc network [10]-[12] because there is a basic question: whether the conventional MAC in ad hoc network has fully exploited the available radio resource. CSMA/CA (Carrier Sense Multiple Access/Collision Avoidance) [13] is a well-known MAC protocol for wireless ad hoc network owing to its flexibility. In order to avoid packet collision, nodes in CSMA/CA network sense other carriers before transmission to know whether the other nodes are transmitting in the same channel. If the channel is busy, the node will delay its transmission. CSMA/CA is able to manage the interferences while keeping the flexibility and scalability of wireless ad hoc network. CSMA/CA has been commonly used in distributed multi-user wireless networks such as Wireless Local Area Networks (WLAN) and Wireless Personal Area Networks (WPAN). It is also expected to play important roles in forthcoming applications of ad hoc networks including vehicle-to-vehicle (V2V) communications [14] and ubiquitous sensor networks [15]. The performance of these networks greatly depends on how far CSMA/CA can coordinate traffic from multiple users. However, due to Hidden Terminal (HT) problem [16], interference cannot be perfectly controlled especially when the radio environment

varies due to fading or shadowing. Since HT problem is the main reason that hinders CSMA/CA, it is necessary to carefully study on the characteristic of HT.

1.2 Hidden Terminal Problem

In a CSMA/CA network, HT problem appears when invisible senders (senders that cannot sense each other) transmit packets at the same time. It causes unexpected packet loss and considerably degrades communication quality [17]. In order to analyze HT problem and improve the network performance, many studies have been done [18]-[25].

Since the generation of HT depends on the instantaneous path loss between a sender and an interferer as well as the carrier-sense sensitivity, location of the HT and radio propagation characteristic have strong influence on the problem. The location and radio propagation characteristic also affect the degree of interference caused by the HT at a receiver. In actual radio environments, fading due to multipath propagation is commonly observed. With the presence of fading, the instantaneous propagation loss between any two nodes fluctuates with time. Therefore, carrier sense may fail occasionally and the appearance of HT depends not only on location but also on time.

Nevertheless, most of the past studies on HT problem did not include fading in their modeling [18]-[23]. This changed the HT analysis into a simpler geographical modeling with only three categories of regions such as carrier sense region, transmission region and interfering region. In this modeling, occurrence of HT is determined by the mutual location, regardless of time. Then an HT can be further classified by its impact [20][22]. However, this modeling does not correctly represent actual radio environments.

Reference [24] studied the probability of HT occurrence under fading environment when the request-to-send/clear-to-send (RTS/CTS) method is employed for the IEEE 802.11 WLANs [26]. In the paper, all nodes are randomly distributed in a circle cell and only the averaged probability of HT appearance is calculated. Thus, it did not discuss the impact of location of HT, which is indispensable in the analysis of HT problem. Reference [25] focused on the impact of fading on packet reception success probability on ALOHA and CSMA. However, it does not consider backoff process that is essential for CSMA/CA.

In order to evaluate packet loss under the existence of HT, it is necessary to analyze both the HT appearance probability and the received CINR at a receiver. With capture effect, packet collision due to HT does not always generate packet loss [21]-[25]. However, not only interference from HT but thermal noise always affects packet reception in the actual radio communication. Therefore, packet loss analysis should take into account fading and capture effect as well as thermal noise, which results in CINR-based probability analysis.

In addition, HT effect on ACK (acknowledgement) packets should be taken into account for evaluating the impact of HT problem on CSMA/CA unicast communication. Since an ACK packet follows a data packet after a Short Inter-Frame Space (SIFS), HT problems for data and ACK packets are not independent each other but strongly correlated. However, no works have analyzed how this interaction affects the performance of CSMA/CA unicast communication.

1.3 Intra-Flow Interference Caused by Hidden Terminal

In order to evaluate the performance of CSMA/CA multi-hop transmission, many studies have been done [27]-[30] by taking into account HT-caused intra-flow interference (IFI, i.e. the interference from the contending links in the same traffic flow). Many of the previous works proposed HT modeling with geographical analysis approach [27]-[29], which shares the same idea with the study of unicast communication, that is, simplifying the analysis without considering fading. In [30], an intriguing approach to model the IFI problem is presented based on the geographical analysis. It analyzed HT effect hop by hop and then evaluated the end-to-end capacity by solving recurrence equation.

Reference [31] evaluated CSMA/CA multi-hop network performance under fading environment. It is based on a CINR probability analysis, in which collision does not always result in packet loss. Not only interference but also thermal noise is taken into account because it severely affects packet reception. However, the paper only studied fading effect on CINR during the signal reception but not on the carrier sense. This is not appropriate because the result of carrier sense, which influences the generation of HT, is significantly affected by fading.

1.4 Intra-Flow Interference Cancellation

The policy of CSMA/CA is to passively avoid collision by deferring prospective transmission when ongoing transmissions are sensed. Based on this policy, the overall time required for a multi-hop transmission will significantly increase when the data traffic becomes high. Moreover, since the HT problem is probabilistic in fading environments, it is difficult for CSMA/CA to protect packets from the collision caused by IFI. Consequently, CSMA/CA is not suitable for efficient multi-hop packet transmission under fading environments. Until now, there have been many studies [18]-[23] that aim to improve CSMA/CA network performance by globally optimizing transmission power, carrier sense level or receiving threshold based on stochastic geometry theory [32]. These methods and analyses employ complex algorithms that are difficult to implement in actual distributed networks. Nevertheless, these methods bring limited performance improvement because they essentially change assignment of radio resources to high SINR links.

If intra-flow interference could be effectively suppressed, simultaneous packet transmission in a multi-hop flow will be possible, yielding highly efficient multi-hop media access. In order to realize this idea, interference cancellation (IC) technology is a promising candidate [33]-[38]. Until now, various IC methods have been studied. Depending on whether the bit information contained in the interfering signal is needed to perform IC, they are categorized into two types: unknown IC [33][34] and known IC [35]-[38]. Here, the question becomes which type is the best choice for multi-hop packet transmission. In many applications realized by multi-hop ad hoc networks, a routing protocol like AODV creates a route before data transmission, so that a series of data packets will be forwarded over the same flow. Hence, the bit information of interfering signal has been received or sent before the node suffers from IFI. This advantage makes known IC easy to implement. However, unknown IC approaches can only function at the sacrifice of diversity gain [33] or under critical SIR (signal to interference ratio) [34] due to the lack of bit information about the interference.

Known IC methods are further categorized into blind known IC [35] and visible known IC [36]-[38], depending on the availability of channel state information (CSI). Blind known IC [35] removes the interference by employing a complex algorithm like

belief propagation [39]. This increases the transmission latency and imposes high computation costs. By contrast, visible known ICs are easier to implement because channel information can be obtained from the received training sequence (TS) before performing IC.

Analog network coding (ANC) in [36] attaches training sequences to both the beginning and end of the packets so that the channel information can be separately obtained if two colliding packets partially overlap. Since the decoding algorithm proposed in [36] is only optimized for minimum shift keying (MSK), applicability to other modulation schemes with amplitude variations and the performance with them has not been presented. Therefore, a more general IC method is needed to cover various applications. ZigZag decoding [37] interactively extracts unknown bits from two interfered signals (different overlapping patterns of two packets). However, it can only be applied when two identical packets collide twice. This is the crucial precondition that makes ZigZag decoding unable to resolve the IFI issue since the downstream interferer does not necessarily transmit the same packet after it causes IFI to an upstream node. Reference [38] proposed an overhearing scheme that captures the signal in the air so that the interfering signal can be subtracted when it appears again. This scheme expands the applicability of existing known IC techniques. Nevertheless, its performance improvement is still limited for two reasons: the overhearing scheme does not help canceling the short-term interference under fading; it essentially causes latency that eventually reduces the achievable throughput of the system.

Although many basic analyses on ICs have been published, previous works did not address the detailed design of ICs in multi-hop network systems. For achieving higher throughput in multi-hop networks, the IFI should be analyzed in more detail, and the performance improvement with IFIC should be examined in practical environments where fading among links is independent. In order to make IC work efficiently, new MAC frame formats and transmission schemes are needed that consider the complex interactions possible among packet flows.

1.5 About the Study

1.5.1 Scope and Structure

After reviewing the pioneering works, it is found that several fundamental questions need more studies.

1) How does HT affect the performance of CSMA/CA networks under fading environment? If fading has little correlation with the impact of HT, optimizing CSL and receiving threshold would be a good solution to improve multi-hop transmission capability for CSMA/CA ad hoc network.

2) How does intra-flow interference affect the high data rate multi-hop transmission in fading environment? This question can also be interpreted as: Is it valuable to make efforts to avoid the effect of intra-flow interferences?

3) If intra-flow interference is the primary reason that reduces the multi-hop relaying capability, is there any method that can better control interferences and improve the performance of wireless ad hoc network?

This thesis gives the answers to the three questions by three steps (chapters) which can be illustrated as in Fig.1-1. This figure shows the scope of each chapter. In Chapter 2, the thesis analyzes HT effect on CSMA/CA unicast communication taking into account actual radio environments including both fading and capture effect. In Chapter 3, a CINR-based (carrier to interference and noise ratio) analysis method is proposed that can well predict the packet delivery probability for CSMA/CA multi-hop network under fading environment considering HT-caused intra-flow interference (IFI). IFI is the interfering signal that belongs to the same multi-hop data flow with the desired signal. The results prove that conventional CSMA/CA media access control cannot support highly efficient multi-hop transmission. Therefore, in Chapter 4, this thesis further proposes IFI-canceling multi-hop transmission (IFIC-MHT) scheme that enables efficient relaying with the highest traffic load for half-duplex multi-hop network. Finally, this thesis studies the effect of intra-flow interference cancellation (IFIC) on large-scale ad hoc network where both intra-flow interference and inter-flow interference take place and together affect the multi-hop transmission.

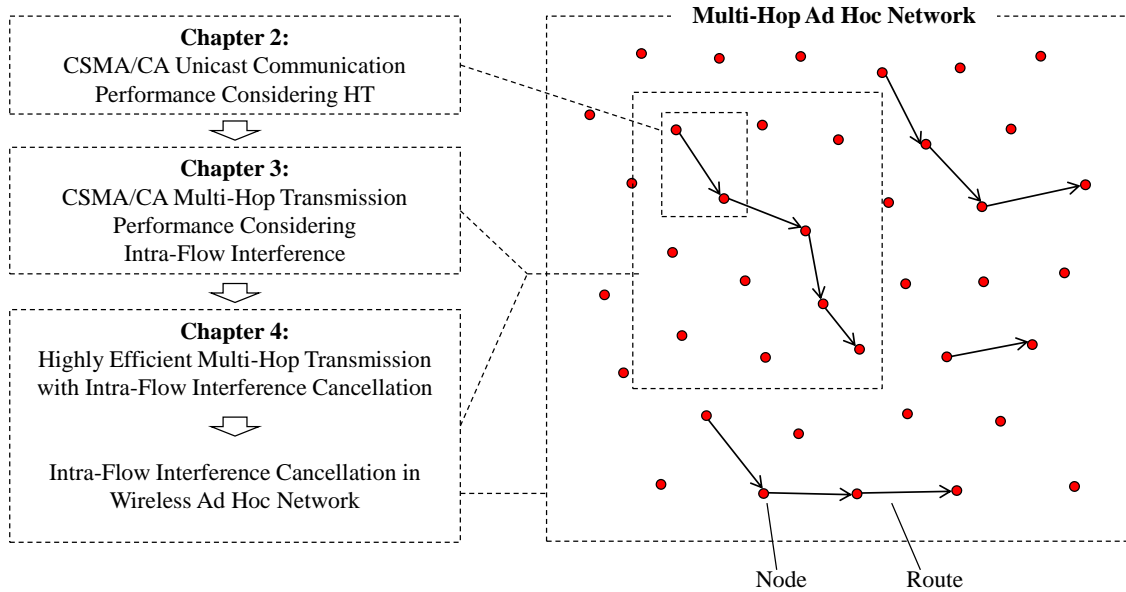


Fig. 1-1 Structure of the thesis and the corresponding scope of each chapter.

1.5.2 Contribution of the Study

The contribution of this thesis can be summarized as follows. Each of them will be explained in detail in Chapter 2 to Chapter 4, respectively.

- Propose an exact analysis method of HT problem under fading environment and reveal the performance of CSMA/CA unicast communication suffering from HT. The analysis method is also validated by comparing the theoretical results with the ones obtained by simulation.
- Propose and validate a precise analysis method to evaluate the performance of CSMA/CA multi-hop network under fading environment considering intra-flow interference. The results imply that in multi-hop communication, end-to-end performance of CSMA/CA is severely affected by IFI if traffic load is high. Improving carrier sensitivity can suppress the occurrence of HT but also increases the transmission latency. Hence high traffic load cannot be supported by CSMA/CA multi-hop network.
- Propose a highly efficient multi-hop transmission (MHT) scheme using intra-flow interference cancellation. Results from theoretical analysis as well as simulation prove that the proposed IFIC-MHT scheme is able to improve the end-to-end throughput even in high traffic load.

- Study the effect of intra-flow interference cancellation on large-scale ad hoc network. Modification of IFIC-MHT is made to adapt itself to large-scale ad hoc networks. The results indicated that IFIC effectively improves the reliability of multi-hop transmission in the scenario where IFI dominates.

Chapter 2

CSMA/CA Unicast Communication Performance with Two-Dimensional Distribution of Hidden Terminal

Until now, there have been numerical studies on CSMA/CA performance. Most of the works assume a fading-free environment and then divide the nodes into two groups: HTs and non-HTs. With the help of capture effect, interferences caused by HTs are harmless as long as the SINR is higher than the reception threshold. Therefore, optimizing the carrier sense level and reception threshold will be the reasonable approaches to improve the CSMA/CA performance. Some extended studies that proposed transmission power management or spectrum alignment are also based on the assumption. However, the fundamental question is, does HT affect CSMA/CA mechanism in the same way in fading and fading-free environment? The purpose of this chapter is to provide more exact analysis method of HT problem under fading environment with capture effect and to reveal the performance of CSMA/CA unicast communication suffering from HT. RTS/CTS mechanism is excluded in our study in order to make HT's effect distinct and keep generality. Retransmission is not applied for simplification.

The analysis model employed in this chapter is simple and basic. It has three nodes, a sender, a receiver and an interferer. They are located in two-dimensional plane. This makes it easy to understand the influence of HT location on the probability of successful communication.

The rest of chapter is organized as follows. Section 2.1 presents the analysis method including HT model and traffic model. Section 2.2 gives some results of analysis and discusses the effect of HT on the probability of successful communication and communication efficiency.

2.1 Analysis

In this section, an HT model is introduced to analyze the effect of HT on the probability of successful communication and communication efficiency for unicast data communication. It is assumed that the communication links follow physical and MAC layer specifications defined by the IEEE 802.11 standard.

2.1.1 Hidden Terminal Model

A basic three-node HT model is employed to obtain general understanding of the HT problem in fading environment. In Fig. 2-1, Node 1 (the focused sender, which is hereafter called "sender") and Node 3 (the interferer) will generate unicast data packets with a fixed size at the same frequency but having independent schedules. They immediately try to send them to Node 2 (the receiver) with CSMA/CA. If a data packet is received successfully by Node 2, the Node replies an ACK packet. The positions of nodes can be assigned arbitrarily in two-dimensional space as illustrated in Fig. 2-1. By changing the position of Node 3, location dependence of the effect of HT can be analyzed.

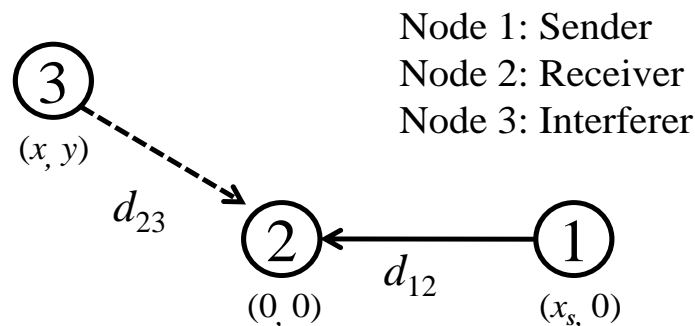


Fig. 2-1. Hidden Terminal analysis model.

2.1.2 Traffic Model

Constant Bit Rate (CBR) traffic is assumed in which each node periodically generates a data packet with a fixed interval of communication, T_{int} . This traffic model is shown in Fig. 2-2. It is supposed that T_{int} is common to the sender and interferer. The

generation timing of the initial packet for each node is random and obeys uniform distribution in T_{int} . As expressed in Eq. 2-1, T_{int} is determined to accept two contending nodes (sender and interferer) to communicate with the receiver based on CSMA/CA mechanism.

$$T_{int} \geq 2(T_p + T_A + SIFS) + DIFS + Back_{max} \quad (2-1)$$

where T_p and T_A are the time required to transmit a data packet and an ACK packet, respectively. $SIFS$ is the time interval between the data packet and its ACK. $DIFS$ (Distributed Inter-Frame Space) is the time interval that a node needs to wait before backoff period during which the medium should be continuously idle. $Back_{max}$ is the maximum backoff time that equals to the initial backoff window time for the network with two contending nodes. With above conditions, a delayed transmission will not overlap with the next transmission from the other node. Retransmission of data packet by the MAC layer is not applied because of simplification.

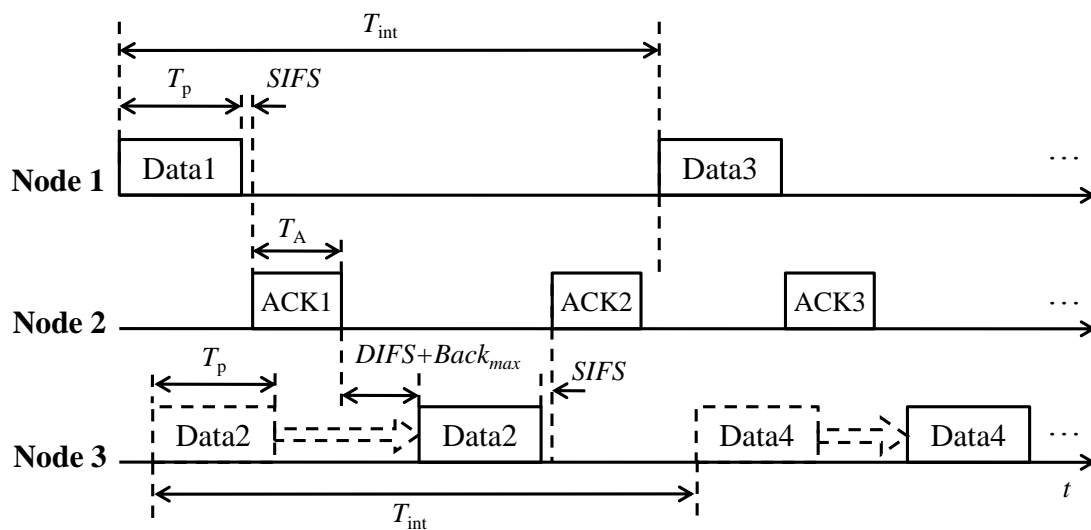


Fig. 2-2. Traffic model used in analysis.

2.1.3 Analysis Model for Deriving Probability of Successful Communication

The successful communication is defined as that Node 1 successfully received the

ACK from Node 2 after Node 1 sent a data packet. The flow chart shown in Fig. 2-3 represents the process to derive Probability of Successful Communication (PSC). The packet schedule overlapping probability, carrier sense failure probability, and packet reception success probability under collision will be calculated for both data and ACK packets.

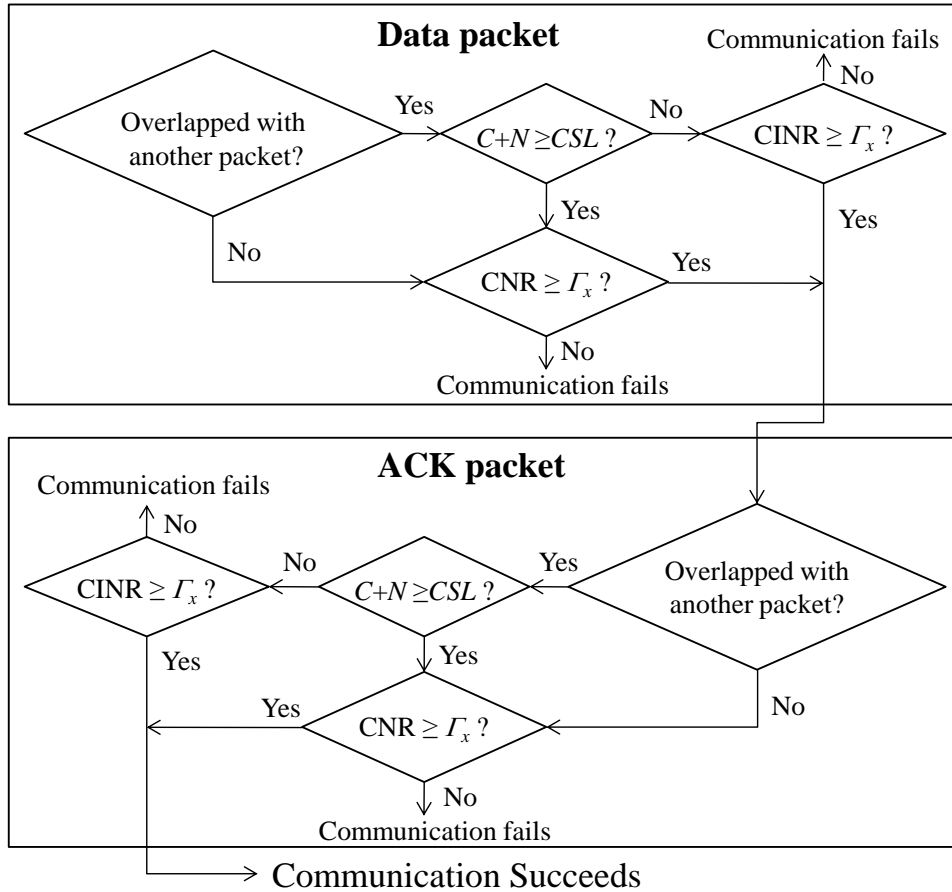


Fig. 2-3. Flow chart for deriving the probability of successful communication.

In the following analysis, the reception success probabilities (p_1, p_2, p_5 and p_7), and carrier sense failure probabilities (p_3, p_4 and p_6), listed below are used.

$$\left. \begin{aligned}
p_1 &= p\left(\frac{C_{12}}{C_{32}+N} \geq \Gamma_x\right) & p_2 &= p\left(\frac{C_{12}}{N} \geq \Gamma_x\right) \\
p_3 &= p(C_{13}+N < CSL) & p_4 &= p(C_{23}+N < CSL) \\
p_5 &= p\left(\frac{C_{21}}{C_{31}+N} \geq \Gamma_x\right) & p_6 &= p(C_{21}+N < CSL) \\
p_7 &= p\left(\frac{C_{32}}{N} \geq \Gamma_x\right)
\end{aligned} \right\} \quad (2-2)$$

where C_{ij} is the instantaneous power of received signal at node j from node i . It is assumed that C_{ij} and C_{ji} have the same distribution. CSL indicates carrier sense level (CSL). N is the power of thermal noise at receiver. Γ_x is the CINR threshold necessary for reception (also the CNR threshold in case of no interference).

It is assumed that Γ_x is common for both data packet and ACK packet for simplicity. This assumption gives good approximation when the transmission data rate is equal for data and ACK packets and data packet length is relatively short. In the actual communication, Γ_x depends on the data packet length and transmission data rate. Transmission power in the analysis is common to all nodes and constant. Transmission Power Control (TPC) is not assumed in this thesis because it requires feedback of receiving quality, thus, another packet should be defined or ACK packet should include channel quality information. However, in most applications using IEEE 802.11 series PHY/MAC, feedback scheme is not specified.

In order to calculate the probabilities p_1, p_2, \dots, p_7 in Eq. 2-2 under fading environment, probability density function (PDF) of the received power is used. In Rayleigh fading, the probability p_2 that received power exceeds $\Gamma_x N$ can be written by

$$\begin{aligned}
p_2 &= 1 - \int_0^{\Gamma_x N} \frac{1}{\sigma^2} \exp\left(-\frac{C}{\sigma^2}\right) dC \\
&= 1 + \exp\left(-\frac{C}{\sigma^2}\right) \Big|_0^{\Gamma_x N} = \exp\left(-\frac{\Gamma_x N}{\sigma^2}\right)
\end{aligned} \quad (2-3)$$

where C denotes the time-variant received power (C_{12}), and σ^2 is the averaged received power which mainly depends on the path loss as a function of the distance between two nodes.

Since an ACK packet follows a data packet, transmissions of data packet and ACK packet correlate each other. Therefore, packet generation time lines for both data and ACK should be carefully classified into possible cases considering the interaction of transmissions from the three nodes. The cases in which communication can succeed are shown in Table 2-1. Probabilities for the cases will be calculated below.

TABLE. 2-1 Cases that Communications Succeed

		Data Packet of Node 1 (D_{N1})			ACK Packet for Node 1 (A_{N1})			
		Overlap with	CS	Collide with	Overlap with	CS	Collide with	
D_{N1} is earlier than D_{N3}	Case 1.1.1	D_{N3}	F(N3)	D_{N3}	D_{N3}	—	D_{N3}	
	Case 1.1.2		S(N3)	—	—	S(N3)	—	
	Case 1.1.3				D_{N3}	F(N3)	D_{N3}	
	Case 1.1.4				—	F(N3)	—	
	Case 1.2.1	—	—	—	D_{N3}	F(N3)	D_{N3}	
	Case 1.2.2					S(N3)	—	
	Case 1.3				—	—	—	
D_{N1} is later than D_{N3}	Case 2.1.1	D_{N3}	F(N1)	D_{N3}	—	—	—	
	Case 2.1.2.1		S(N1)	—	—	—	—	—
	Case 2.1.2.2			S(N1)	—	—	—	—
	Case 2.1.2.3			F(N1)	—	—	—	—
	Case 2.2	A_{N3}	S(N1)	—	—	—	—	
	Case 2.3	—	—	—	—	—	—	
status F(X): Node X fails to carrier sense; status S(X): Node X has successfully carrier sensed								

Case 1 The generation of data packet at Node 1 is earlier than that of Node 3. This probability is 1/2 (since Node 1 and Node 3 have the same possibility to access the channel first). The following cases from 1.1 to 1.3 are subcases of case 1.

Case 1.1 <Schedule overlap case 1> Node 3's data packet transmission schedule overlaps with Node 1's data packet transmission. Define the overlapping probability for

case 1.1 as α that equals to T_p/T_{int} . Note that if the order of the two transmissions is not limited, the overlapping probability for the two data packets is $(2T_p/T_{int})$.

Case 1.1.1 <Packet collision occurs, condition #1> As shown in Fig. 2-4, Node 3 failed to sense Node 1's data packet D_{N1} with probability of p_3 . Then Node 3 will send its packet D_{N3} to Node 2 and collision will happen between them. Moreover, Node 3's packet will collide with Node 2's ACK packet A_{N1} with high probability (because SIFS is very short). Thus reception of the data packet as well as ACK packet is interfered. PSC for this case can be expressed as

$$P_{1.1.1} = \{\alpha p_3\} p_1 p_5 \quad (2-4)$$

where $\{\alpha p_3\}$ is the probability that Case 1.1.1 happens. p_1 is the data reception probability and p_5 is the ACK reception probability, both under collision.

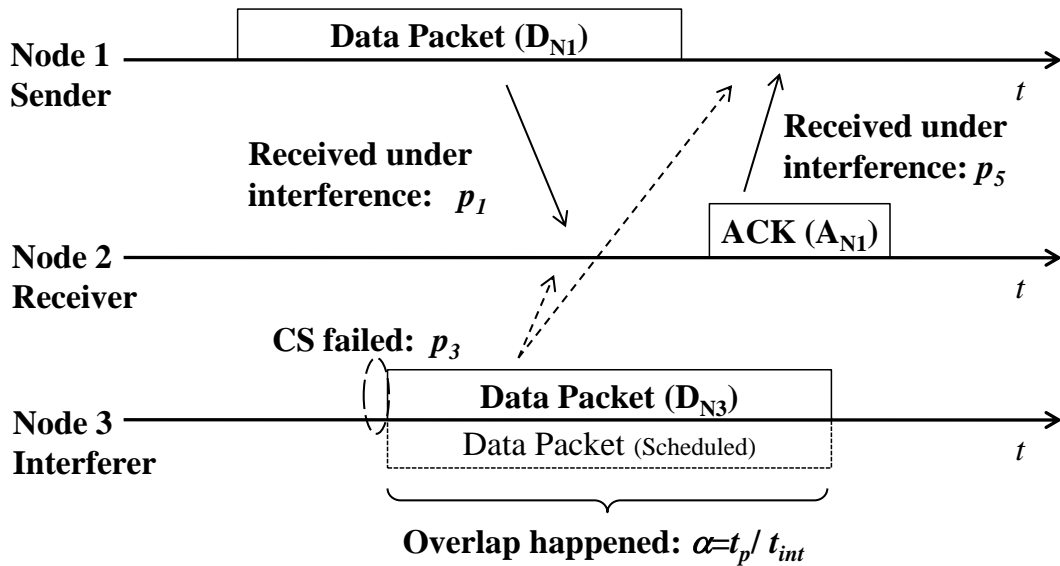


Fig. 2-4. Communication sequence for case 1.1.1.

Case 1.1.2 If Node 3 can sense both D_{N1} and the following ACK A_{N1} from Node 2, the transmission will be completed without interference. The corresponding probability is

$$p_{1.1.2} = \{ \alpha (1 - p_3)(1 - p_4) \} p_2^2 \quad (2-5)$$

where p_2 is the reception probability both for data and ACK packets without interference.

Case 1.1.3 <Packet collision occurs, condition #2> If Node 3 only sensed D_{N1} but failed in sensing A_{N1} , and if the transmission of A_{N1} has not finished by the end of backoff time, the collision will occur at Node 1. The probability that A_{N1} has not finished by the end of backoff time is denoted as γ , which is

$$\gamma = \frac{\lceil (T_A + SIFS - DIFS) / slot \rceil}{W} \quad (2-6)$$

where $slot$ is the unit slot time for backoff and W denotes the initial backoff window size. The output of function $\lceil a \rceil$ is the smallest integer that is no smaller than a . PSC for this case can be expressed as

$$p_{1.1.3} = \{ \alpha (1 - p_3) p_4 \gamma \} p_2 p_5 \quad (2-7)$$

Case 1.1.4 If Node 3 only sensed D_{N1} , and transmission of A_{N1} has finished by the end of backoff time of Node 3 (with probability of $1-\gamma$), Node 2 can transmit A_{N1} without collision even if Node 3 failed to sense A_{N1} . PSC for this case can be expressed as

$$p_{1.1.4} = \{ \alpha (1 - p_3) p_4 (1 - \gamma) \} p_2^2 \quad (2-8)$$

Case 1.2 <Schedule overlap case 2> Node 3's data packet transmission schedule overlaps with Node 2's ACK packet transmission. This overlap probability is denoted as β , which equals to $(T_A + SIFS)/T_{int}$. In this situation, Node 1 can transmit D_{N1} without interference, but the receiving of A_{N1} may be interfered

Case 1.2.1 <Packet collision occurs, condition #3> If Node 3 failed to sense A_{N1} , PSC that Node 1 successfully received A_{N1} with interference is

$$p_{1.2.1} = \{\beta p_4\} p_2 p_5 \quad (2-9)$$

Case 1.2.2 If Node 3 sensed A_{N1} , the communication will be completed without interference. PSC of this case is given by

$$p_{1.2.2} = \{\beta(1 - p_4)\} p_2^2 \quad (2-10)$$

Case 1.3 <No overlap case 1> D_{N3} is generated at Node 3 after the communication of Node 1 has been finished. This situation occurs if Node 3's transmission schedule is later than Node 1 (with probability of 1/2) and does not overlap with D_{N1} (with probability of α) or A_{N1} (with probability of β). Therefore Case 1.3's occurrence probability is $(1/2 - \alpha - \beta)$. In this situation, the transmission will be free from interference. PSC of Case 1.3 can be expressed as

$$p_{1.3} = \left\{ \frac{1}{2} - (\alpha + \beta) \right\} p_2^2 \quad (2-11)$$

The time cost for a successful communication for any case above is

$$T_{1.1.1} = T_{1.1.2} = \dots T_{1.3} = T_p + SIFS + T_A \quad (2-12)$$

Case 2 The generation of data packet at Node 3 is earlier than Node 1. This probability is 1/2. The following cases from 2.1 to 2.3 are subcases of case 2.

Case 2.1 <Schedule overlap case 3> Node 1's data packet transmission schedule overlaps with Node 3's data packet transmission. This overlap probability is also α , same as the case 1.1.

Case 2.1.1 <Packet collision happens, condition #4> Node 1 failed to sense D_{N3} . Then Node 1 will send D_{N1} to Node 2 and HT problem happens. Even in this situation, D_{N1} still has chance to be received by Node 2 if D_{N3} cannot be received properly and discarded by Node 2. PSC of this case can be written as

$$p_{2.1.1} = \{\alpha p_3(1 - p_7)\}p_1p_2 \quad (2-13)$$

The time cost for this case ($T_{2.1.1}$) is $T_p+SIFS+T_A$.

Case 2.1.2 Node 1 sensed D_{N3} .

Case 2.1.2.1 It is possible that D_{N3} can be sensed by Node 1 but cannot be received properly by Node 2. If this situation happens, Node 1 will occupy the idle channel after the data packet transmission by Node 3. PSC of this case can be written as

$$p_{2.1.2.1} = \{\alpha(1 - p_3)(1 - p_7)\}p_2^2 \quad (2-14)$$

The average waiting time for this case is $(T_p/2+DIFS)$. Considering the average time of backoff, the time cost for this case ($T_{2.1.2.1}$) is $T_p/2+DIFS+T_p+SIFS+T_A+Back_{av}$.

If D_{N3} was received correctly and Node 2 sends ACK A_{N3} to Node 3, there will be two cases.

Case 2.1.2.2 If Node 1 sensed A_{N3} , it will wait until the ACK transmission ends and can transmit its packet after that. PSC of this case can be expressed as

$$p_{2.1.2.2} = \{\alpha(1 - p_3)p_7(1 - p_6)\}p_2^2 \quad (2-15)$$

The average waiting time for case 2.1.2.2 is $(T_p/2+SIFS+ T_A+DIFS)$. The time cost for this case ($T_{2.1.2.2}$) is $T_p/2+SIFS+ T_A+DIFS +Back_{av}+T_p+SIFS+T_A$.

Case 2.1.2.3 If Node 1 failed to sense A_{N3} and the transmission of ACK has finished by the end of backoff time with probability of $1-\gamma$, Node 1 can transmit D_{N1} without collision. PSC of this case is

$$p_{2.1.2.3} = \{\alpha(1 - p_3)p_7p_6(1 - \gamma)\}p_2^2 \quad (2-16)$$

The time cost ($T_{2.1.2.3}$) is $T_p/2+SIFS+T_A+DIFS+Back'+T_p+SIFS+T_A$, where

$$Back' = \frac{\{[(T_A + SIFS - DIFS) / slot] + W\} \times slot}{2} \quad (2-17)$$

If Node 1 failed to sense A_{N3} and the transmission of ACK has not finished by the end of backoff time, <Packet collision happens, condition #5>, Node 1 transmits D_{N1} during the ACK transmission. Then Node 2 cannot receive the signal from Node 1.

Case 2.2 <Schedule overlap case 4> Node 1's data packet transmission schedule overlaps with Node 2's ACK packet transmission if Node 3's data packet has been correctly received. The overlap probability is βp_7 . Similar to the case 2.1.2.2, Node 1 has to sense A_{N3} and wait until the ACK transmission ends. PSC of this case is

$$p_{2.2} = \{\beta p_7 (1 - p_6)\} p_2^2 \quad (2-18)$$

Otherwise <Packet collision happens, condition #6>, Node 1 transmits D_{N1} during the ACK transmission. Then the D_{N1} cannot be received by Node 2.

The average waiting time for Case 2.2 is $(SIFS+T_A)/2+DIFS$. The time cost for this case ($T_{2.2}$) is $(SIFS+T_A)/2+DIFS+Back_{av}+T_p+SIFS+T_A$.

Case 2.3 <No overlap case 2> If Node 3's data packet has not been received correctly, Node 2 will not send ACK to Node 3. Then Node 1 will sense the channel idle and begin to transmit D_{N1} to Node 2. The occurrence probability is $\beta(1-p_7)$. Also, similar to Case 1.3, if D_{N1} is generated after Node 3's communication has been finished (no matter whether it has been successful or not) with occurrence probability of $(1/2-\alpha-\beta)$, Node 1 can communicate with Node 2 without interference. All the corresponding PSC above is given by

$$p_{2.3} = \left\{ \beta(1 - p_7) + \left[\frac{1}{2} - (\alpha + \beta) \right] \right\} p_2^2 \quad (2-19)$$

The time cost for this case ($T_{2.3}$) is $T_p+SIFS+T_A$.

Consequently, there are 4 schedule overlap cases (Case 1.1, 1.2, 2.1 and 2.2) and 2 no overlap cases (Case 1.3 and Case 2.3). The sum of overlap probabilities (occurrence probabilities) of Cases 1.1, 1.2 and 1.3 where Node 1 transmits first is 1/2 and the sum of the other cases is also 1/2.

Finally, the time-averaged PSC of communication between sender and receiver, P , can be obtained by summing all the probabilities corresponding to all above events. It is given by

$$P = p_{1.1.1} + p_{1.1.2} + \dots + p_{2.3} \quad (2-20)$$

The probability inside { } from Eq. 2-4 to Eq. 2-19 also represents the transmission probability. As can be seen, transmission probability is space-time function and determined by the interaction between nodes.

Contribution of each case (from 1.1.1 to 2.3) to PSC given by Eq. 2-20 strongly depends on the data-data overlap probability α and data-ACK overlap probability β . When the data packet size is greater than the ACK packet size, α is larger than β . In this case, the collision between data packets has greater impact on the communication between sender and receiver.

As for collision probability, it can be found that there are 6 conditions in total, between data packets, or between data packet and ACK packet. The probabilities of collisions between data packets for conditions #1(Case 1.1.1) and #4 (Case 2.1.1) are the most important and given by

$$P_{C1} = P_{C4} = \alpha p_3 \quad (2-21)$$

In order to make our HT analysis independent from the overhead size of data packet, communication efficiency is used to evaluate HT effect instead of throughput. The communication efficiency S in this chapter is defined as the ratio of average time used to successfully transmit a data packet to the average time used for the communication.

$$S = \frac{P \times T_p}{(p_{1.1.1} T_{1.1.1} + p_{1.1.2} T_{1.1.2} + \dots + p_{2.3} T_{2.3}) + (1 - P)(T_p + SIFS)} \quad (2-22)$$

Here the average time used for a failure transmission is approximated as $T_p + SIFS$. The maximum communication efficiency S_{\max} is defined as

$$S_{\max} = T_p / (T_p + T_A + SIFS) \quad (2-23)$$

The equations from Eq. 2-4 to Eq. 2-20 are in general form and independent from the channel condition (e.g. path loss and fading), node position, traffic amount and many other parameters. All variables in the equations could be adjusted for a specific purpose.

TABLE. 2-2 Major parameters for evaluation

Radio frequency	2.4G Hz
Data rate	2 M bps
Transmission power	15 dBm
Antenna height	1.5 m
Pathloss model	ITU-R p.1411-6, LOS, lower bound
Fading model	Rayleigh
CNR/CINR threshold (I_x)	10 dB
Receiver noise level (N)	-91 dBm
Carrier sense level (CSL)	-76dBm, -81dBm, -86dBm
Data payload size for a packet	512 byte
Packet length (T_p)	2382 μ s
Packet generation interval (T_{int})	6 ms
Retransmission	0 (No retransmission)

2.2 Analytical Results

As an example, the effect of HT problem will be analyzed in a specific scenario by using the equations derived in the previous section. The propagation and traffic conditions are assumed that may happen in actual environments. The major parameters for evaluation are shown in Table 2-2. The physical and MAC layers follow IEEE 802.11b standard. Data payload size is set as 512 byte, which results in the data packet length (T_p) of 2,382 μ s for the transmission data rate of 2 Mbps. It is longer than that of the ACK packet ($T_A=248\mu$ s). T_{int} is set as 6 ms for most of results, which is expressed as

$$T_{int} = 2(T_p + T_A + SIFS + DIFS) + Back_{max} \quad (2-24)$$

The overlap probabilities α and β for the T_{int} of 6 ms are 0.397 and 0.043, respectively. The maximum communication efficiency S_{max} is 0.9. *SIFS* and *DIFS* are 10 μ s and 50 μ s, respectively. Initial backoff window size W is 31 and *slot* is 20 μ s.

Considering ubiquitous applications for short-range outdoor and indoor communications, fading environment with the ITU-R P.1411-6 path loss model [40] is assumed. Fading is flat Rayleigh fading commonly observed in wireless environments. MATLAB is used for the calculation of probabilities p_1, p_2, \dots, p_7 in Equation 2-2 to obtain the theoretically analyzed results.

2.2.1 HT Effect on Probability of Successful Communication

2.2.1.1 One-Dimensional Node Layout Case

For the first, arrange the nodes on a straight line (i.e. $y=0$ in Fig. 2-1), which is the simplest nodes layout. The interferer is located in the opposite side to the sender across the receiver. The distances d_{12} and d_{23} are assigned with independent values from 20 m to 320 m. The CSL value is -81dBm.

Figure 2-5 shows a global view of the PSC with various d_{12} and d_{23} . PSC is

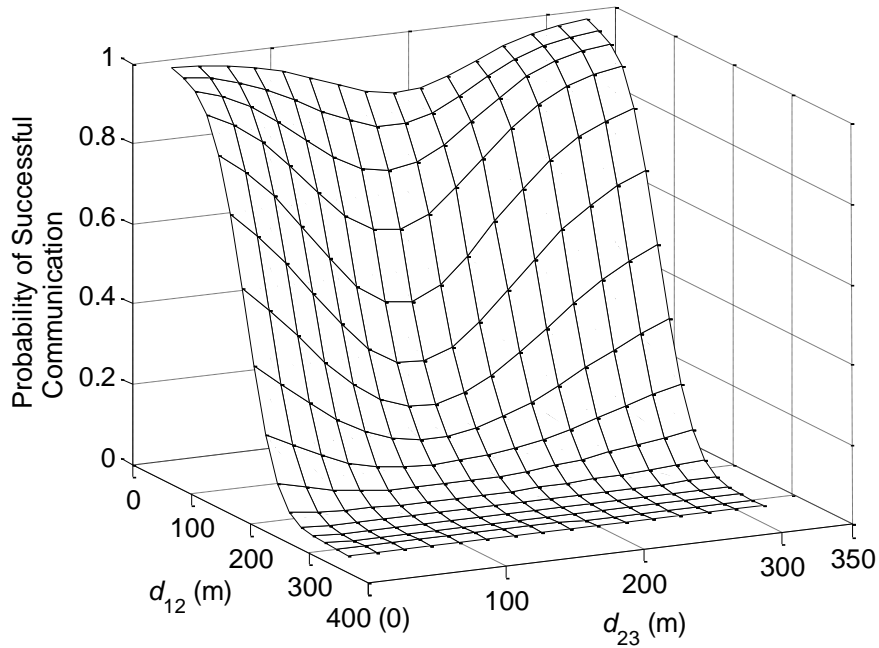


Fig. 2-5. Analyzed PSC for one-dimensional nodes layout.

calculated with Eq. 2-20 in which all cases in Section 2 are included. It is obvious that the probability has a trend of decline when d_{12} increases. It results from the fact that the received power of the signal sent by Node 1 decreases when the distance increases. It can be also found that the probability will temporarily decrease when d_{23} is from 100 to 200 m. It results from HT problem. This phenomenon is further discussed in the next section.

In order to validate the analysis method presented in Section 2, a network simulation by the QualNet software is conducted with the same conditions in Table 2-2. The result is shown in Fig. 2-6. Comparing Fig. 2-5 with Fig. 2-6, it is found that our mathematical analysis well predicted the PSC and described the characteristics of the successful transmission probability suffering from HT. The average difference of the PSCs between analysis and simulation is less than 4%. PSCs with data payload sizes of 100 byte and 250 byte have also been investigated by analysis and simulation. The differences between analysis and simulation are also less than 4%. This difference is mainly due to the difference of bit error rate characteristics employed by analytical model and QualNet simulator.

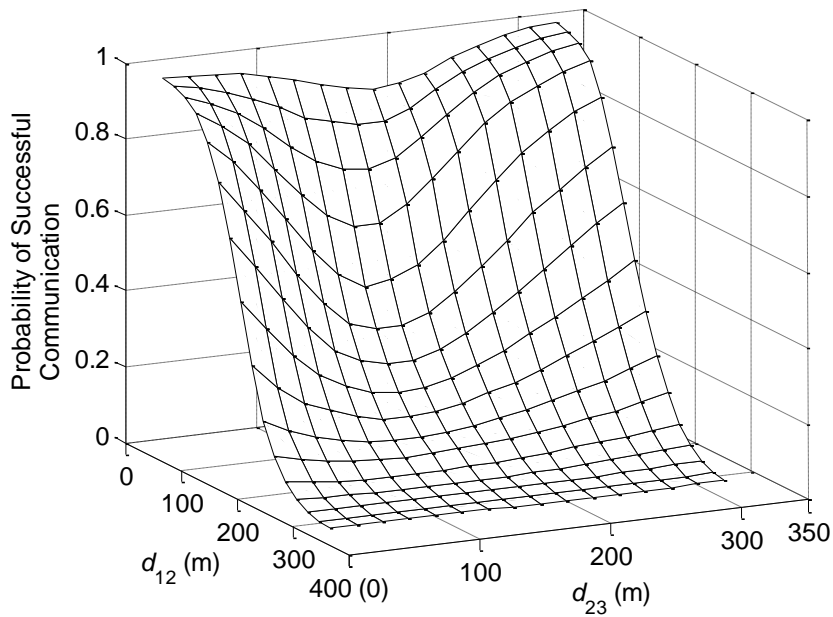


Fig. 2-6. Simulated PSC for one-dimensional nodes layout.

2.2.1.2 Two-Dimensional Node Layout Case

In this section, Section 3.2, and Section 3.3, the coordinates of sender (Node 1) and receiver (Node 2) are fixed at (100,0) and (0,0) in meter, respectively. Thus, the distance between the sender and receiver (d_{12}) is fixed as 100 m while distances to interferer, d_{13} and d_{23} , are variable. With this node arrangement, the variation of PSC is mostly due to HT problem.

2.2.1.2.1 Collision Probability

Fig. 2-7 shows $2ap_3$, the probability of collision between data packets for Cases 1.1.1 and 2.1.1, when CSL is -76 dBm. Cases 1.1.1 and 2.1.1 are the two major collision cases with each transmission probability of ap_3 . Thus, $2ap_3$ is the total collision probability for the two cases. This map is made by placing interferer (Node 3) at every point (x, y) in the plane.

In this map, there is a hollow centering on the sender. When interferer is placed far from the sender, the collision probability increases because possibility of carrier sense failure increases as the distance d_{13} increases. Thus, the probability that HT problem takes place increases.

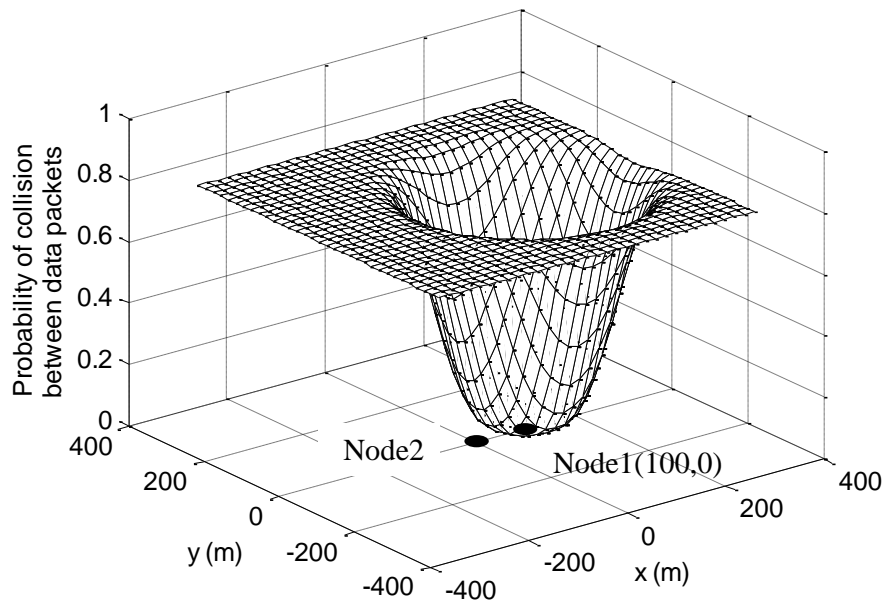


Fig. 2-7. Probability of collision between data packets for Cases 1.1.1 and 2.1.1

2.2.1.2.2 CINR

Fig. 2-8 is the map of the probability $1-p_1$ that CINR at receiver is less than the Γ_x . The probability p_1 is used in calculating PSC for the major collision Cases 1.1.1 and 2.1.1. There is a circular bulge in the Figure. However, its center locates at the receiver, because the CINR at receiver increases when d_{23} increases under a fixed d_{12} . The distance that gives the probability of 50% corresponds to the CINR of around 10 dB.

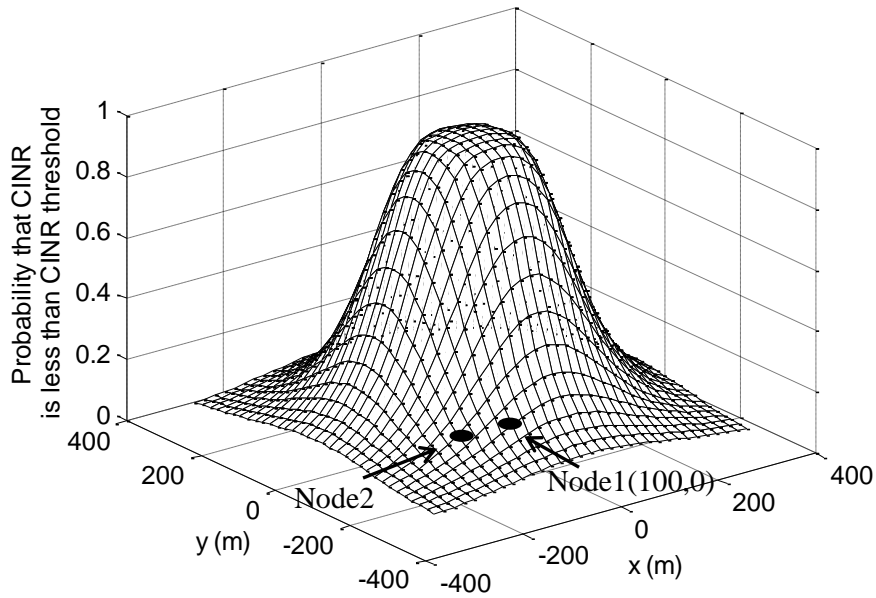


Fig. 2-8. Probability $1-p_1$ that $CINR$ is less than $CINR$ threshold Γ_x .

2.2.1.2.3 Data Packet Error Probability

Fig. 2-9 is the joint probability that data packet collision happens (Fig. 2-7) and $CINR$ is less than Γ_x (Fig. 2-8). It represents data packet error probability for the Case 1.1.1 and 2.1.1. It can be found that HT problem for data packet is severe for the area where the both probabilities are high, such as behind the receiver.

2.2.1.2.4 Probability of Successful Communication

By using Eq. 2-20, PSC that includes all cases in Section 2 can be obtained. Fig. 2-10 shows the map of the PSC for considering all cases when CSL is -76dBm. The reception success probability of ACK packet is also considered. With this map, the effect of HT becomes well visualized. In the figure, the top position of bulge shifts to a

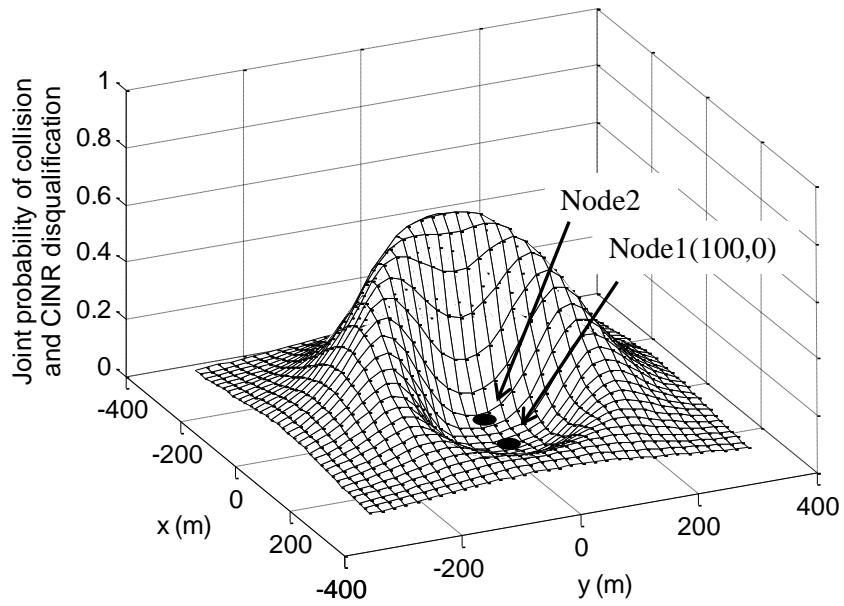


Fig. 2-9. Joint probability that data packet collision happens and $CINR$ is less than the threshold I_x (rotated view) for Cases 1.1.1 and 2.1.1.

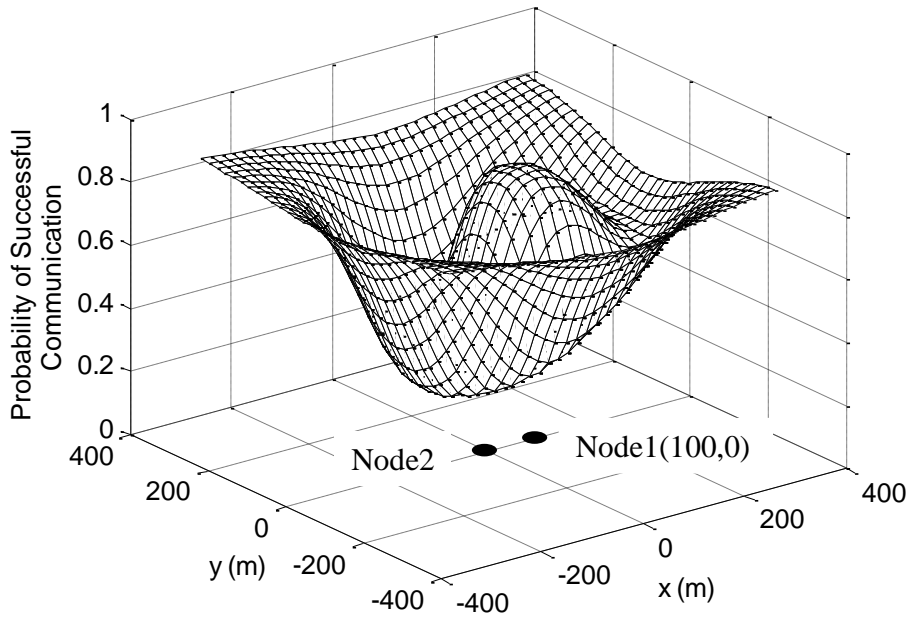


Fig. 2-10. PSC, $CSL=-76dBm$.

place between sender and receiver compared to Fig. 2-8. It locates near (70, 0). PSC at the top of the bulge is about 0.87. If there is no interferer, PSC is equal to p_2^2 . It is 0.91 when the sender is 100 meters away from receiver. Therefore, packet loss due to collision is 0.04, which shows that CSMA/CA achieves high performance even under fading environment if the interferer is close to the sender.

However, when the interferer is away from the sender and receiver, the average received power from them decreases according to the increase of path loss for each path. In the middle distance, it becomes difficult for the interferer to sense the signals from the sender or receiver, although the signals from the interferer still affect CINR at the receiver for the data packet, and at the sender for the ACK packet. Thus, PSC decreases in the middle distance. This situation forms a circular hollow around the receiver and sender.

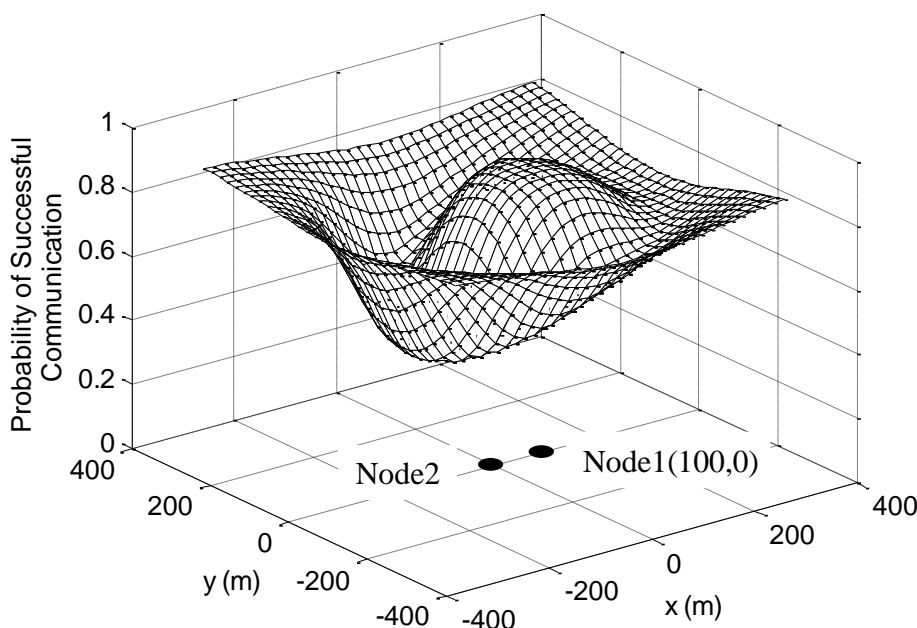


Fig. 2-11. PSC, CSL=-81dBm.

In particular, when the interferer is behind the receiver, HT problem affects the performance most severely. The lowest place of the hollow in Fig. 2-10 at (-120, 0) shows PSC of less than 0.25. Thus, the seriously damaged area forms a crescent behind the receiver.

Since HT problem depends on the carrier sense level, PSC with a CSL of -81dBm,

5 dB more sensitive than the previous example, is shown in Fig. 2-11. By comparing Fig. 2-10 with Fig. 2-11, it can be understood that

- There also exist a bulge and a hollow in Fig. 2-11. PSC corresponding to the top of the bulge in Fig. 2-11 is 0.90, which is closer to the upper bound (0.91). Although the CINR could be the worst in the center bulge area, high success probability of carrier sense prevents collision. Then HT problem seldom happens there. This area is wider in Fig. 2-11 than that in Fig. 2-10.
- Decrease in PSC in the hollow area is smaller than that in Fig. 2-10. It is because collision probability in the hollow area is smaller than that for the CSL of -76dBm. The lowest probability of successful communication is 0.42, which takes place near (-140,0). It is 20 meters far compared to Fig. 2-10.
- The interference free area is considered as the area where the successful communication is possible without carrier sense. It is outside the hollow area and its geographical center is mainly determined by receiver's position. In this area, the probability that CINR is less than I_x is very small (i.e. the average power of interferer's signal is no longer comparable with thermal noise power N). Therefore, communications between sender and receiver will not be disturbed. Since CINR is not a function of CSL, the range of the interference free area does not depend on CSL. It can be found by comparing Fig. 2-10 and Fig. 2-11. The area is approximately more than 320 meters away from the receiver, mostly depends on the propagation loss model.

2.2.2 Comparison with Fading-Free Case

PSC map under no fading environment is also calculated by Eq. 2-20 and shown in Fig. 2-12. CSL is set at -81dBm. When fading is not considered, the probabilities p_1, p_2, \dots, p_7 can only take either 0 or 1.

Remarkable difference can be found comparing Fig. 2-12 with Fig. 2-11. For convenience, PSC($x, 0$) (a slice of PSC at $y=0$) from Fig. 2-12 and Fig. 2-11 are compared in Fig. 2-13.

Analysis without fading gives optimistic result of PSC compared with fading except in the hollow area. The maximum difference (about 45%) between the two results appears when interferer is at (-100,0). The averaged difference is about 19%.

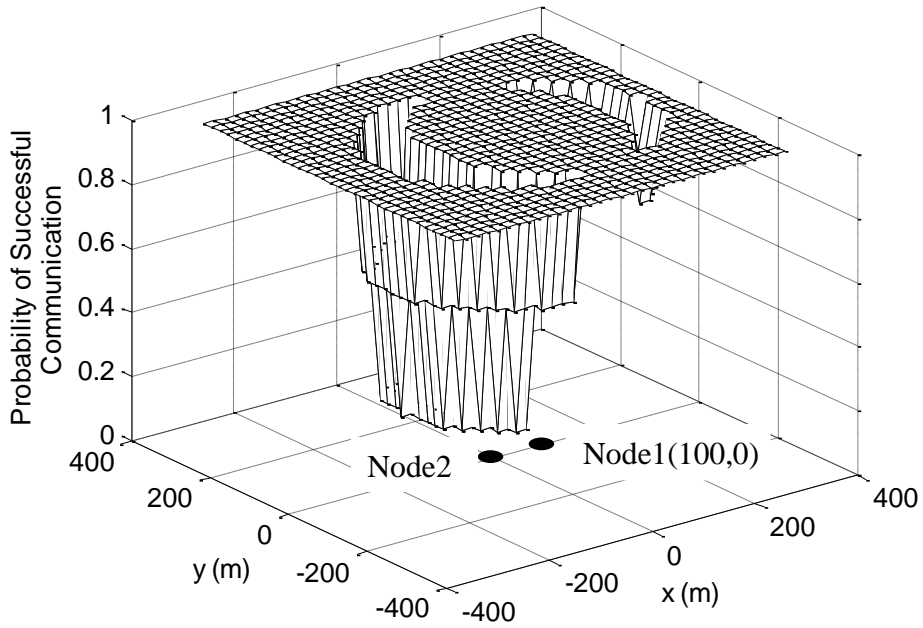


Fig. 2-12. PSC without fading, CSL=-81dBm.

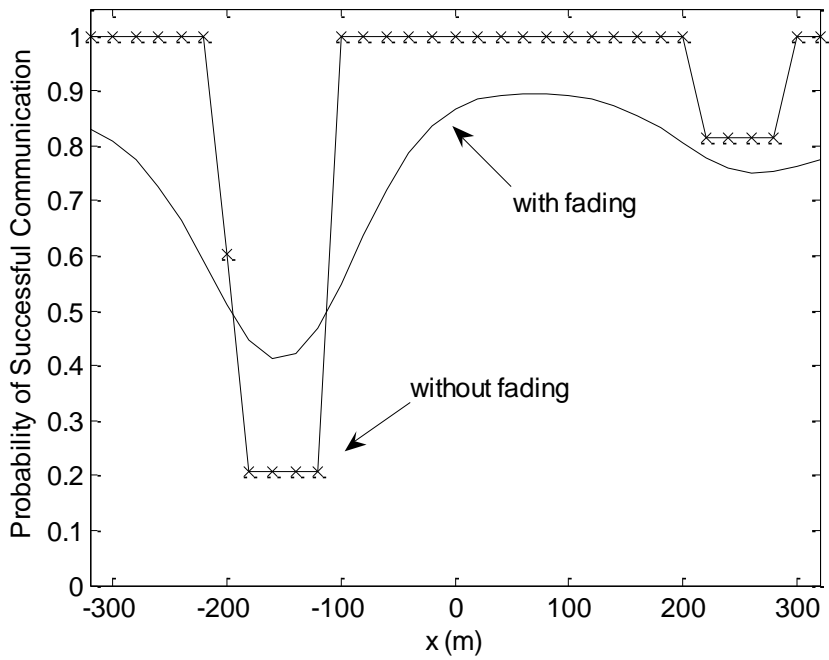


Fig. 2-13. PSC(x, 0), with or without fading, CSL=-81dBm.

2.2.3 Hidden Terminal Effect on Communication Efficiency

By using Eq. 2-22, communication efficiency map corresponding to different position of interferer (Node 3) is obtained. The result is shown in Fig. 2-14 for the CSL of -81dBm. Similar with Fig. 2-11, hollow and bulge can be found in Fig. 2-14. When interferer is in hollow area behind the receiver, sender's communication efficiency seriously suffers from HT problem. It decreases to less than 0.4, while that for the interference free area keeps around 0.7.

When interferer locates in the bulge area that is near sender and receiver, HT problem seldom occurs because of high probability of successful carrier sense. However, when carrier sense succeeds, sender's transmission is delayed. Therefore, communication efficiency decreases. This can be observed in Fig. 2-14 where the communication efficiency for the top of bulge is still lower than that in the interference free area.

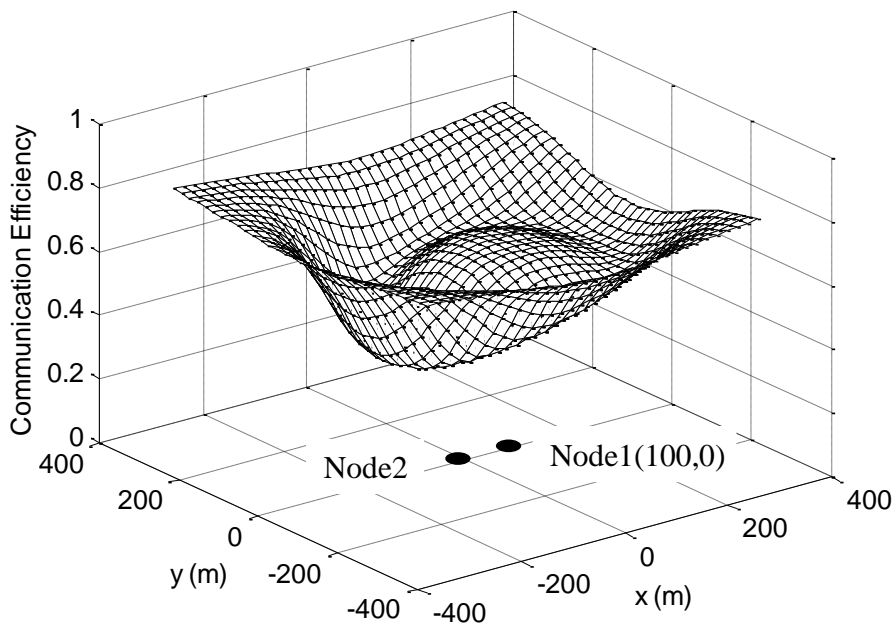


Fig. 2-14. Communication efficiency, CSL=-81dBm.

The effect of interferer's position, communication interval and CSL on sender's communication efficiency can be studied with Fig. 2-15. The horizontal axis is communication interval normalized by $T_{int}/2$.

When communication interval becomes longer, the overlap probabilities (α and β) decrease and the communication efficiency increases. When interferer is in hollow area (-140, 0) where HT problem severely affects the communication efficiency, higher CSL improves the network performance. On the other hand, if the interferer locates in interference free area (340, 0), higher CSL slightly reduces the network performance due to Exposed Terminal problem [41].

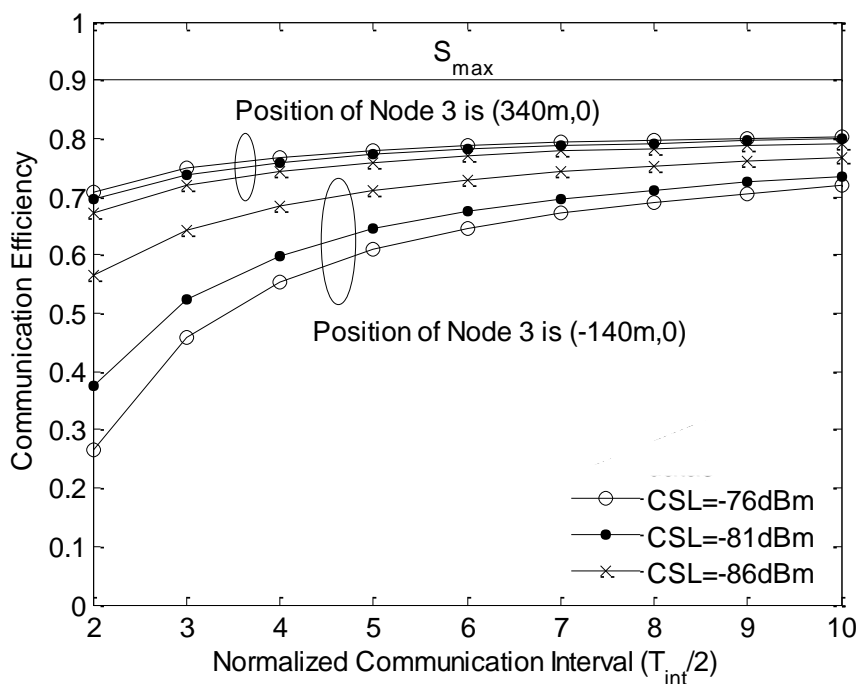


Fig. 2-15. Communication efficiency vs. communication interval, CSL=-81dBm.

2.3 Conclusion of Chapter 2

In this chapter, a mathematical analysis method for HT problem has been proposed that takes both fading and capture effect into account. With this method, performance of CSMA/CA unicast communication suffering from HT is revealed including the interaction of data and ACK packets. Analysis on the probability of successful communication with two-dimensional HT distribution makes it easy to understand the influence of HT location and carrier sense level.

The most important conclusion is that there is considerable difference on the probability between fading and fading-free environments. In fading environment, HT

problem has much wider influential area in which a node becomes a HT of the concerned link and causes fatal collision. In multi-hop ad hoc network scenario, it is highly possible that one or more nodes are within this area.

It is also found that CSMA/CA with lower carrier sense level (higher sensitivity of carrier sense) can

- expand the region where an interferer inside does not severely affect communication of focused nodes, and
- mitigate the worst effect of HT problem, while
- slightly degrade the communication efficiency if interferer is near interference free area.

The obtained results as well as the proposed analysis method are quite useful for the following chapters.

Chapter 3

CSMA/CA Multi-Hop Transmission Performance Considering Intra-Flow Interference Caused by Hidden Terminal

The findings obtained in Chapter 2 indicate that CSMA/CA multi-hop transmission will also suffer from HT problem because in multi-hop transmission scenarios, it is highly possible that transmitting nodes are located at the opposite sides corresponding to the receiver. As shown in Fig. 3-1, the transmitting nodes are in the same data flow and far from each other. The interference signal generated from the down-stream transmitting nodes is called intra-flow interference. Since the multi-hop transmission performance is significantly affected by intra-flow interference, a performance analysis method considering intra-flow interference is necessary. This analysis method will help us find the highest PDR and end-to-end throughput that CSMA/CA is able to achieve in fading environment.

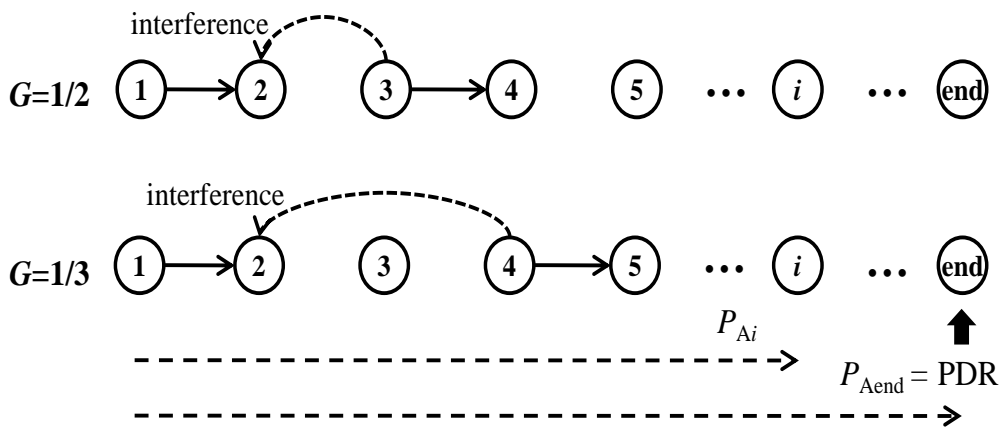


Fig. 3-1. Multi-hop traffic flows and Intra-flow Interference.

In this chapter, a precise analysis method is proposed to evaluate the performance of CSMA/CA multi-hop network under fading environment. In order to analyze the effect of intra-flow interference caused by HT, several important interactions among

contending links are concerned. Collision between ACK and data packets is also taken into account in the analysis of the interactions. After a general expression of per-link successful transmission probability (STP) is derived, the packet delivery ratio and system throughput are provided by solving recurrence equation.

3.1 Analysis

3.1.1 Multi-Hop Network Model

A chain topology network is employed to obtain general understanding of intra-flow interference. The distance between all neighboring nodes is fixed as D meters. It is assumed that each link follows the PHY and MAC layer specification defined by the IEEE 802.11 series standard [15].

Assume a multi-hop communication using single frequency channel, in which a source node constantly generates packets with a fixed communication interval, T_{int} . Since the transceivers in the multi-hop chain are half-duplex, the interval should not be shorter than twice of the packet communication period T_{com} , which is necessary for the transmitter and receiver to complete a unit transmission. In order to quantify the density of given traffic rate, defined a normalized load G , which is :

$$G = T_{com}/T_{int} \quad (G \leq 1/2) \quad . \quad (3-1)$$

Fig.3-1 shows the traffic flows in a one-way relay network when G is 1/2 and 1/3. The word “high traffic” used in this thesis means that G is 1/2 or 1/3.

To evaluate the performance of multi-hop chain network under fading, the probability of successful transmission of each link (link $i-1$ between *Node i-1* and *Node i*) will be analyzed considering HT-caused intra-flow interference. In Chapter 2, it is proved that HT’s occurrence and its effect depend on the mutual position of nodes. Thus, it is necessary to analyze the combinations of the concerned link (solid arrow) and its potential contending links (dashed arrows) as shown in Fig. 3-2. Fig. 3-2 shows the initial status of cases (combinations) when offered load traffic occupies 1/2 of the possible transmission time resource. Assume that node does not transmit data packets

continuously in single chain topology network. Thus there's no potential contending link between *Node i-2* and *Node i-1*. In Chapter 2, it is also proved that HT problem is the severest when senders are at different sides of receiver. Therefore, the network model where nodes are one dimensionally placed is used in order to investigate how HT problem limits the network performance. Then it is reasonable to assume that: 1) state of Link *i-1* is determined by the interaction of nodes from *Node i-3* to *Node i+2*; 2) the signal from a distance $3 \times D$ or farther cannot be sensed.

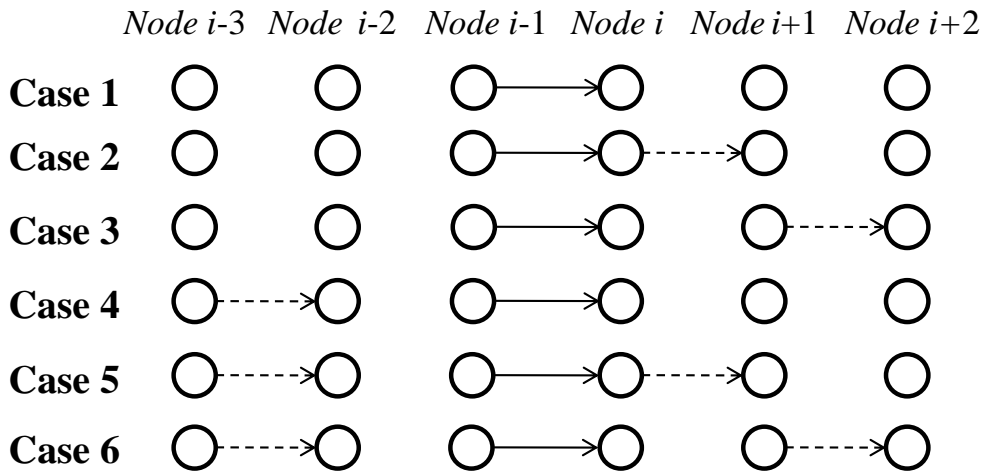


Fig. 3-2. Potential contending links with G equals to $1/2$.

3.1.2 Traffic Model

Assume that the source node generates CBR traffic with a fixed interval of communication, T_{int} . The offered load traffic rate G can be $1/2$ or $1/3$. When G is $1/2$, T_{int} is twice of the averaged communication time T_{ave} , which is necessary for each node to transmit a data packet and receive an ACK packet.

$$T_{ave} = T_p + T_A + SIFS + DIFS + Back_{av} \quad (3-2)$$

where T_p and T_A are the time required to transmit a data packet and an ACK packet, respectively. $Back_{av}$ is the averaged backoff time that is defined as half of the initial backoff window time.

In order to simplify the analysis and to obtain basic view, retransmission of data

packet by the MAC layer is not applied. RTS/CTS mechanism is excluded in order to make HT's effect distinct and for simplicity.

3.1.3 Analysis Model for Deriving Packet Delivery Ratio

3.1.3.1 Packet Delivery Ratio with G of 1/2

In the following analysis, carrier sense failure probabilities (p_1 , p_2 and p_3) and the reception failure probabilities (p_4 , p_5 , p_6 , p_7 and p_8) are used. They are listed below.

$$\begin{array}{ll}
 p_1 = p(C_2 + N < CSL) & p_2 = p(C_1 + N < CSL) \\
 p_3 = p(2C_2 + N < CSL) & p_4 = p\left(\frac{C_1}{N} < \Gamma_{CNR}\right) \\
 p_5 = p\left(\frac{C_1}{C_2 + N} < \Gamma_{CINR}\right) & p_6 = p\left(\frac{C_1}{C_1 + N} < \Gamma_{CINR}\right) \\
 p_7 = p\left(\frac{C_2}{N} < \Gamma_{CNR}\right) & p_8 = p\left(\frac{C_1}{C_3 + N} < \Gamma_{CINR}\right)
 \end{array} \quad \left. \vphantom{\begin{array}{l} p_1 \\ p_3 \\ p_5 \\ p_7 \end{array}} \right\} \quad (3-3)$$

C_a is the instantaneous power of received signal from the node $a \times D$ meters away. For instance, C_2 can either indicate the power of received signal at *Node i-1* transmitted by *Node i+1*, or the power of received signal at *Node i-1* transmitted by *Node i-3*. CSL indicates the global CSL. N is the power of thermal noise at receiver. Γ_{CNR} and Γ_{CINR} are the CNR and CINR thresholds necessary for reception, respectively. The probabilities p_1 , $p_2 \dots p_8$ in Eq. 3-3 can be obtained by using PDF of the received power under fading environment. The packet arrival probability P_{Ai} is illustrated in Fig. 3-1. It is the percentage of the packets that have been correctly delivered from source node to *Node i*. An important performance index is the packet delivery ratio (PDR) P_{Aend} , defined as the arrival probability at the end node.

Based on the above assumptions, the per-link STP for link $i-1$ ($i=2, 3 \dots n+1$) will be analyzed, by categorizing the interactions in the multi-hop chain into the cases shown in Fig. 3-2. *Node i* is hereafter denoted as N_i for abbreviation.

Case 1: Case 1 happens with two conditions: i) N_i directly forwarded the previous packet but N_{i+1} didn't receive this packet with probability of P_{Ei} , or the previous packet has not been received by N_i with probability $1-P_{Ai}$ (where P_{Ai} denotes the arrival

probability that a data packet is received by N_i); ii) N_{i-3} doesn't have packet to send (with probability $1-P_{Ai-3}$). Then the probability that Case 1 happens is $(1-P_{Ai-3})[(1-P_{Ai})+P_{Ei}]$. STP of link $i-1$ for Case 1 is given by

$$p_{C1} = 1 - p_4 \quad (3-4)$$

Case 2: N_i schedules to transmit a data packet during N_{i-1} is transmitting a packet. This happens if N_i delayed its transmission after carrier sensing. The probability that Case 2 occurs is $(1-P_{Ai-3})P_{Di}$, where P_{Di} denotes the probability that a packet was received by N_i but N_i delayed its transmission after the previous carrier sensing. Since N_i should remain silent for a random backoff time after DIFS, N_{i-1} will transmit first with high possibility. Then N_i should receive N_{i-1} 's signal regardless of having the waiting packet for N_{i+1} . Thus N_i keeps its receiving mode and the reception of N_{i-1} 's signal will not be affected by the attempt of transmitting the delayed packet for N_{i+1} . STP for this case is

$$p_{C2} = 1 - p_4 \quad (3-5)$$

Case 3: N_{i-1} and N_{i+1} are going to transmit almost at the same time. This happens if N_i sent a data packet immediately and N_{i+1} received it. The probability is denoted as P_{Ni} . Then Case 3's occurrence probability is $(1-P_{Ai-3})P_{Ni}$. N_{i-1} and N_{i+1} have comparable possibility to transmit first. The following cases from 3.1.1 to 3.2.2 are the subcases of Case 3.

Case 3.1: N_{i+1} transmits first with probability of $(1-f_1)$ where f_1 denotes the probability that the previous node transmits first.

Case 3.1.1: N_{i-1} has sensed N_{i+1} 's signal with probability $1-p_1$, and N_{i+2} has received N_{i+1} 's signal. Since N_{i-1} can hardly sense the signal from N_{i+2} , the possibility that the packet transmitted by N_{i-1} collides at N_i with N_{i+2} 's ACK or data packet is very high. However, N_{i-1} 's packet can be received by N_i if the CINR is larger than threshold. STP for this subcase is

$$p_{C3.1.1} = (1 - f_1)(1 - p_1)(1 - p_4)(1 - p_5) \quad (3-6)$$

Case 3.1.2: N_{i-1} has sensed N_{i+1} 's signal, and N_{i+2} cannot receive the packet from N_{i+1} correctly. N_{i-1} can transmit without interference after backoff. STP for this subcase is

$$p_{C3.1.2} = (1 - f_1)(1 - p_1)p_4(1 - p_4) \quad (3-7)$$

Case 3.1.3: N_{i-1} has not sensed N_{i+1} 's signal, thus, N_{i-1} and N_{i+1} transmit simultaneously. if N_i ' signal strength is strong that can satisfy CINR threshold, N_i can receive it properly. STP for this subcase is

$$p_{C3.1.3} = (1 - f_1)p_1(1 - p_6) \quad (3-8)$$

Case 3.2: N_{i-1} transmits first with probability of f_1 .

Case 3.2.1: N_{i+1} has not sensed N_{i-1} 's signal. Collision will occur at N_i . STP for this subcase is

$$p_{C3.2.1} = f_1 p_1(1 - p_6) \quad (3-9)$$

Case 3.2.2: N_{i+1} has sensed N_{i-1} 's signal. N_{i-1} can transmit without interference. STP for this subcase is

$$p_{C3.2.2} = f_1(1 - p_1)(1 - p_4) \quad (3-10)$$

Case 4: Transmission schedules of N_{i-1} and N_{i-3} overlap. This probability is $P_{Ai-3}[(1 - P_{Ai}) + P_{E1}]$. The following cases are the subcases of Case 4.

Case 4.1: N_{i-1} transmits first with probability $(1 - f_1)$.

Case 4.1.1: N_{i-3} has not sensed N_{i-1} 's signal. N_{i-1} will transmit under interference. STP for this subcase is

$$p_{C4.1.1} = (1 - f_1)p_1(1 - p_8) \quad (3-11)$$

Case 4.1.2: N_{i-3} has sensed N_{i-1} 's signal. N_{i-1} will transmit without suffering interference. STP for this subcase is

$$P_{C4.1.2} = (1 - f_1)(1 - p_1)(1 - p_4) \quad (3-12)$$

Case 4.2: N_{i-3} transmits first with probability of f_1

Case 4.2.1: N_{i-1} has not sensed N_{i-3} 's signal. N_{i-1} will transmit under interference. STP for this subcase is

$$P_{C4.2.1} = f_1 p_1 (1 - p_8) \quad (3-13)$$

Case 4.2.2: N_{i-1} has sensed N_{i-3} 's signal; N_{i-2} has received the packet from N_{i-3} and forwards the packet to N_{i-1} right after sending ACK packet (with DIFS interval). On the other hand, N_{i-1} should keep sensing channel for a random backoff time after DIFS, thus always sensed N_{i-2} 's signal before backoff and delays its transmission. (For simplification, it is assumed that in Case 4.2.2 N_{i-2} can always receive N_{i-3} 's signal, and N_{i-1} can always sense N_{i-2} 's signal.) Hereafter there are three possible situations may occur: 1) N_{i-3} has begun to send another packet with probability P_{Ai-3} and N_{i-1} sensed this packet during backoff, thus Case 4.2.2 occurs again. N_{i-1} will increase its backoff timer; 2) N_{i-3} has begun to send another packet but N_{i-1} failed to sense N_{i-3} , thus Case 4.2.1 occurs; 3) There's no packet in N_{i-3} , thus Case 1 occurs. If situation 1 reaptely occurs and N_{i-1} still cannot transmit even the backoff timer reaches to backoff limit K , the current packet is dropped. The STP for this case is expressed by Eq. 3-14.

$$P_{C4.2.2} = f_1 \times \left(p_1 (1 - p_8) \sum_{k=1}^K (1 - p_1)^k P_{Ai-3}^k + P_{Ai-3} (1 - p_4) \sum_{k=1}^K (1 - p_1)^k P_{Ai-3}^{k-1} \right) \quad (3-14)$$

The averaged STP for all the cases is denoted as p_L . The relationship between P_{Ai} and P_{Ai-1} can be expressed by the following recurrence equation,

$$P_{Ai} = P_{Ai-1} p_L \quad (3-15)$$

where p_L can be calculated by the equation below.

$$\begin{aligned}
P_L &= p_{C1}(1 - P_{Ai-3})[(1 - P_{Ai}) + P_{Ei}] \\
&+ p_{C2}(1 - P_{Ai-3})P_{Di} + p_{C3}(1 - P_{Ai-3})P_{Ni} \\
&+ p_{C4}P_{Ai-3}[(1 - P_{Ai}) + P_{Ei}] + p_{C5}P_{Ai-3}P_{Di} + p_{C6}P_{Ai-3}P_{Ni}
\end{aligned} \tag{3-16}$$

If i equals to $n+1$, the arrival probability is also the n -hop network's PDR. That is,

$$P_{PDR} = P_{An+1} \tag{3-17}$$

The probability P_{Di-1} can be obtained by analyzing the cases where the node has delayed its transmission after CS. P_{Di-1} is given by

$$\begin{aligned}
P_{Di-1} &= \{(1 - P_{Ai-3})P_{Ni}(1 - f_1)(1 - p_1) \\
&+ P_{Ai-3}[(1 - P_{Ai}) + P_{Ei}]f_1(1 - p_1) + P_{Ai-3}P_{Di}f_1(1 - p_1) \\
&+ P_{Ai-3}P_{Ni}[\hat{p}_{D6}]\}P_{Ai-1}.
\end{aligned} \tag{3-18}$$

where \hat{p}_{D6} is delay probability of Case 6.

In cases 3.1.1 and 3.1.2, N_{i-1} can successfully deliver the data packet to N_i after backoff. Therefore, the probability P_{Ni-1} can be derived by eliminating those cases' corresponding STP from P_{Ai} . It is given by

$$\begin{aligned}
P_{Ni-1} &= P_{Ai} - (p_{C3.1.1} + p_{C3.1.2})(1 - P_{i-3})P_{Ni}P_{Ai-1} \\
&- p_{C4.2.2}P_{Ai-3}[(1 - P_{Ai}) + P_{Ei}]P_{Ai-1} \\
&- [\hat{p}_{N5}]P_{Ai-3}P_{Di}P_{Ai-1} - [\hat{p}_{N6}]P_{Ai-3}P_{Ni}P_{Ai-1}.
\end{aligned} \tag{3-19}$$

where \hat{p}_{N5} and \hat{p}_{N6} are the corresponding probabilities in Case 5 and Case 6, respectively.

The relationship between P_{Ei-1} , P_{Ni-1} , P_{Di-1} and P_{Ai-1} is given by

$$P_{Ei-1} = P_{Ai-1} - P_{Di-1} - P_{Ni-1} \tag{3-20}$$

Not all of the cases presented above happen for every hop. For example, for last hop,

only Case 4 and Case 1 happen.

For each hop, four equations, Eq. 3-15, Eq. 3-18, Eq. 3-19 and Eq. 3-29 have been obtained. For n -hop network, there are totally $4n$ variables and $4n$ equations. Then they can be solved by using computing software. The $4n$ variables include:

$$P_2, P_3 \cdots P_{A_{n+1}}; P_{N_1}, P_{N_2} \cdots P_{N_n}; P_{D_1}, P_{D_2} \cdots P_{D_n}; P_{E_1}, P_{E_2} \cdots P_{E_n} .$$

3.1.3.2 Packet Delivery Ratio with G of 1/3

Because the nodes having $3 \times D$ or farther distance cannot sense each other, the nodes will not delay their transmissions when G is 1/3 or lower. The case analysis for G is 1/3 is similar to the last section but much simpler.

3.2 Analytical Results

Since the property of HT problem has been well revealed in Chapter 2, the major radio parameters including CSL range are not changed. The parameters employed for evaluation are listed in Table 3-1. The physical and MAC layers follow IEEE 802.11b standard. Data payload size is set as 512 byte, which results in the data packet length (T_p) of 2,382 μ s for the transmission data rate of 2 Mbps. T_A is 248 μ s. T_{int} is set as 6 ms for G of 1/2, and 9 ms for G of 1/3. It is assumed that all contending nodes have equal probability to transmit first. This results in the factors f_1 equal to 1/2.

Considering ubiquitous applications for short-range outdoor and indoor communications, fading environment with the ITU-R P.1411-6 path loss model [43] is assumed. Fading is flat Rayleigh fading commonly observed in wireless environments. D is set as 100 m, which results $(1-p_4)$ equals to 0.9522, (i.e. the link has high reliability if there is no interference.) while the averaged received signal power at 300 m drops to -87dBm, which is no longer significant and can be ignored.

TABLE 3-1 Configuration and fixed parameters

Radio frequency	2.4G Hz
Data rate	2 Mbps
Transmission power	15 dBm
Antenna height	1.5 m
Path loss model	ITU-R p.1411-6, LOS, lower bound
Fading model	Rayleigh
CNR/CINR threshold ($\Gamma_{\text{CNR}}/\Gamma_{\text{CINR}}$)	10 dB
Receiver noise level (N)	-91 dBm
Carrier sense level (CSL)	-81 dBm, -85 dBm
Data payload size for a packet	512 byte
Packet length (T_p)	2382 μ s
Packet generation interval (T_{int})	6 ms, 9 ms
Backoff limit (K)	6 times
Space between neighboring Nodes (D)	100 m, 120 m

3.2.1 Arrival Probability and Packet Delivery Ratio

Fig. 3-3 shows the arrival probability and PDR when CSL is -81dBm and G is 1/2. PDR is the arrival probability at destination node that is marked with black arrow. When the multi-hop chain has only 2 hops, the arrival probability at Node 2 is 0.952 and PDR is as high as 0.907. However, as the number of hops increases from 2 to 3, the arrival probability at Node 2 remarkably drops to 0.635 and the PDR decreases to 0.527. This means that the first hop becomes the bottleneck and restricts the network's PDR. This phenomenon is caused by intra-flow interference due to HT problem. When the network only has two hops, Node 3 is the destination node that does not transmit data packet. However, when the network has three or more hops, Node 3 is relay node, thus it is possible that Node 1 and Node 3 are both willing to transmit at the same time (Case 3). If CS failed, then collision occurs at Node 2.

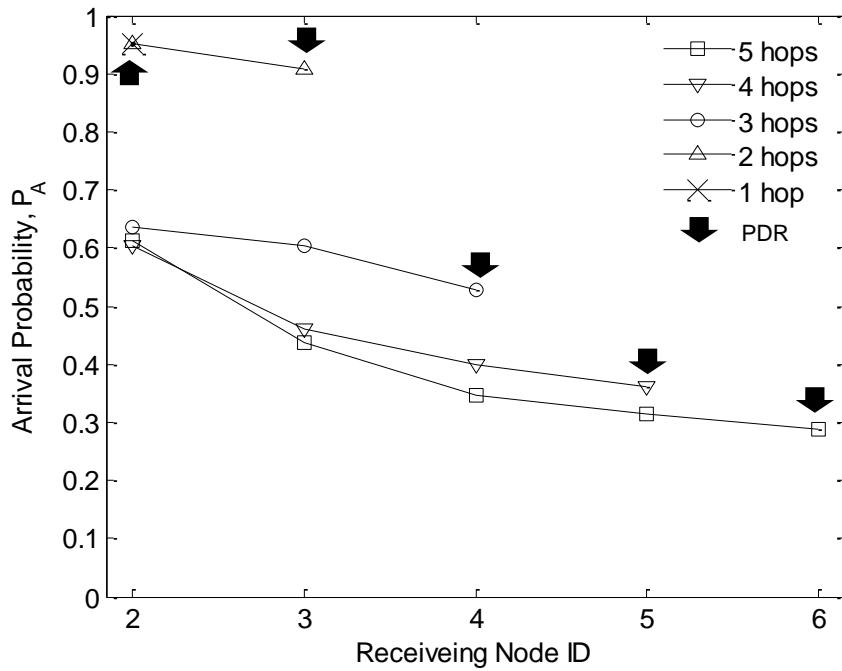


Fig. 3-3. Arrival probability and PDR, CSL=-81dBm, $G=1/2$.

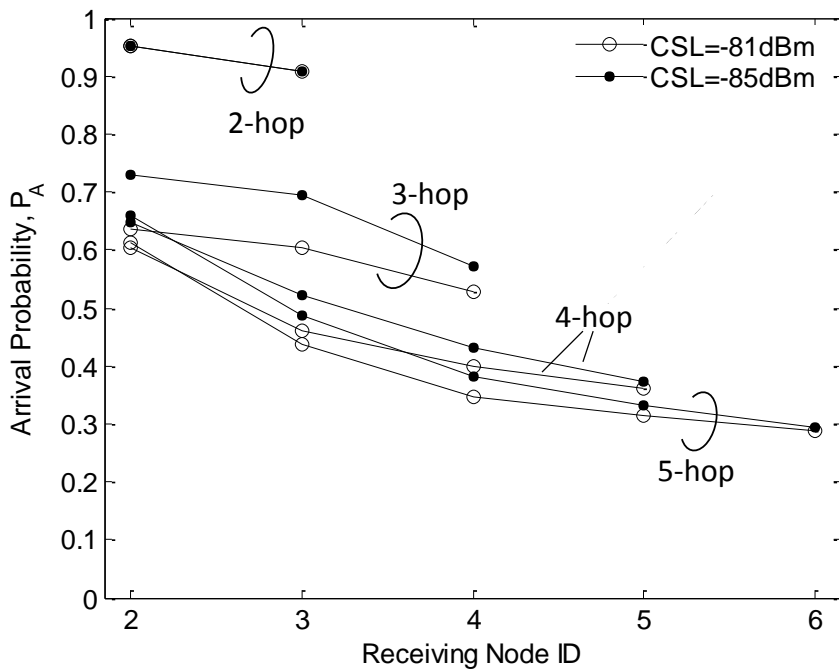


Fig. 3-4. Arrival probability and PDR, CSL=-81dBm & -85dBm, $G=1/2$.

Since HT problem depends on the carrier sense level, the arrival probability with other *CSL* is also investigated. The results with *CSL* of -85dBm are shown in Fig. 3-4. It is found that degradation of the arrival probability at Node 2 is severer when lower

sensitivity of -81 dBm is employed.

The probability of successful transmission after delay and the probability of transmission failure after delay of N_{i-1} are denoted as $P_{DN_{i-1}}$ and $P_{DE_{i-1}}$, respectively. The sum of $P_{DN_{i-1}}$ and $P_{DE_{i-1}}$ is $P_{D_{i-1}}$. Considering Eq. 3-20, $P_{A_{i-1}}$ can be written as

$$P_{A_{i-1}} = P_{DN_{i-1}} + P_{DE_{i-1}} + P_{N_{i-1}} + P_{E_{i-1}} \quad (3-21)$$

Fig. 3-5 shows the percentages of probabilities of P_{DN} , P_{DE} , P_E and P_N to P_A at each node in 5-hop network. With Fig. 3-4 and Fig. 3-5, it is found that:

-- Higher carrier sensitivity improves the arrival probability at the first relay node by suppressing P_E and increasing P_{DN} . $P_{E_{i-1}}$ is mainly due to intra-flow interference caused by HT problem.

--However, the sum of P_E and P_{DE} increases when carrier sensitivity becomes higher. Thus higher carrier sensitivity also decreases the STP of the 3rd hop and the following hops. Then PDR at destination may not be improved significantly. This phenomenon will be addressed in Section III-B.

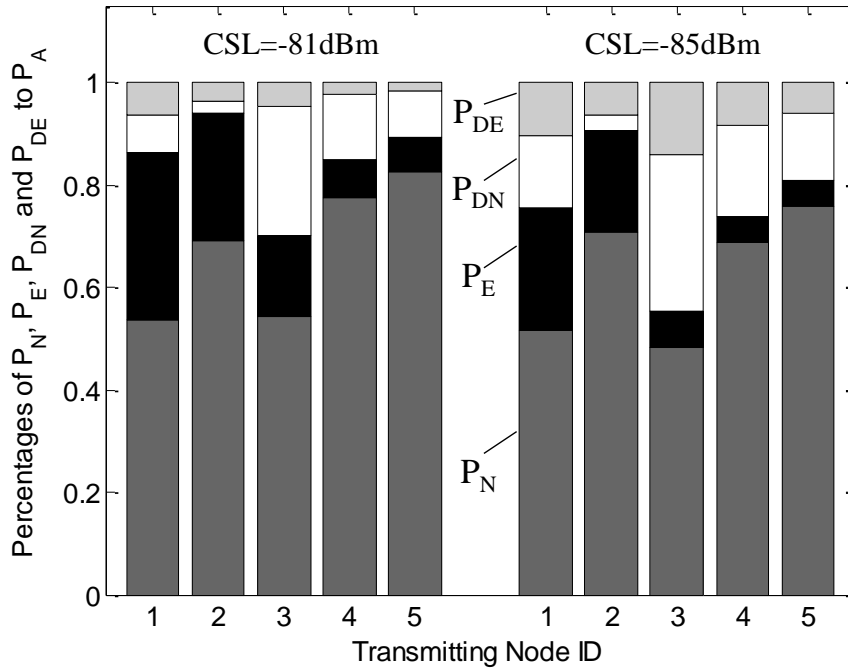


Fig. 3-5. Percentages of P_N , P_E , P_{DN} and P_{DE} to P_A at each transmitting node, 5-hop.

In order to validate the analysis presented in Section II, network simulation by QualNet 4.5 is conducted with the same conditions in TABLE 3-1. For comparison, the results with *CSL* of -81dBm and -85dBm are shown in Fig. 3-6. It is found that our mathematical analysis can well describe the characteristics of the arrival probability suffering from HT and precisely predicts the arrival probability and PDR when the hop number is 4 or more (absolute error is less than 2%). The average differences of the arrival probabilities between analysis and simulation with different hop numbers, *CSL* and *D* (distance between neighbor nodes) are always less than 3.5%.

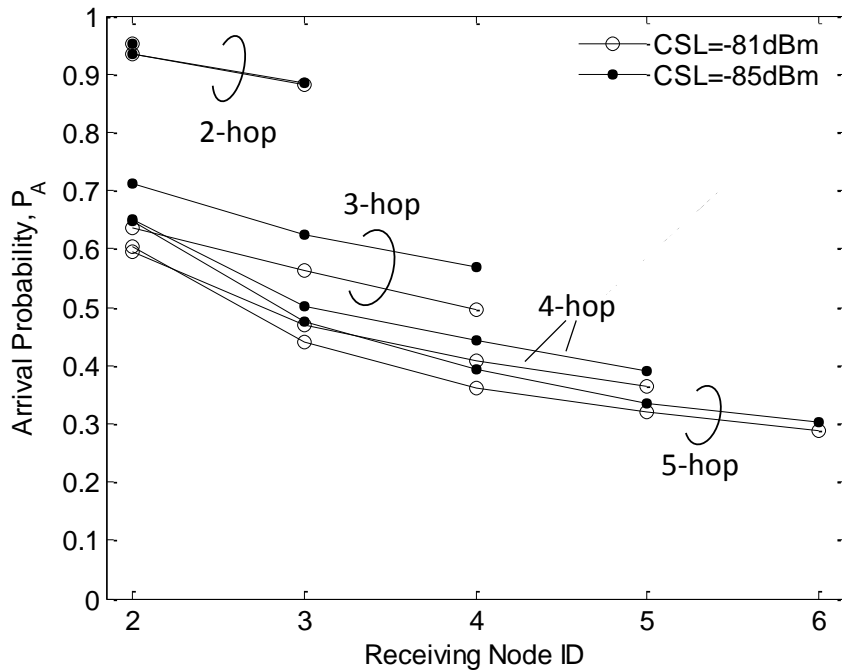


Fig. 3-6. Simulated arrival probability and PDR, $CSL = -81dBm$ & $-85dBm$, $G = 1/2$.

3.2.2 Delay Probability

The delay probability P_D is a by-product of the derivation of arrival probability P_A . Fig. 3-7 shows the delay probability P_D in 5-hop network with different *CSL*. It can be found that source node and Node 3 are more likely to delay their transmission. When the carrier sense sensitivity is high, the possibility increases that Node 3 will continue to sense Node 1's transmission and delay its transmission (Case 4.2.2). Since Node 1 is the

source node and periodically generates packet, the packets to be transmitted by Node 3 will be discarded due to backoff limit. On the other hand, if source node sensed the signal from Node 3 and delayed its transmission, it will not continue so long because Node 3 does not generate any packet by itself, which results in higher delay efficiency at source node. Consequently, high carrier sensitivity prevents packet forwarding at the later hops.

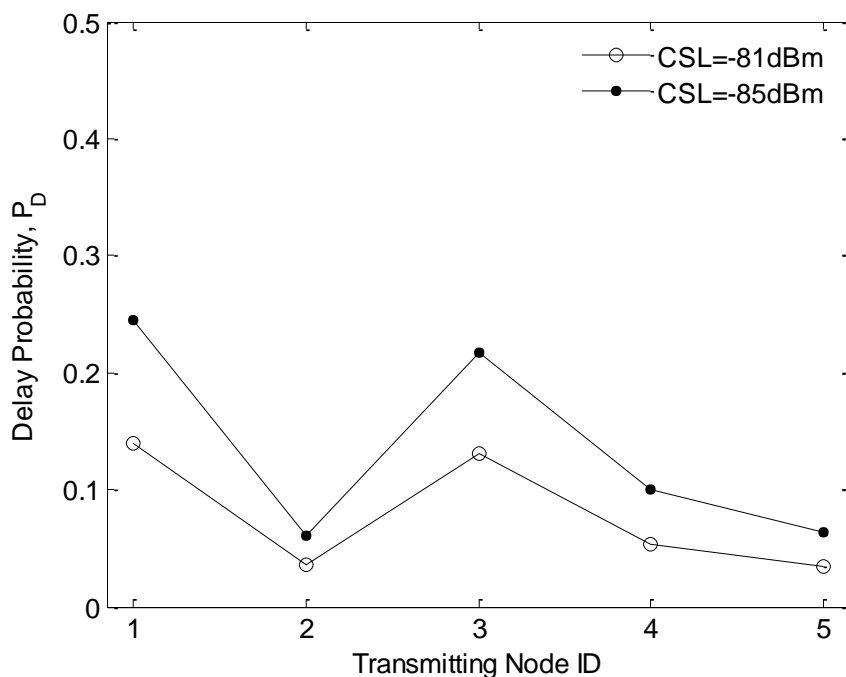


Fig. 3-7. Delay probability, CSL=-81dBm & -85dBm, $G=1/2$.

3.2.3 Normalized Throughput

As can be seen in Section III-A, intra-flow interference due to HT problem severely affects the network's performance. Then, it is natural to ask whether the network's performance can be improved by reducing the offered load traffic rate G .

Fig. 3-8 shows the arrival probability and PDR when G is $1/3$ and CS level is -81dBm. Compared with Fig. 3-3, the similar phenomenon can be observed: arrival probability severely decreases by around 30% at Node 2 when the network's hop number increases from 3 to 4. The important difference is that the arrival probability for G of $1/3$ severely decreases between hop numbers of 3 and 4, instead of 2 and 3 for G of

1/2. Another remarkable point is that the arrival probability at Node 2 of 4-hop network is smaller than the one of 5-hop network. This results from the fact that the occurrence probability of HT problem is relatively higher in 4-hop network.

When G is 1/3, the packet arrival probability, as well as PDR, is globally much higher than that when $G=1/2$. However, it costs more time to transmit a packet. Thus, the normalized throughputs for both cases are calculated. The normalized system throughput S is defined as

$$S = G \times P_{PDR} \quad (3-22)$$

The results are shown in TABLE 3-2 and Fig. 3-9. It can be found that

--The throughput with $G=1/2$ is superior to the one with $G=1/3$ when the hop number is 1 or 2.

--The throughput performance gradually becomes comparable for $G=1/2$ and $G=1/3$ when the network's hop number is 3 or larger.

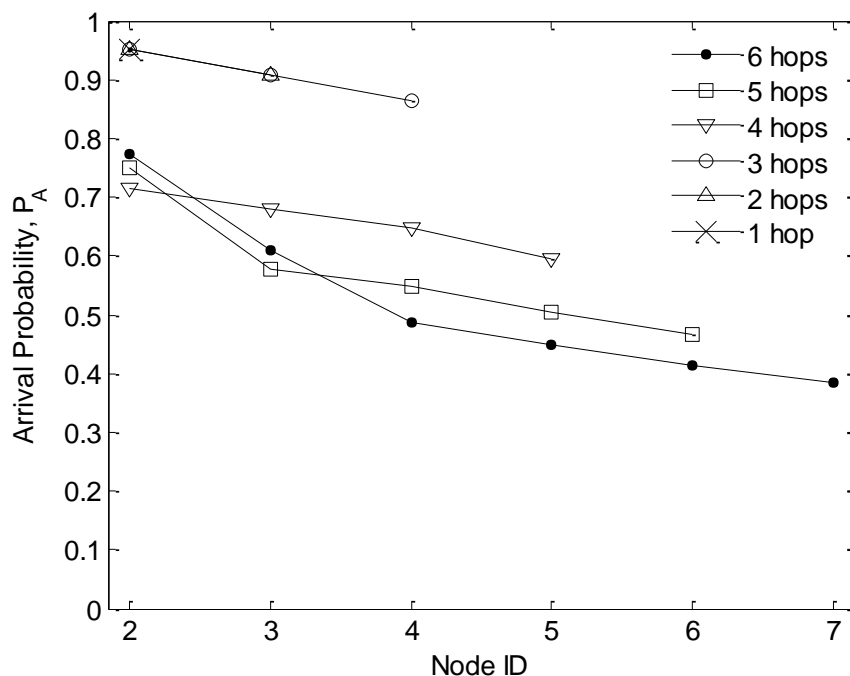


Fig. 3-8. Arrival probability and PDR, CSL=-81Bm, $G=1/3$.

TABLE 3-2 Normalized Throughput, CSL=-81dBm

	1 hop	2 hops	3 hops	4 hops	5 hops	6 hops
G=1/3	0.317	0.302	0.288	0.198	0.155	0.128
G=1/2	0.476	0.453	0.264	0.181	0.144	0.121

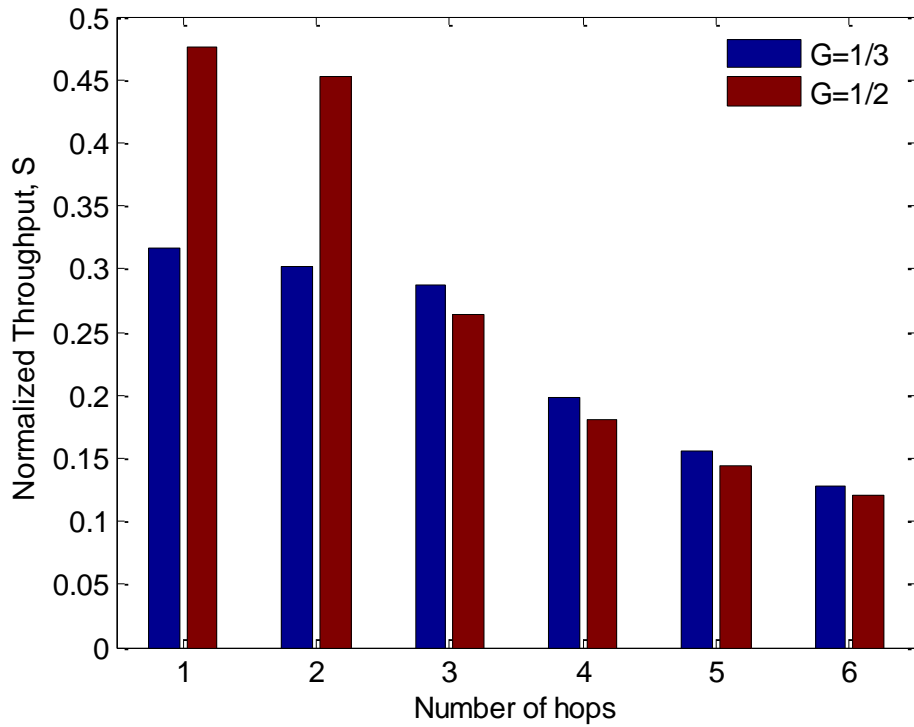


Fig. 3-9. Throughputs of CSMA/CA multi-hop network for different number of hops.

3.3 Performance Limitation in CSMA/CA Multi-Hop Transmission

Intra-flow interference caused by HT problem severely degrades the per-link STP of the first hop. The network's performance is therefore affected due to bottleneck effect. Higher carrier sensitivity can alleviate HT-caused intra-flow interference at the first hop however cannot improve the network's Packet Delivery Ratio significantly.

Normalized load G determines the upper limit of the end-to-end throughput.

However, achievable throughputs in actual CSMA/CA multi-hop communications saturate before G reaches to $1/2$. This phenomenon can be found in Fig. 3-10. In this chapter, it has been revealed that this phenomenon is caused by intra-flow interference due to HT problem. Furthermore, when traffic is high, employing higher carrier sensitivity cannot improve the throughput because it introduces much more waiting time and clogs transmission.

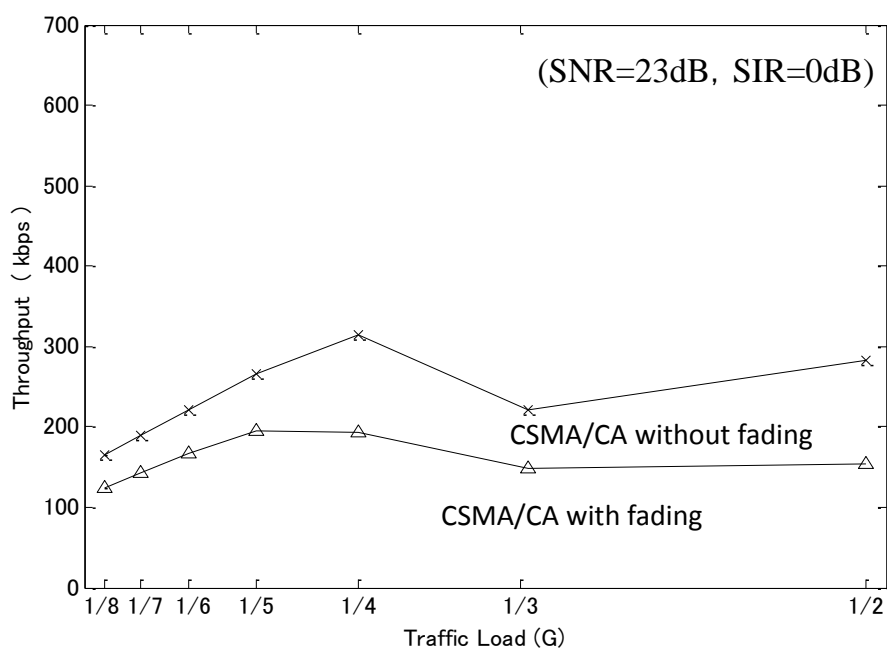


Fig. 3-10. Throughputs of CSMA/CA multi-hop network.

In Fig.3-1, the previously forwarded packets are sent from Node 3 to Node 4 for $G = 1/2$, and from Node 4 to Node 5 for $G = 1/3$. They collide with the next packet from Node 1 and may cause packet loss. Since Node 2 knows all bit information of the interfering signal that has previously sent by itself, the receiver of Node 2 may cancel the interference and increase the communication performance. Thus, it is natural to consider the use of interference cancellation (IC).

3.4 Conclusion of Chapter 3

In this chapter, a CINR-based probability analysis method that well predicts the packet delivery ratio for CSMA/CA multi-hop network under fading environment is proposed. With the method, the impact of HT-caused intra-flow interference and the effect of carrier sense level have been analyzed. The multi-hop network's performance with offered load traffic rate of $1/2$ and $1/3$ was also compared.

Intra-flow interference (IFI) caused by HT problem severely degrades the per-link successful delivery probability of the first hop. The network's performance is therefore affected due to bottleneck effect. Higher carrier sensitivity can alleviate HT-caused intra-flow interference at the first hop however cannot improve the network's Packet Delivery Ratio significantly.

The network with offered load traffic rate of $1/3$ shows much better performance in the aspect of packet delivery rate compared with the one with $1/2$. However, it has little advantage in end-to-end throughput, that is, CSMA/CA multi-hop transmission has performance limitation for high traffic load. An optimal CSL will make the stochastic CINR status just satisfies the requirement for the current data rate in the flow. The relationship between CINR requirement and data rate is determined by the Shannon capacity. If the multi-hop network attends to relay data in higher speed, CSMA/CA will delay some of the transmissions by back off mechanism so that neighboring transmitting nodes will not be too close to each other and the CINR status will keep steady. Consequently, the throughput cannot be increased. If the IFIs can be removed, CNR condition will become the one that limits the channel capacity instead of CINR therefore higher data rate can be supported.

Chapter 4

Highly Efficient Multi-Hop Packet Transmission Using Intra-Flow Interference Cancellation

In Chapter 3, it has been revealed that IFI limits the multi-hop transmission performance and that IC will be a promising method to enable the network to support higher traffic load. This chapter 1) proposes a known IC technique against IFI that uses normalized least mean square (NLMS) equalization. It is applicable to a variety of modulation schemes as well as a wide range of SIR (signal to interference ratio). Moreover, it is capable of canceling multiple known interference from different hidden terminals; 2) designs an IFI-canceling multi-hop transmission scheme to facilitate IC so that the nodes can efficiently relay packets under high traffic loads in half-duplex networks; and 3) discusses a collaboration approach that combines IFIC with the maximal-ratio combining (MRC) reception by which MRC can still provide diversity gain in the presence of interference. The performance of our proposal is evaluated in the presence of Rayleigh fading.

The rest of the chapter is organized as follows. In Section 4.1, the traffic model for multi-hop transmission is introduced; in Section 4.2, a method of canceling IFI by using adaptive equalization with NLMS will be presented; the detailed design of IFI-canceling multi-hop transmission (IFIC-MHT) scheme including packet format, multi-hop transmission scheme and receiving operation will be introduced in Section 4.3; the mathematical analysis model for performance evaluation of IFIC-MHT is presented in Section 4.4, where the impact of maximum Doppler frequency is considered; After the performance evaluation settings are introduced in Section 4.5, the results and related analysis will be presented in Section 4.6; The applications of IFIC for other scenarios will be discussed in Section 4.7 and Section 4.8.

4.1 Modeling for Multi-Hop Transmission

4.1.1 Traffic Model

Assume multi-hop communication over a single frequency channel, in which a source node constantly generates a packet stream with a fixed packet generation interval, T_{int} . All transceivers in the multi-hop links are half-duplex, so that the interval should not be shorter than twice of the packet communication period T_{com} , which is necessary for the sender and receiver to complete unicast transmission. To quantify the density of given traffic rate, normalized load G , is defined as:

$$G = T_{com} / T_{int} \quad (G \leq 1/2) \quad (4-1)$$

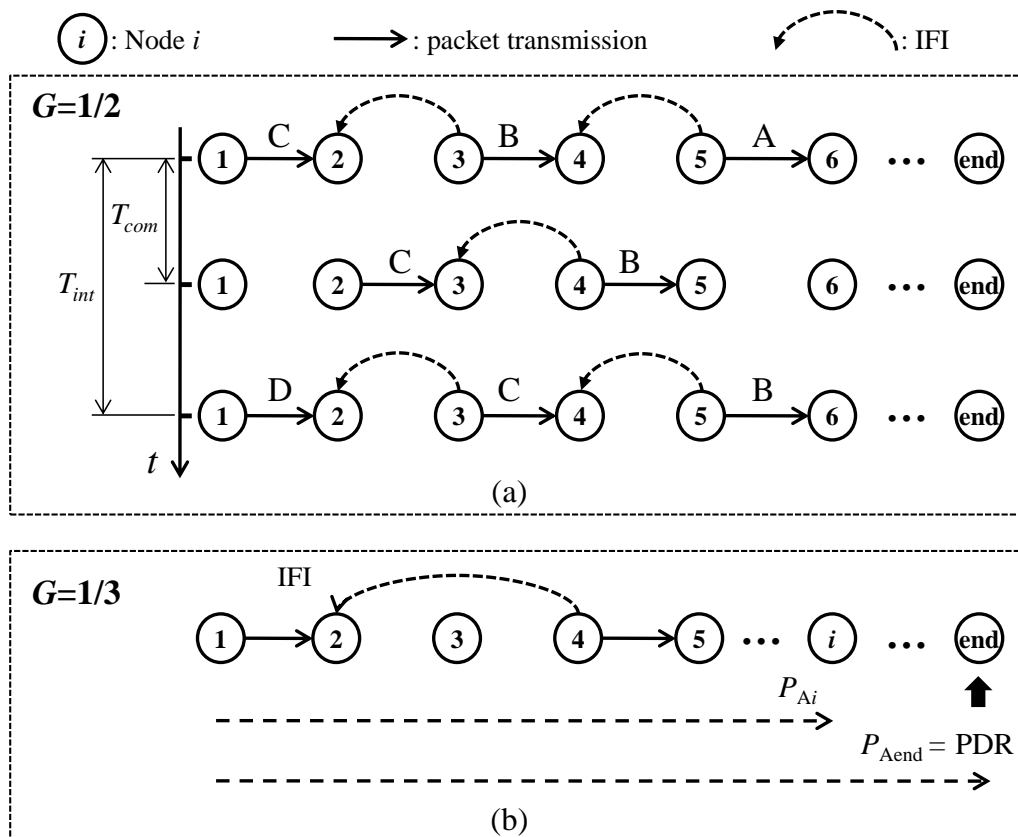


Fig. 4-1. Ideal multi-hop traffic flows and intra-flow interference.

G is the upper limit of the end-to-end throughput normalized by the transmission data rate. Fig. 4-1 shows the ideal traffic flows in a one-way multi-hop network when G is $1/2$ and $1/3$ based on the assumption that all packets can be received correctly under known IFI¹ (shown by dashed lines). The word “high traffic load” in this chapter means that G is $1/3$ or higher. As an example, Fig. 4-1(a) illustrates how the packets (A, B, C, D) are forwarded when G is $1/2$ (i.e. the source node periodically generates one new packet every $2T_{com}$). The packet arrival probability P_{Ai} is shown in Fig. 4-1(b). It is the percentage of the packets that have been correctly delivered from source node to Node i .

4.1.2 Antenna Settings

All the antennas in the nodes are assumed omnidirectional. Multiple receiving antennas can be used for MRC reception to further improve the performance of IFIC. However, since MRC does not change the essence of the proposed IFIC-MHT scheme, it is assumed that each node equips single antenna for transmitting and receiving except for the MRC case.

4.2 Intra-Flow Interference Canceller

4.2.1 Mechanism of Cancellation

Given that signal $x(t)$ is transmitted over time-variant channel $h(t)$, received signal $y(t)$ can be written as (* represents convolution)

$$y(t) = x(t) * h(t) + n(t) \quad (4-2)$$

where $n(t)$ is AWGN with power spectrum density (PSD) of N_0 . The samples of the received signal $\{y_n\}$, input to the equalizer, can be represented in z domain as:

$$Y(z) = X(z)H(z) + N(z) \quad (4-3)$$

If the channel response is known, the ideal equalizer to recover the signal by the minimum mean-square error (MMSE) criterion [42] is given by:

$$F(z) = \frac{H^*(1/z^*)\Phi_X(z)}{H(z)H^*(1/z^*)\Phi_X(z) + N_0}, \quad (4-4)$$

where $F(z)$ denotes the z transform of the equalizer's impulse response and $\Phi_X(z)$ is the z transform of the autocorrelation of sampled $x(t)$. The transmitted signal can be recovered by the equalizer if noise power is small, i.e. $X(z) \approx Y(z)F(z)$.

For time-varying channels, the adaptive equalizer estimates the channel response based on a known sequence received in the training phase (TP). If two training sequences of the desired and undesired signals are received separately as shown in Fig. 4-2, two signals can be unbundled.

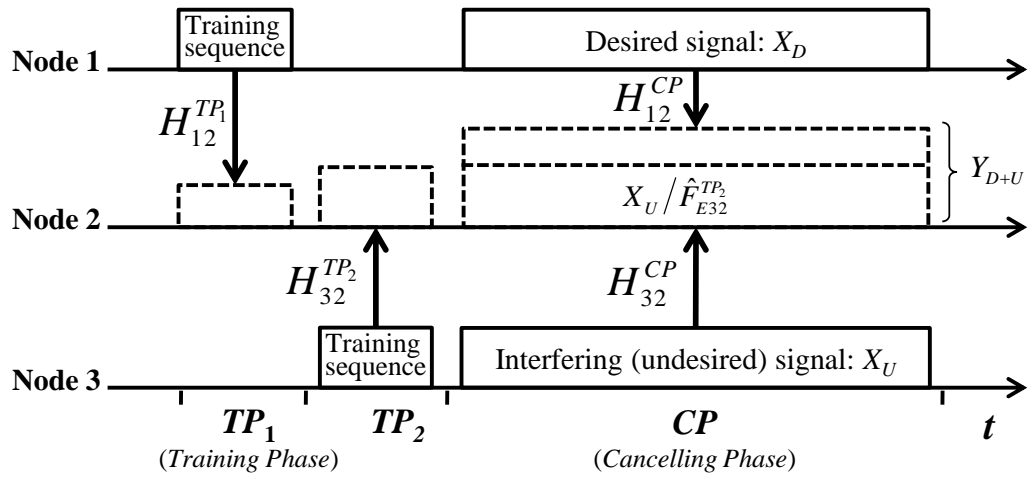


Fig. 4-2. Interference cancellation algorithm.

during the canceling phase (CP) as shown below. At the end of TP_1 , the impulse response of adaptive equalizer $\hat{F}_{E12}^{TP_1}(z)$ that uses the MSE cost function is given by

$$\hat{F}_{E12}^{TP_1}(z) \approx \frac{H_{12}^{TP_1*}(1/z^*)\Phi_{TS_D}(z)}{H_{12}^{TP_1}(z)H_{12}^{TP_1*}(1/z^*)\Phi_{TS_D}(z) + N_0}. \quad (4-5)$$

Here, H_{ij} denotes the channel response from Node i to Node j . Similarly, at the end of TP_2 , the impulse response for the undesired signal is given by

$$\hat{F}_{E32}^{TP_2}(z) \approx \frac{H_{32}^{TP_2^*}(1/z^*)\Phi_{TS_U}(z)}{H_{32}^{TP_2}(z)H_{32}^{TP_2^*}(1/z^*)\Phi_{TS_U}(z) + N_0}. \quad (4-6)$$

When Node 1 transmits desired signal $X_D(z)$ and Node 3 transmits another signal $X_U(z)$ (which is undesired for Node 2 and causes interference), the received interfered signal can be expressed as:

$$Y_{D+U}(z) = X_D(z)H_{12}^{CP}(z) + X_U(z)H_{32}^{CP}(z) + N(z). \quad (4-7)$$

If the following three conditions are satisfied, the desired signal $X_D(z)$ can be demodulated under interference: 1) The channel responses during *TP* and *CP* have strong correlation, (i.e. $H_{12}^{TP_1}(z) \approx H_{12}^{CP}(z)$, $H_{32}^{TP_2}(z) \approx H_{32}^{CP}(z)$); 2) Noise is small; 3) The interfering signal $X_U(z)$ is known by the receiver. Accordingly, $X_U(z)$ can be cancelled with the operation shown in (8).

$$\begin{aligned} [Y_{D+U}(z) - X_U(z)/\hat{F}_{E32}^{TP_2}(z)]\hat{F}_{E12}^{TP_1}(z) &\approx \left[X_D(z)H_{12}^{CP}(z) + X_U(z)H_{32}^{CP}(z) + N(z) - X_U(z) \frac{H_{32}^{CP}(z)H_{32}^{CP^*}(1/z^*)\Phi_{TS_U}(z) + N_0}{H_{32}^{CP^*}(1/z^*)\Phi_{TS_U}(z)} \right] \hat{F}_{E12}^{TP_1}(z) \\ &\approx \left[X_D(z)H_{12}^{CP}(z) + N(z) - \frac{X_U(z)N_0}{H_{32}^{CP^*}(1/z^*)\Phi_{TS_U}(z)} \right] \frac{H_{12}^{CP^*}(1/z^*)\Phi_{TS_D}(z)}{H_{12}^{CP}(z)H_{12}^{CP^*}(1/z^*)\Phi_{TS_D}(z) + N_0} \\ &\approx \left[X_D(z)H_{12}^{CP}(z) + N(z) - \frac{X_U(z)N_0}{H_{32}^{CP^*}(1/z^*)\Phi_{TS_U}(z)} \right] \frac{1}{H_{12}^{CP}(z) + N_0/[H_{12}^{CP^*}(1/z^*)\Phi_{TS_D}(z)]} \\ &\approx X_D(z) + \frac{N(z)}{H_{12}^{CP}(z)} - \frac{X_U(z)}{H_{32}^{CP^*}(1/z^*)\Phi_{TS_U}(z)} \frac{N_0}{H_{12}^{CP}(z)} \approx X_D(z) \quad (|N(z)| \ll |H_{12}^{CP}(z)| \text{ and } N_0 \ll |H_{12}^{CP^*}(1/z^*)\Phi_{TS_D}(z)|). \end{aligned} \quad (4-8)$$

4.2.2 Channel Estimation with LMS or NLMS

Since practical applications must consider the costs of power consumption and hardware, least mean square (LMS) [43] equalization and its extensions are preferred to fulfill the task described above. LMS equalization is based on an approximated steepest-descent method and is known for its simplicity and applicability of implementation [42]. LMS updates the filter's parameters $f_k(n)$ as

$$f_k(n+1) = f_k(n) + \mu f_k(n) e(n), \quad (4-9)$$

where μ is the step size and $e(n)$ is the error at sample n . The adjustment error, ε , of basic LMS can be approximately represented by (10) as reference [44],

$$\varepsilon \approx \frac{1}{2} \mu \sum_{k=1}^M \lambda_k = \frac{1}{2} \mu \sum_{k=1}^M E[u^2(n-k+1)], \quad (4-10)$$

where M is filter length and $u(n-k+1)$ is the input of the k^{th} tap of the adaptive filter. λ_k is the eigenvalue of the correlation matrix [45]. As this equation implies, to keep the estimation error consistent, the step size should be adjusted depending on the input signal power. However, it is not practical to optimize the step size at the receiver for a specific signal in actual systems. In this context, normalized LMS (NLMS) is chosen [46] [47] for IFIC. In contrast to basic LMS, NLMS updates the filter's parameters $f_k(n)$ with μ normalized by the sum of instantaneous signal power at each tap. That is,

$$f_k(n+1) = f_k(n) + \frac{\mu}{\eta + \sum_{k=1}^M |u(n-k+1)|^2} f_k(n) e(n), \quad (4-11)$$

where η is a positive bias. This algorithm increases the calculation complexity but greatly improves the stability of adaptation for signals with different received powers.

4.3 Detailed Design for Intra-Interference Cancellation

4.3.1 Packet Format

Identity of IFI and CSI are essential elements for performing IFI-cancellation. The key to designing an IFIC-MHT scheme is to guarantee that they can be received without being interfered. To realize this, the desired and IFI packets are assigned different formats as shown in Fig. 4-3. Both formats consist of three parts: α , β and γ , while a blank period (T_B) is inserted between β and γ for the case of Format 2. The α part,

which contains the training sequence for channel estimation, is the PHY/MAC header defined in IEEE 802.11 standards [15]. Fig. 4-3 illustrates an example for 802.11b. The β part carries the IP payload that will overlap with other packet's β part if packet collision occurs. The α and β parts together form the original IEEE 802.11 packet. The newly added γ part includes *ACK* (acknowledgment) information and *payload identifier*. The blank period is longer than the time for transmitting α and γ parts ($T_\alpha + T_\gamma$) so that the two parts can be received without interference. It also can be set wider if two or more interfering packets should be cancelled (discussed in Section VIII).

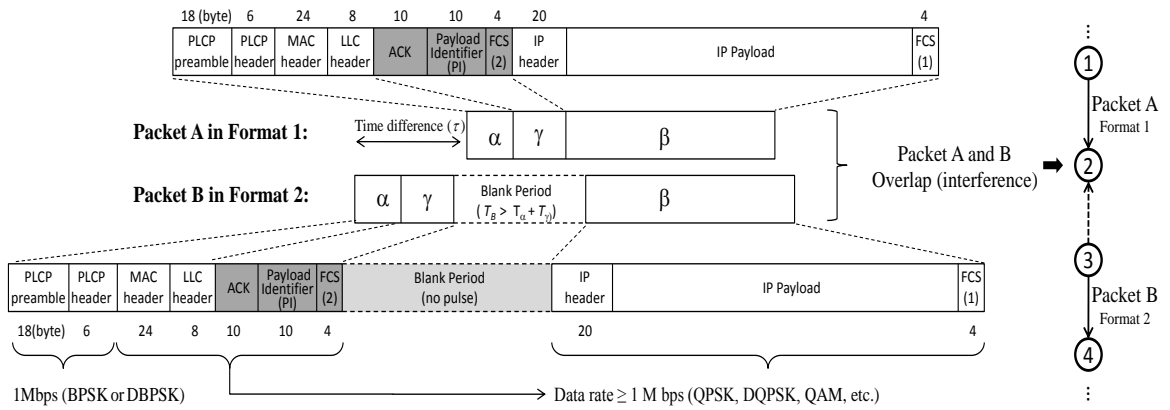


Fig. 4-3. Overlapping pattern of two packets and the packet formats for IFIC-MHT scheme.

4.3.1.1 Payload Identifier

The identifier that indicates the IP payload of IFI is carried by the *payload identifier* (PI) in Fig. 4-3. Every node maintains a list table that consists of the IP payload copies and the corresponding identifiers that have been transmitted recently. A receiver that suffers interference can use this identifier to find a copy of the IP payload and then utilize it for IC. In order to guarantee that the γ part is received correctly, an additional frame check sequence (FCS) is attached right after the PI.

4.3.1.2 ACK

Since the γ part can be received without IFI, ACK information is placed inside so that no dedicated ACK packet needs to be transmitted in the IFIC-MHT scheme. This keeps the length of communication period T_{com} constant and eliminates the overhead that would otherwise be caused by transmitting dedicated ACK packets.

4.3.1.3 Comparison of Packet Format with Analog Network Coding

Analog network coding (ANC) [36] is a visible known-IC method that also uses TSs to obtain CSI. However, there are significant differences between ANC and IFIC-MHT. In ANC, packet transmissions take place asynchronously. TS and pilot information are attached at the beginning and ending of packets as shown in Fig. 4-4 (a). Since the transmission timing is random, overlapping pattern of two packets should be considered. If the desired signal and interfering signal overlap partially, the training sequences for both signal can be received without being interfered. However, there are several demerits for such design. For explanation, Fig. 4-4 (b) and Fig. 4-4 (c) give the comparisons of packet overlapping patterns between IFIC-MHT and ANC in some circumstances. ANC cannot well support the cases when desired signal and interfering signal have significant difference in packet length. As shown in Fig.4-4 (b), IC cannot be performed for the case of ANC because the two training sequences of Signal 2 are both interfered. However, it does not take place in IFIC-MHT because it introduces the slot-frame structure. Also, the packet format used in ANC cannot be directly used in the situation when multiple interferences present. As illustrated in Fig. 4-4 (c), the training sequences of Signal 2 are interfered and the receiver must remove Signal 3 (another known-interference) at first. Meanwhile, the residual error introduced by cancelling Signal 3 will degrade the channel estimation accuracy for cancelling Signal 2. In contrast to ANC, the proposed packet format ensures that multiple interferences can be cancelled in parallel, because the training signals for three packets can be received independently. Furthermore, ANC use energy detection to detect the arrival timing of the interfering packet, which limits the modulation method in order to keep the signal envelop constant. By contrast, since interference arrives during the blank period, the starting of interference can be easily detected by simple energy detection without the requirement of constant envelop.

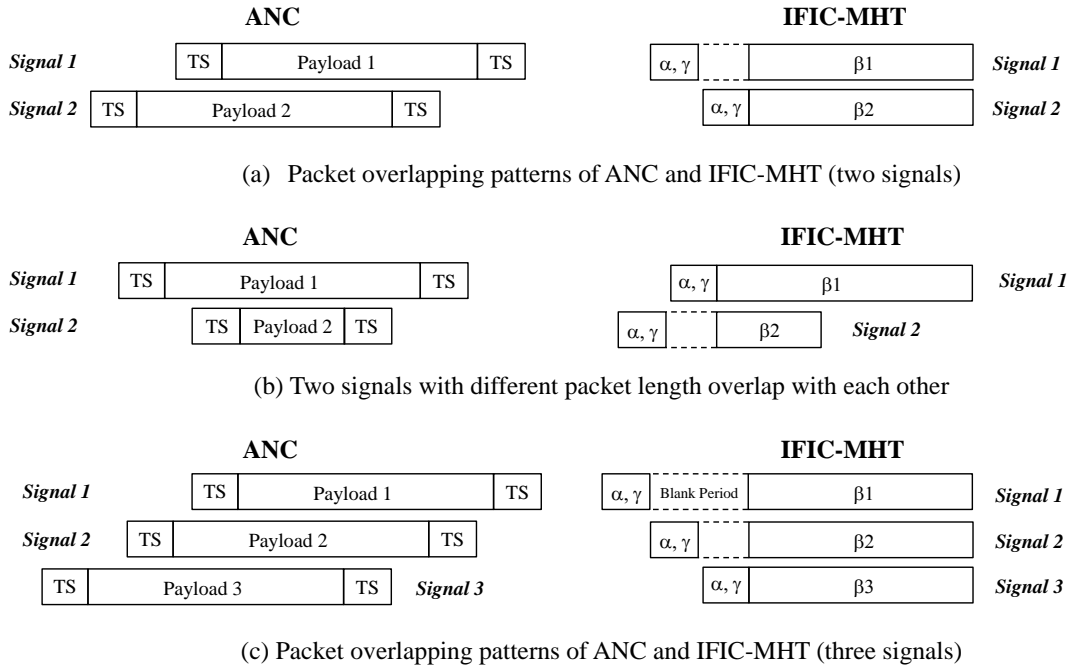


Fig. 4-4. Difference of packet format between ANC and IFIC-MHT.

4.3.2 Relay Process

Since the IFIC-MHT process aims at maximum throughput for packet streaming applications such as video streaming, the time scale is divided into slots of fixed length which equals one communication period, T_{com} . All nodes refer to a common time reference to synchronize their frame structure. Time adjustment is performed by inserting an occasional packet that carries the time stamp information instead of data. The receiving nodes can adjust their time according to the stamp. The nodes in IFIC-MHT follow the 4 rules shown below. Variable i is a global variable that satisfies: $i \in \mathbb{N}^+$ and $i \leq 1/G$.

- Node i , Node $i+1/G$, Node $i+2/G$, ... , Node $i+k/G$ ($k \in \mathbb{N}$) transmit during the same time slot m ($m \in \{i, i+1/G, i+2/G, \dots\}$).
- Node i , Node $i+2/G$, Node $i+4/G$, ... , Node $i+2k'/G$ ($k' \in \mathbb{N}^+$) transmit packets in Format 2.
- Node $i+1/G$, Node $i+3/G$, Node $i+5/G, \dots$, Node $i+(2k''+1)/G$ ($k'' \in \mathbb{N}$) transmit packets in Format 1 with delay τ (the time difference in Fig. 4-3). Delay τ should satisfy

$$T_\alpha + T_\gamma < \tau \leq T_B. \quad (4-12)$$

- Each node is ready to receive signal before and after its transmission time slot in order to get a new packet and check the ACK, respectively. If G is $1/2$, the two tasks are accomplished in the same time slot.

To highlight the essence of the proposed IFIC-MHT process, the following two relay scenarios are illustrated in Fig. 4-5 and Fig. 4-6 for 5-hop transmission with $G = 1/2$.

4.3.2.1 Scenario 1: Idea Relay without Packet Loss

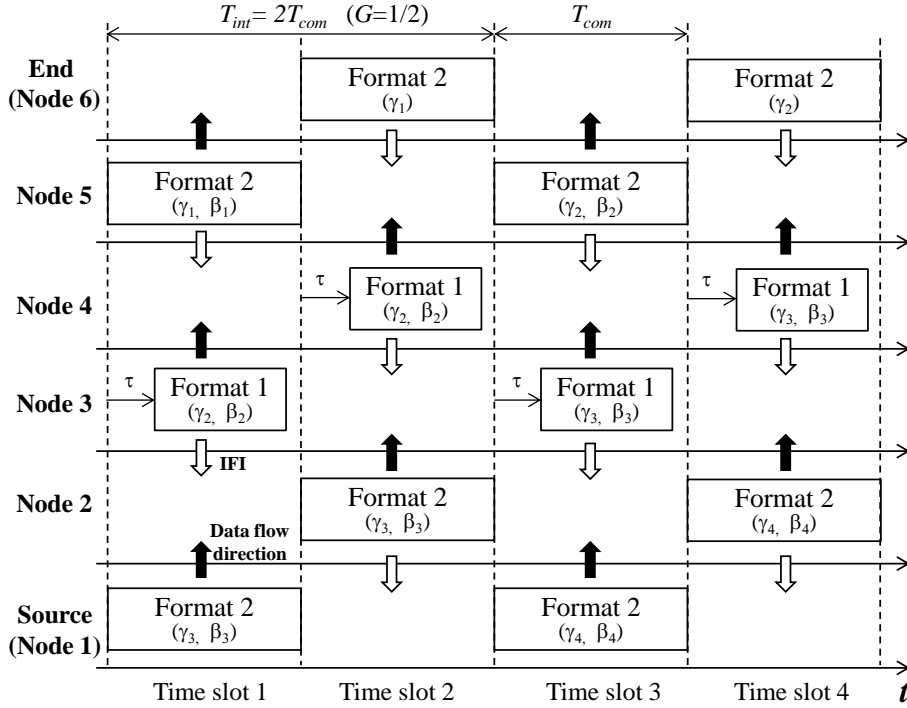


Fig. 4-5. Relay process of 5-hop IFIC-MHT for scenario 1 (without packet loss).
(Subscripts for γ and β represent the IDs of ACK and payload, respectively.)

During time slot 1, according to the first rule, the odd numbered nodes transmit packets to their next nodes. Transmitted signals will interfere at Node 2 and Node 4. According to the second and third rules, the signals transmitted by Node 1 and Node 5 have different packet formats from that of Node 3, thus their α and γ parts are free from interference from Node 3. Then at Node 2, for example, the receiver demodulates

payload β_3 with IFI-cancellation using the estimated CSI obtained from the α parts. During time slot 2, even numbered nodes transmit packets starting from the beginning of the time slot while Node 4 transmits packet after delay τ .

4.3.2.2 Scenario 2: Relay Process with Packet Loss and Retransmission

Figure 4-6 shows the case that Node 4 has failed to receive the desired signal from Node 3 in time slot 1. Node 4 will not transmit any packet during time slot 2. Since the expected ACK (for payload β_2) has not returned in time slot 2, Node 3 should push the newly received packet into a FIFO (first in first out) buffer and transmit the packet with payload β_2 in time slot 3. Note that the γ part of this packet carries ACK information for β_3 . If Node 3 fails in transmitting a packet before the retransmission amount exceeds the limit, it will discard the packet. If the FIFO buffer is full, the newly arriving packet will also be discarded.

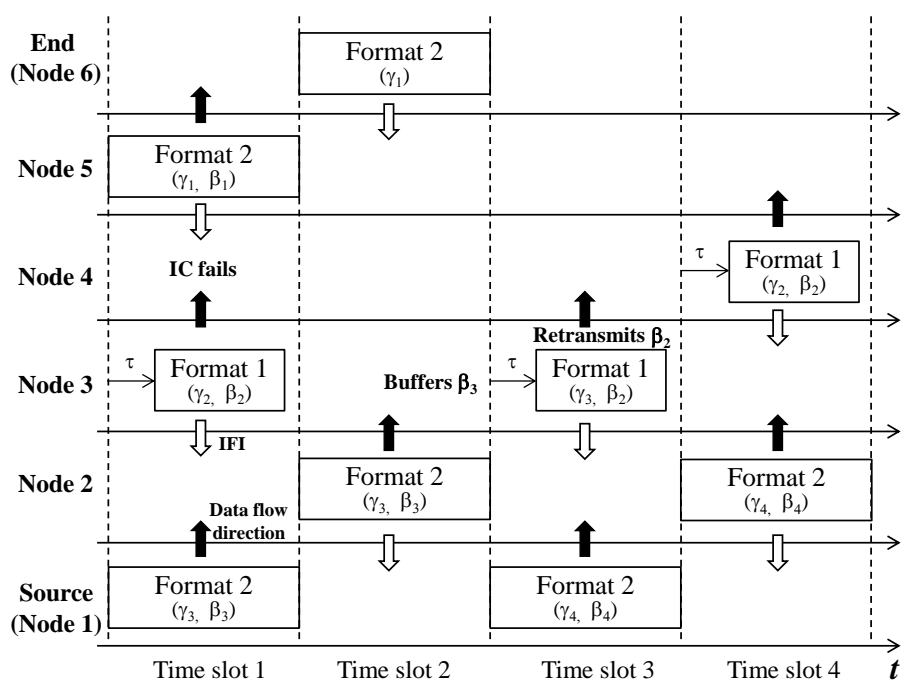


Fig. 4-6. Relay process of 5-hop IFIC-MHT for scenario 2.

(Subscripts for γ and β represent the ID of ACK and payload, respectively.)

4.3.3 Receiving Operation

The flow chart of receiving operation is shown in Fig. 4-7 where the desired signal (Signal 1 in flowchart) carries the packet in format 2 while the interfering signal 2 is in format 1. The receiver will enter into one of three different demodulation modes according to IFI status.

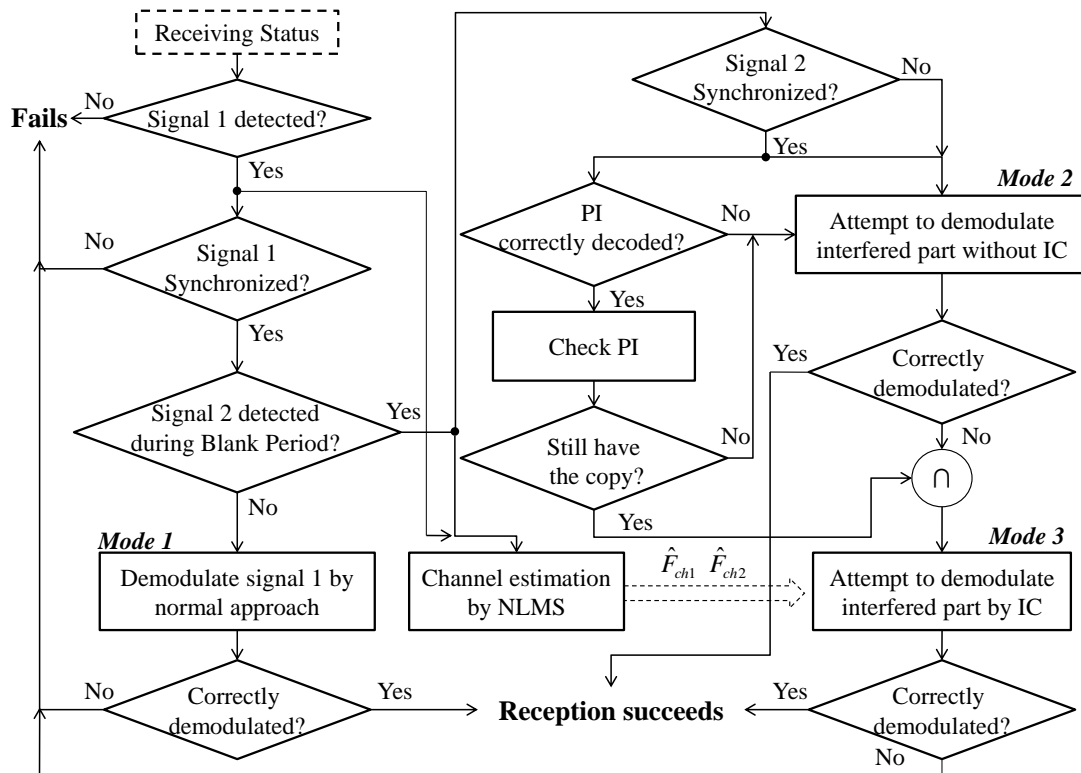


Fig. 4-7. Flow-chart of the receiving operation.

4.3.3.1 Demodulation Mode 1

The receiver demodulates the signal via the normal approach if IFI has not been detected.

4.3.3.2 Demodulation Mode 2

If IFI has been detected, the receiver will first attempt to demodulate the interfered β part without performing IC. Since SINR under fading environment dynamically changes, there is a chance of satisfying the required SINR. If this requirement is not satisfied, the receiver moves to Demodulation Mode 3.

4.3.3.3 Demodulation Mode 3

From the decoded γ part, the receiver can identify the β part of the interfering packet. The receiver then demodulates the desired signal by performing IC.

Figure 4-8 illustrates the IFIC processes sequentially including the detection of signal, channel estimation, IC and demodulation. Based on the relay process introduced in Section 4.3.2, the beginnings of two signals can be easily detected by energy detection because they are interference-free guaranteed. Therefore, the clock synchronizations for desired signal and interfering signal can be carried out independently and the receiver is able to subtract the interference at the right timing. It is not necessary to synchronize the two signals in symbol level because the cancelling process can be performed in higher sampling rate.

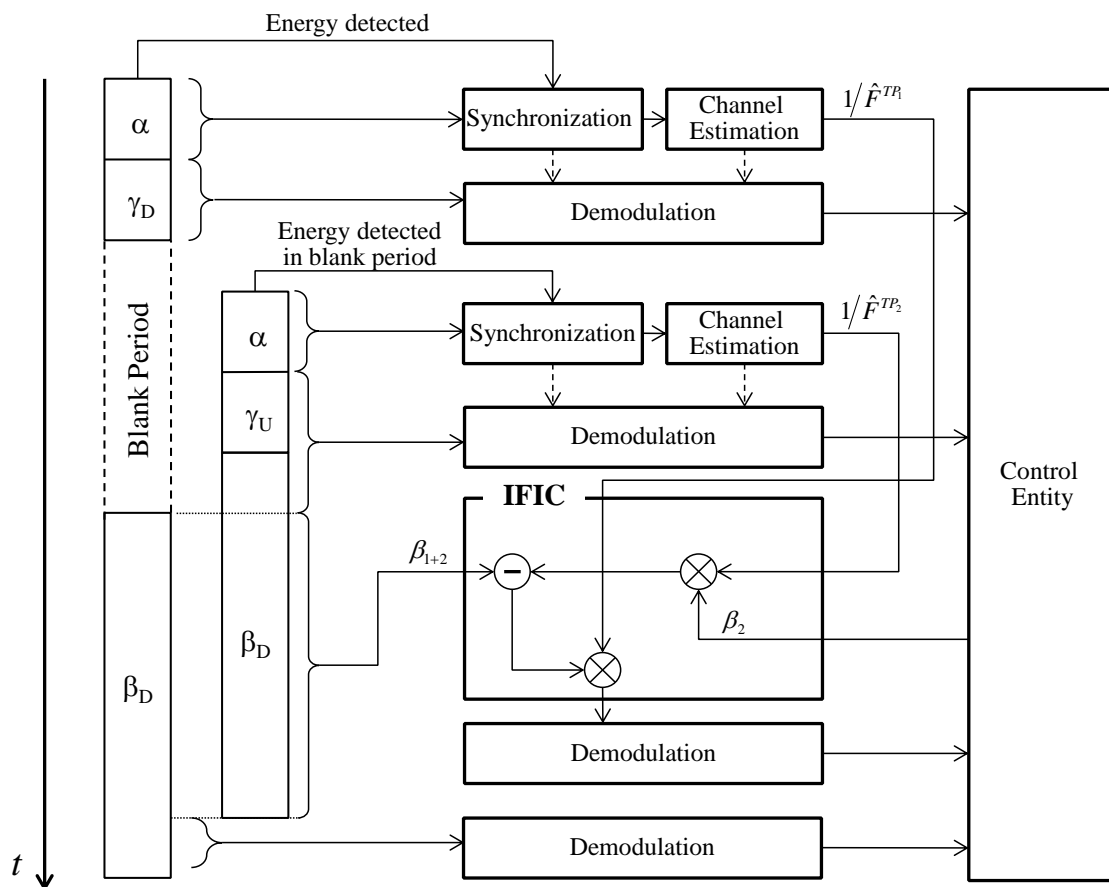


Fig. 4-8. Process of IFIC.

4.3.4 Buffering Process

Figure 4-9 is an example that demonstrates the buffering process in IFIC-MHT. In Time Frame 1, Node 3 transmits packet No.18 with ACK information of No.18. Although this causes IFI at Node 2, Node 2 can correctly receive both packet No. 20 and 18 with IFIC. At Time Frame 2, Node 2 will transmit packet No.19. The γ part of this packet contains ACK for No.20. If Node 1 fails to receive the ACK, it will retransmit the packet No.20. As a result, the buffer of Node 1 is full. Then the new coming payload of No.23 will be discarded. On the other hand, if Node 1 correctly receives the ACK for No. 20, it will accept new payload No. 23 into the buffer.

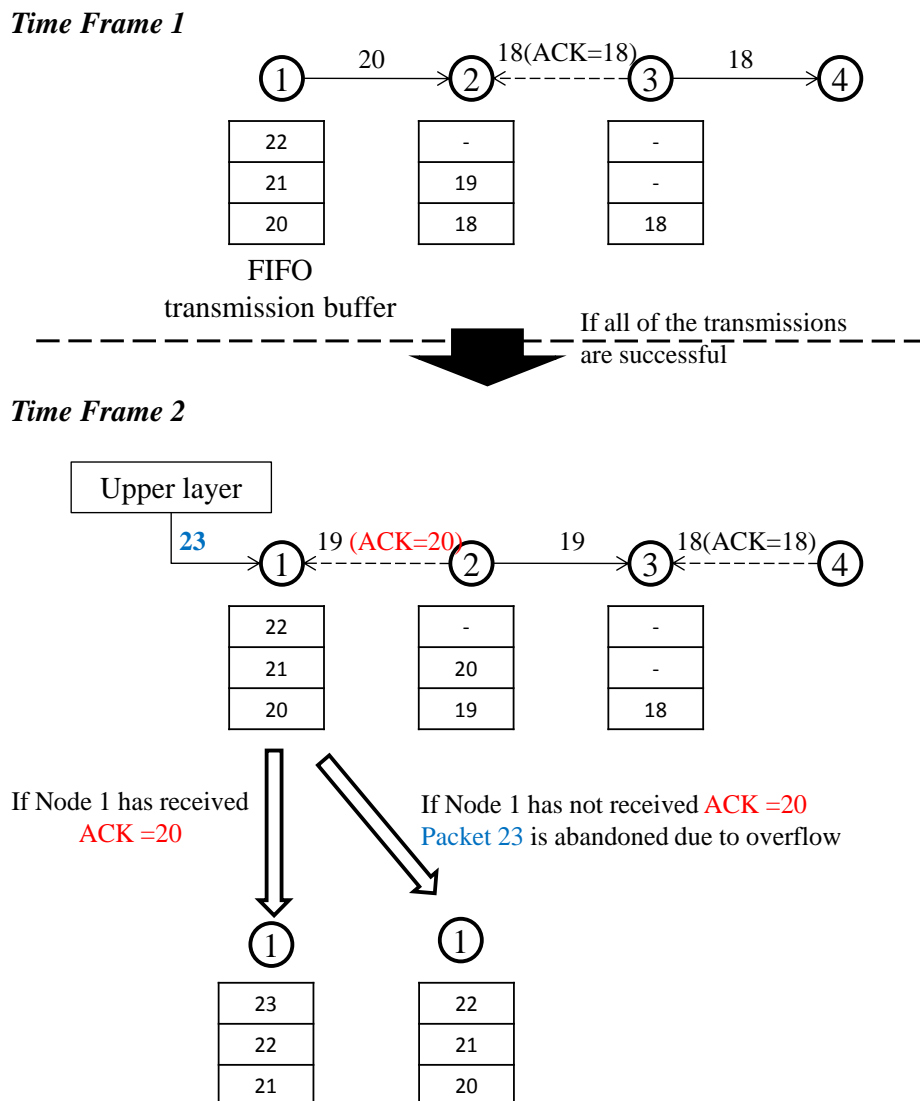


Fig.4-9. Example that demonstrates the buffering process in IFIC-MHT

4.4 Analysis

Packet delivery ratio and the end-to-end throughput (S) are the two main performance indexes considered here. For an N -hop IFIC-MHT, where the source node is Node 1 and the end node is Node $N+1$, P_{Ai} can be expressed by the following recurrence equation:

$$P_{Ai} = \begin{cases} p_{Hi-1} P_{Ai-1} & (N+1 \geq i \geq 2) \\ 1 & (i=1) \end{cases}, \quad (4-13)$$

where p_{Hi-1} is STP for the hop $i-1$, between Node $i-1$ and Node i . STP is the key to solving (13) and has different forms depending on the retransmission policy. Accordingly, its detailed analysis is presented in the next two subsections. Note that the analysis model assumes $G=1/2$. The analysis models for other traffic loads can take a similar approach.

It is notable that the analysis model in this chapter is created for verifying and predicting the performance of *multi-hop transmission* based on the *single-hop* BER/PER (bit error rate/packet error rate) performance with interference canceler (it will be presented in Section VII-C.). Since it is very difficult to theoretically analyze the BER/PER performance with interference canceler under fading environment, the following probabilities, referred to hereinafter, are obtained by simulation. 1) p_{nor} : the probability that a packet is received correctly with no interference present (demodulation mode 1); 2) p_{int} : the probability that an interfered packet is received without using cancellation (demodulation mode 2); 3) p_{can} : the probability that an interfered packet is received correctly by canceling interference (demodulation mode 3, including the probability that PI can be received properly).

4.4.1 Analysis Model for No-Retransmission Case

If retransmission is not employed, p_{Hi-1} can be calculated considering the cases where IFI is present or not. This is expressed as

$$p_{Hi-1} = P_{Ai+1} [p_{int} + (1 - p_{int})p_{can}] + (1 - P_{Ai+1})p_{nor}, \quad (4-14)$$

where the first part on the right side of the equation is the successful transmission probability when Node $i-1$ and Node $i+1$ both have packets to transmit (i.e. IFI present), while the later part represents the successful transmission probability when only Node $i-1$ transmits (No IFI). The arrival probability of each node can be obtained by interactively solving (13) and (14). The end-to-end throughput S is defined as

$$S = K P_{PDR} L / T_{total}, \quad (4-15)$$

where K is the total number of packets generated, L indicates the payload size in bits and T_{total} is the total time taken to deliver the packets.

4.4.2 Analysis Model Considering Time-Correlated Retransmission

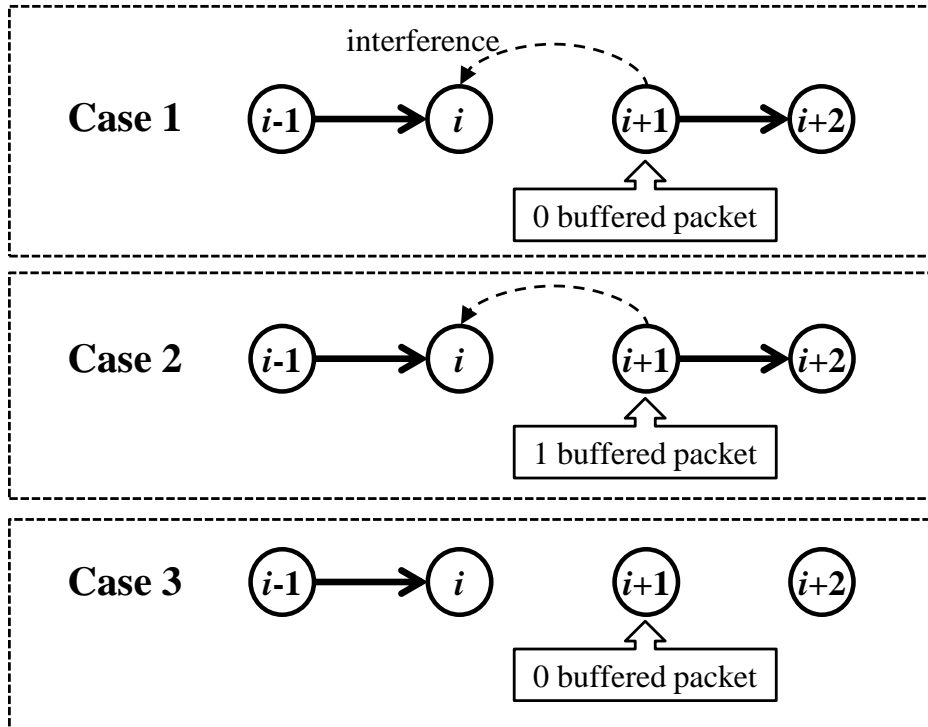


Fig. 4-10. Three cases for analyzing the STP of hop $i-1$.

To precisely calculate the arrival probability when multiple-retransmission is employed under fading while considering the time correlation of signals, the analysis model is so complex that its practicability is impaired. And since the room for performance improvement dwindles with each additional retransmission, an analysis model for deriving the arrival probability with single-retransmission is presented in the following section. In general, the appearance of IFI depends on the state of packet flow over the multi-hop network. Retransmission makes packet flows more complicated, which needs more detailed classification. For quick reference, Fig. 4-10 illustrates the three cases that may take place.

When retransmission is employed, STP of hop $i-1$ between Nodes $i-1$ and i can be written as:

$$P_{Hi-1} = (P_{Ai+1} - P_{Bi+1})p_{C1} + P_{Bi+1}p_{C2} + (1 - P_{Ai+1})p_{C3}, \quad (4-16)$$

where $(P_{Ai+1} - P_{Bi+1})$, P_{Bi+1} and $(1 - P_{Ai+1})$ represent the occurrence probabilities of Cases 1, 2, and 3, respectively; p_{Cl} is the sum of STPs of the corresponding sub cases for Case l ; and P_{Bi+1} is the retransmission occurrence ratio of Node $i+1$ multiplied by P_{Ai+1} . Suppose that among the arrived packets at Node $i+1$, M packets are successfully transmitted without retransmission while R packets are retransmitted, P_{Bi+1} is defined as:

$$P_{Bi+1} = [R/(M + R)]P_{Ai+1}, \quad (4-17)$$

For hop $i-1$, P_{Bi-1} can be calculated as

$$P_{Bi-1} = (P_{Ai+1} - P_{Bi+1})p_{R1} + P_{Bi+1}p_{R2} + (1 - P_{Ai+1})p_{R3}, \quad (4-18)$$

where p_{Rl} is the sum of retransmission occurrence probabilities of the corresponding sub cases for Case l . The key to solving Equations 4-13, 4-16 and 4-18 is to obtain probabilities p_{Cl} and p_{Rl} for each case.

Case 1: Both Node $i-1$ and Node $i+1$ have packets to transmit and there's no buffered packet in Node $i+1$. There are several sub-cases that may occur depending on the success/failure states of reception.

Case 1.1: Node $i-1$ transmits a new packet to Node i and Node i correctly receives this packet. The STP of hop $i-1$ for this sub-case is given by the sum of demodulation success probabilities for demodulation modes 2 and 3. That is:

$$P_{C1.1} = P_{int} + (1 - P_{int})P_{can}. \quad (4-19)$$

Even if the new packet has been successfully received by Node i , and if Node $i-1$ cannot receive the corresponding ACK from Node i with probability of $(1-p_{nor})$, Node $i-1$ will still retransmit the packet. The retransmission occurrence probability for Case1.1 is:

$$P_{R1.1} = [P_{int} + (1 - P_{int})P_{can}](1 - P_{nor}). \quad (4-20)$$

Case 1.2: Node $i-1$ has failed to deliver the packet to Node i the first time and so buffers the packet for retransmission. The retransmission occurrence probability for Case1.2 is

$$P_{R1.2} = (1 - P_{int})(1 - P_{can}). \quad (4-21)$$

One of the two sub cases, Case 1.2.1 and Case 1.2.2, may take place if Case 1.2 has occurred.

Case 1.2.1: In the next transmission time slot, Node $i+1$ has received a new packet from Node i . This packet should be a buffered packet from Node i . The occurrence possibility of Case 1.2.1 is so small that it can be ignored without the loss of too much accuracy.

Case 1.2.2: Node $i+1$ has no packet to transmit, thus only Node $i-1$ transmits during the transmission slot. As can be proved hereinafter, the failure of IC at Node i strongly correlates with the fading gain of the channel between Node $i-1$ and Node i while it has little correlation with the channel state between Node i and Node $i+1$. Therefore it is reasonable to infer that the SNR (signal to noise ratio) at Node i was less than the SNR threshold in the previous time slot. Considering the time correlation, the corresponding STP for hop $i-1$ can be written as:

$$P_{C1.2.2} = (1 - P_{int})(1 - P_{can})\tilde{q}_{nor}. \quad (4-22)$$

Here \tilde{q}_{nor} is the conditional probability of successful transmission given that the previous transmission was not successful. The relationship between the success/failure states of current and previous transmissions under fading environments can be described as a first-order Markov chain model [47]. The transition probability matrix is given by

$$\mathbf{P} = \begin{pmatrix} \tilde{p}_{nor} & 1 - \tilde{p}_{nor} \\ \tilde{q}_{nor} & 1 - \tilde{q}_{nor} \end{pmatrix}, \quad (4-23)$$

where \tilde{p}_{nor} represents the conditional probability of successful transmission given that the previous transmission was successful. The steady-state probability that a packet transmission fails (i.e. packet error rate, PER) is denoted as p_E which is equal to $(1-p_{nor})$. Based on the property of Markov chain, p_E can be expressed as

$$p_E = p_E(1 - \tilde{q}_{nor}) + (1 - p_E)(1 - \tilde{p}_{nor}). \quad (4-24)$$

\tilde{p}_{nor} and \tilde{q}_{nor} can be derived by using the method introduced in reference [48].

Case 2: Node $i-1$ and Node $i+1$ both have packets to transmit; There's one buffered packet in Node $i+1$. The occurrence probability for Case 2 is P_{Bi+1} .

Case 2.1: Node $i-1$ transmits a new packet to Node i and Node i correctly receives this packet. The STP of hop $i-1$ for this case is given by:

$$P_{C2.1} = p_{int} + (1 - p_{int})p_{can}. \quad (4-25)$$

Similar to Case 1.1, Node $i-1$ will retransmit the packet if it fails to receive the ACK. The retransmission probability is

$$p_{R2.1} = [p_{int} + (1 - p_{int})p_{can}](1 - p_{nor}). \quad (4-26)$$

Case 2.2: Node $i-1$ has failed to transmit the packet at the first time but will retransmit

the packet during the next transmission time slot. The retransmission probability is

$$P_{R2.2} = (1 - p_{int})(1 - P_{can}). \quad (4-27)$$

Because Node $i+1$ has a buffered packet, Node i will also transmit during the next transmission slot. Similar to Case 1.2.2, STP of Case2.2 can be approximately represented as

$$P_{C2.2} = (1 - p_{int})(1 - P_{can})\tilde{q}_{nor}. \quad (4-28)$$

Case 3: Only Node $i-1$ has a packet to transmit. The occurrence probability is $(1 - P_{Ai+1})$. Due to the time correlation of the fading channel, the STP of current transmission is dependent on the transmission status held as history. Because Node $i+1$ doesn't have a packet to transmit, one of the following 3 possible cases (Case 3.1 to 3.3) has occurred. The total occurrence probability of the three cases is $(1 - P_{Ai} + P_{Bi})$.

Case 3.1: The previous packet has arrived at Node $i-1$ but not Node i (i.e. the previous packet has been lost during transmission from Node $i-1$ to Node i thus the corresponding occurrence probability is $P_{Ai-1} - P_{Ai}$). It implies that the SIR at Node i has been unsatisfactory, thus the STP of hop $i-1$ for the current transmission under Case3.1 can be expressed as:

$$P_{C3.1} = \frac{P_{Ai-1} - P_{Ai}}{1 - P_{Ai} + P_{Bi}}\tilde{q}_{nor}. \quad (4-29)$$

Case 3.2: The previous packet has arrived at Node i but not Node $i+1$. Node i has failed to transmit the previous packet to Node $i+1$ at the first time but will retransmit the packet in the next transmission time slot. The occurrence probability is P_{Bi} . Under such circumstance, it is reasonable to presume that the SIR at Node i has been satisfactory, thus the STP of hop $i-1$ for the current transmission can be expressed as:

$$P_{C3.2} = P_{Bi} / (1 - P_{Ai} + P_{Bi})\tilde{p}_{nor}, \quad (4-30)$$

Case 3.3: The previous packet has arrived at Node $i-1$, the STP of hop $i-1$ for the current transmission can be expressed as:

$$p_{C3.3} = (1 - P_{Ai-1}) / (1 - P_{Ai} + P_{Bi}) p_{nor} \cdot \quad (4-31)$$

For the Cases of 3.1 to 3.3, Node $i-1$ will retransmit if it fails to receive the ACK. Thus,

TABLE 4-1 RADIO TRANSMISSION PARAMETERS

Fading model / RF frequency	Flat Rayleigh (Jakes) / 2.4GHz
Maximum Doppler frequency	3 Hz
Noise at receiver	AWGN
Path loss model	ITU-R p.1411-6, LOS, lower bound [43]
Node interval	100 m
Transmitting power	15 dBm
Antenna height	1.5 m
Modulation	BPSK (TS in α part), QPSK (other parts)
Payload length	512 byte
Training sequence length	144 bit
Data rate	1 Mbps (α part), 2 Mbps (β and γ parts)
Normalized traffic load	1/2, 1/3, ..., 1/8
Communication period	3.082 ms
Adaptive mechanism (IFIC)	Normalized LMS (Filter length: 1)
Step size (IFIC)	0.02
Bias η in Eq.4-11 (IFIC)	0
Carrier sense level (CSMA/CA)	-81dBm

the total retransmission probability for the three cases is:

$$p_{R3.1} + p_{R3.2} + p_{R3.3} = (p_{C3.1} + p_{C3.2} + p_{C3.3}) (1 - p_{nor}) \cdot \quad (4-32)$$

Case 3.4: Node $i-1$ has failed to transmit the packet the first time but will retransmit in the next transmission time slot. Thus, the retransmission probability can be written as

$$p_{R3.4} = (1 - p_{C3.1} - p_{C3.2} - p_{C3.3}), \quad (4-33)$$

and the corresponding STP is

$$p_{C3.4} = (1 - p_{C3.1} - p_{C3.2} - p_{C3.3})\tilde{q}_{nor}. \quad (4-34)$$

Finally, by solving Equations 4-13, 4-16, and 4-18, PDR of IFIC-MHT with time-correlated retransmission is obtained.

4.5 Performance Evaluation Settings

4.5.1 Simulation Conditions

A simulation program suite by using MATLAB[®] and Simulink[®] is created. A Simulink model is created to simulate the propagation channel and the essential part of physical layer including LMS-IFIC. The MATLAB program acts as the upper-layer that controls all the actions needed to perform IFIC multi-hop transmission. MATLAB program and Simulink model work interactively every time slot. This cooperation enables the IFIC simulator to simulate the dynamic behavior among nodes, which depends on the fading and noise on each channel. For comparison, the performance of IEEE 802.11b CSMA/CA is also obtained by using the QualNet[®] network simulator. The common parameters for both simulations are listed in Table 4-1. The blank period (T_B) is adjusted as 522 μ s so that IFIC-MHT and CSMA/CA have the same T_{com} . This setting makes the airtime for IFIC-MHT and CSMA/CA identical for the same G , so that their performance can be fairly compared. In order to find out the lower bound of IFIC-MHT's performance, 1) delay τ is fixed to 522 μ s, so the β parts of two signals will completely overlap if IFI occurs; 2) channel coding is unused so that even one bit error will lead to the failure of packet reception.

The propagation channel is a 2.4 GHz flat Rayleigh channel. In this thesis, a slow fading environment is assumed where the nodes have fixed position while other objects (e.g., human beings) in the environment are moving slowly. The walking speed of

human beings is about 1m/s, which causes maximum Doppler shift f_D (maximum Doppler frequency) about 8 Hz. In this section, the maximum Doppler frequency of 3Hz is set at first to obtain the basic characteristic of IFIC and then verify the performance of IFIC with f_D from 1Hz to 25Hz. Distance between two adjacent nodes (denoted as D) is set as 100 m so the link has high reliability for 2.4GHz signals if no interference exists. The link quality significantly decreases if the distance is longer. Thus the signal transmitted from the node $3D$ or farther away has little impact on reception.

4.5.2 Optimizing the Step Size of Equalizer

The bit error rate performance with different step sizes for optimization is obtained. The result, plotted in Fig. 4-11, shows that owing to the property of NLMS, IFIC performs well under a wide range of SNR conditions when the step size is around 0.02. Therefore, a step size of 0.02 is employed. If the IFIC is used in a faster fading environment, the step size should be increased.

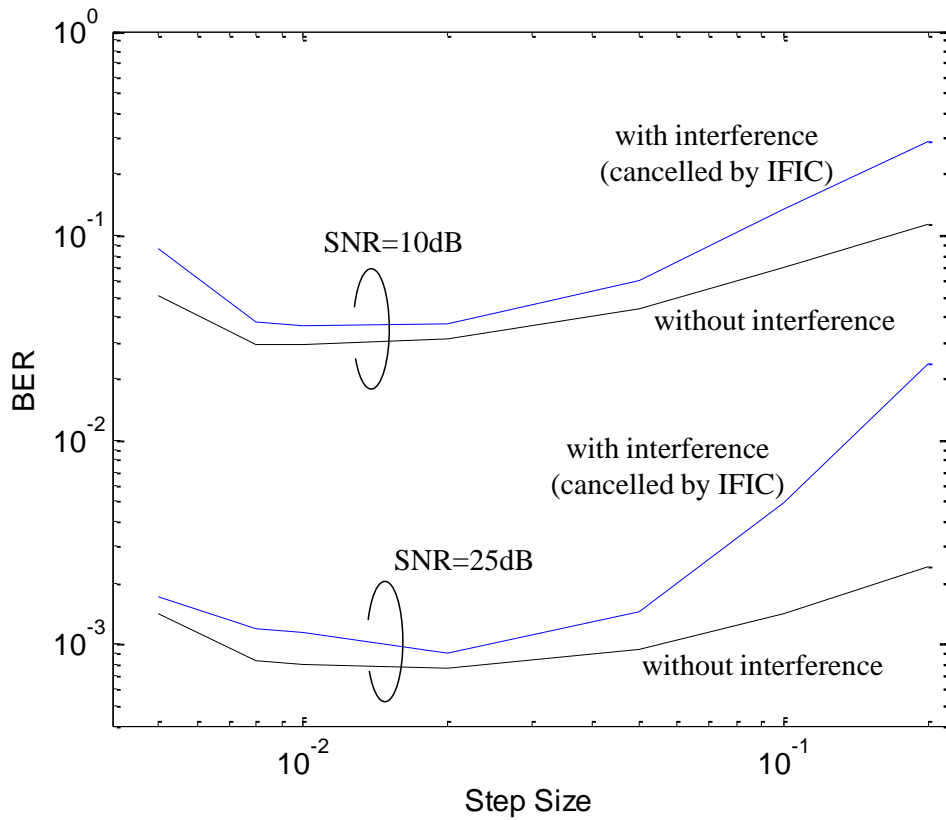


Fig. 4-11. BER performance of IFIC with different step sizes. ($f_D=3\text{Hz}$)

4.6 Performance of IFIC Multi-Hop Transmission

4.6.1 Basic Behavior of IFIC

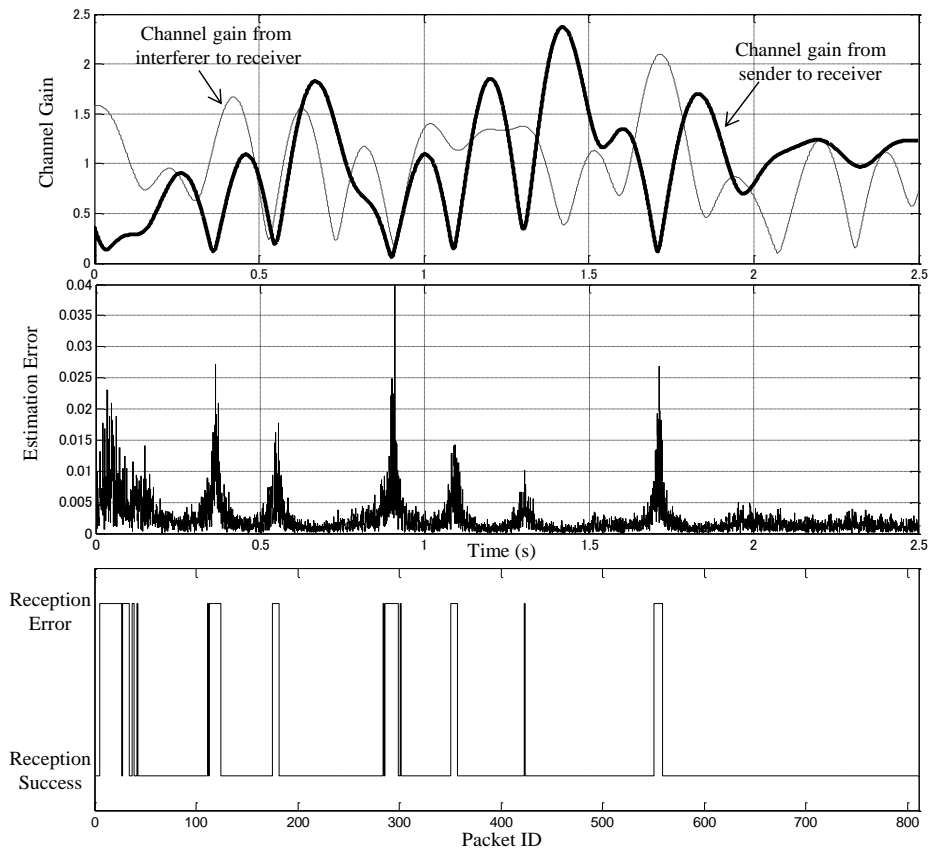


Fig. 4-12. Relationship between channel gain, LMS estimation error and packet reception error.

In order to verify the interference-canceling performance of IFIC in Rayleigh fading environments and understand its basic property, single-hop scenario with 3 nodes: Sender (Node 1), Receiver (Node 2) and Interferer (Node 3) is examined at first. Fig. 4-12 shows examples of simulation results of normalized channel gains, estimation error, and packet reception error. Both average SNR and INR (interference to noise ratio) at the receiver are 23 dB, which corresponds to the link distance of 100 m. The figure shows that the estimation error is strongly correlated with the channel gain from sender to receiver but little correlation with the gain from interferer to receiver. Another

phenomenon observed is that only large estimation error for desired signal due to deep fade causes packet reception failure. This impacts the error tolerance capability of the modulation scheme.

4.6.2 Further Performance Improvement by Combining IFIC with MRC

As described above, reception error takes place when the channel experiences deep fade. This problem can be offset by diversity techniques. In this chapter, 2-branch MRC is adopted. In Fig. 4-13, the antenna space can be set 0.2 times of wavelength or wider, so that the cross-correlation of two antenna outputs is less than 0.5 in scattered multi-path environment. It has been proved that this condition is enough for obtaining sufficient diversity gain [51]. Equalizers used for IC can provide the phase information for the MRC combiners to enable co-phasing. To make the discussion concise and focused, it is assumed that Nodes 1 and 2 use only 1 antenna during transmission. With the help of MRC diversity, the reception error only occurs when h_{12} and h'_{12} suffer deep fading at the same time. The weight assigned for each MRC branch is the square root of averaged signal power after IC at the corresponding branch.

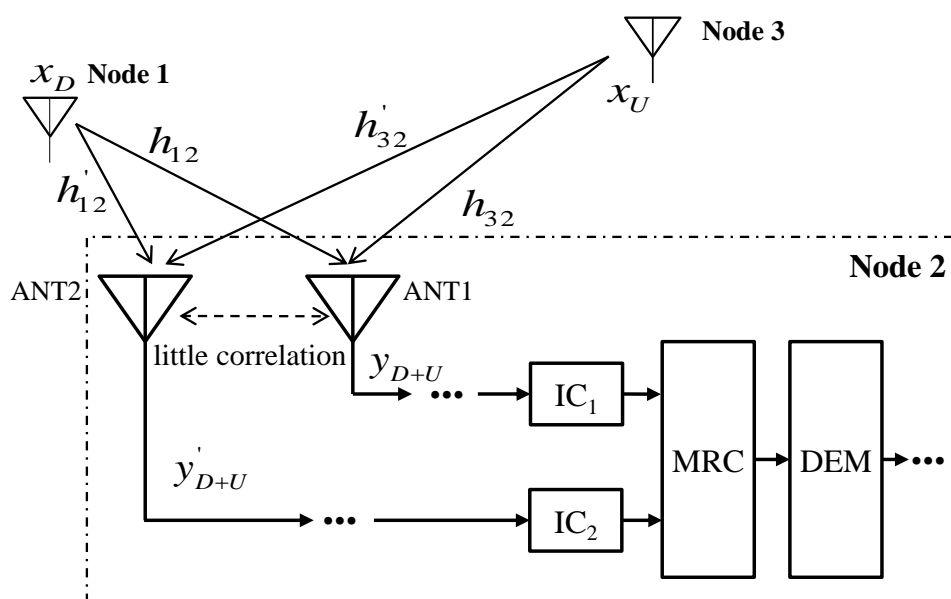


Fig. 4-13. Two-branch IFIC-MRC receiver.

MRC can also be carried out before performing IC as shown in Fig. 4-14. Since the TSs of signals are not interfered, MRC weights can be determined from independently measured desired and undesired signals. When MRC combiner co-phases the desired signals, the phases of interfering signals (i.e. U and U') are also shifted accordingly. Therefore, it is necessary to consider the phase shift during IC. There are two methods to determine the weights for MRC branches. The first method (*MRC-IFIC Method 1*) is to measure the square root of averaged signal power for desired signal; another method (*MRC-IFIC Method 2*) is to measure the square root of averaged combined signal power at every input of MRC combiner.

There have been many studies that use multiple antennas to remove interferences not by interference canceller but interference alignment [33][49]-[52]. In this thesis, multiple antennas are used only for suppressing the fading effect. Discussion on the method that uses multiple antennas for interference alignment is beyond the scope of this thesis.

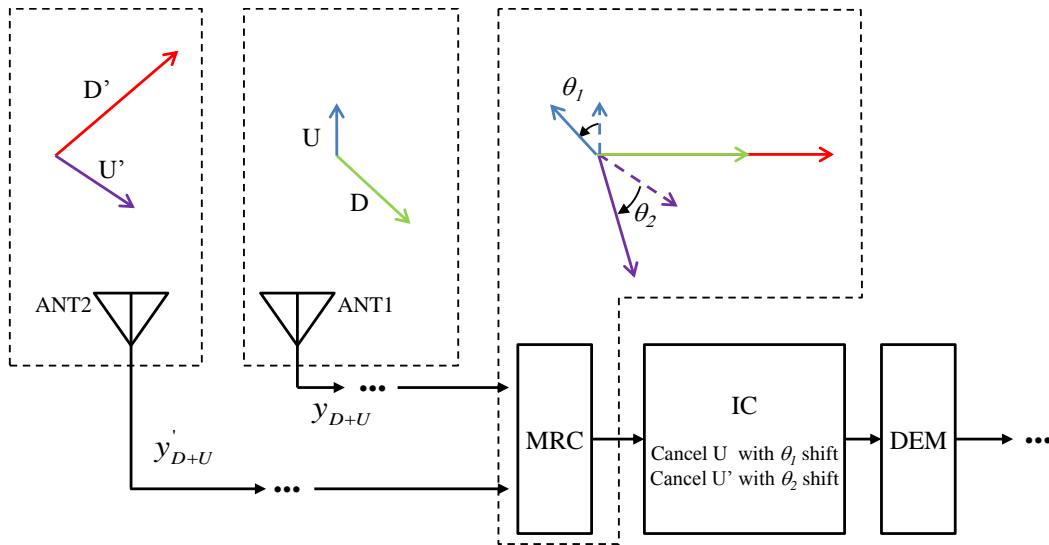


Fig. 4-14. Two-branch MRC-IFIC receiver.

4.6.3 Basic BER/PER Performance of IFIC and IFIC-MRC

BER/PER performance of IFIC for the single-hop scenario under fading environment is investigated by simulation. In this section, noise and interfering signal power at the receiver are fixed as -91dBm and -68dBm, respectively, so that INR is

always 23dB. And the desired signal power at receiver is changed to obtain different SNR conditions. The settings of SNR and INR are illustrated in Fig. 4-15.

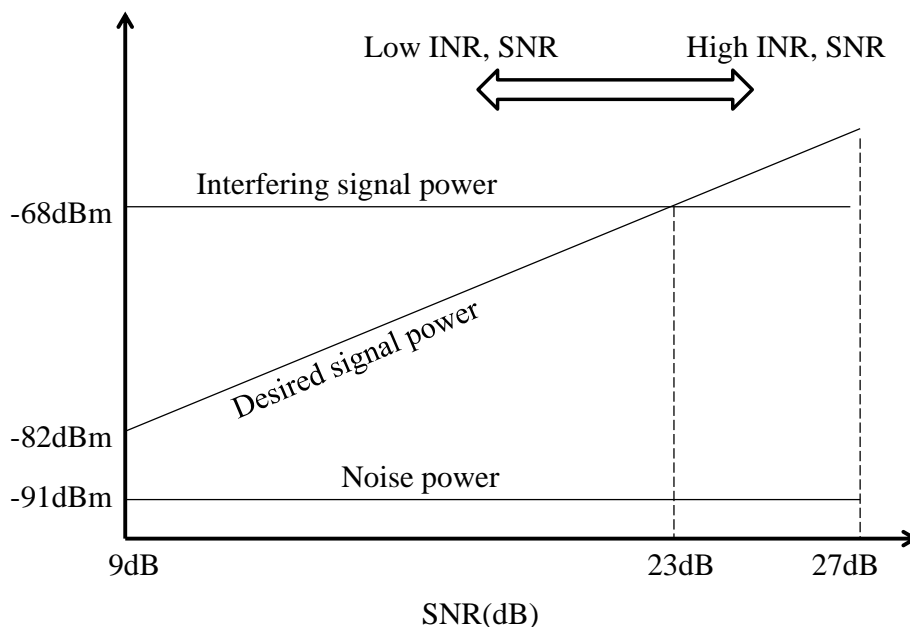


Fig. 4-15. Settings of SNR and INR.

The performance with the single antenna arrangement is shown in Fig.4-16. In the figure, PER without IFIC is always higher than 35%, which is unacceptable if the target is multi-hop transmission. On the other hand, BER/PER with IFIC are very close to their lower bounds (i.e. BER/PER without interference). This proves that IFIC can efficiently cancel the interference in a wide range of SNR as well as SIR.

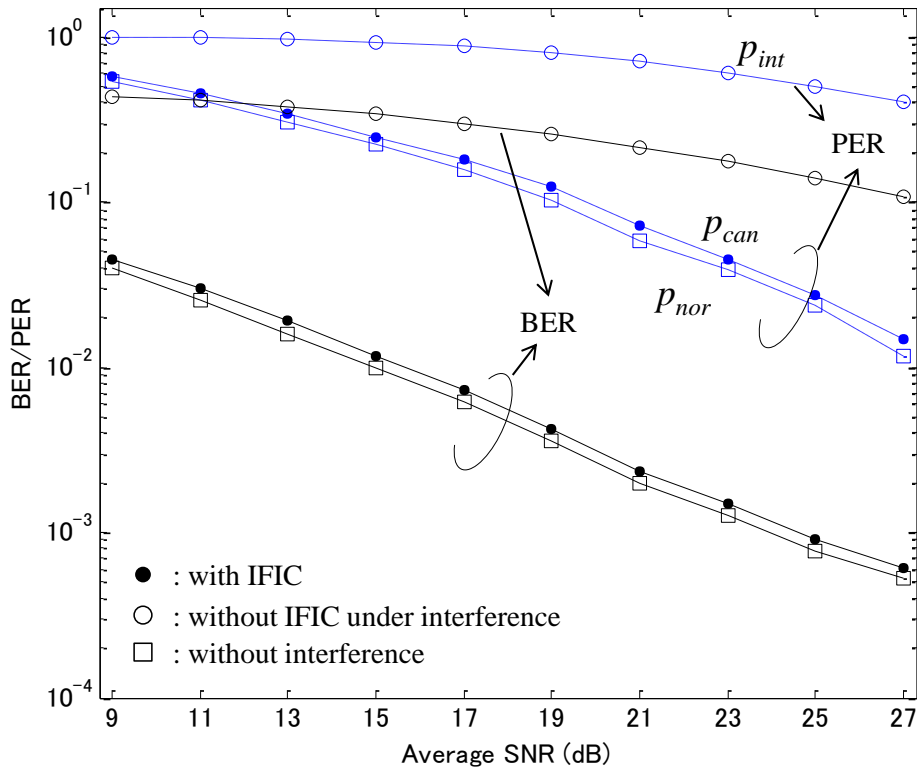


Fig. 4-16. BER/PER performance of IFIC with single-antenna receivers for single-hop scenario.

Figure 4-17 gives the comparison of BER/PER performance for different combinations of IFIC and MRC. All combinations of IFIC and MRC gain BER/PER improvement. When MRC is performed before IC (Fig. 4-14), MRC-IFIC Method-1 provides the same BER/PER as that of IFIC-MRC. Meanwhile, for MRC-IFIC Method-2, the BER/PER performance will experience degradation around 1dB compared with IFIC-MRC. For MRC-IFIC Method-2, the branch with a higher (S+I)/N will be weighted more based on the MRC principle. If the average power of interference signal is comparable to that of the desired signal and has little correlation with it, the MRC cannot be optimal for the desired signal and the diversity gain decreases. Consequently, the IFIC-MRC structure is used in the following simulations.

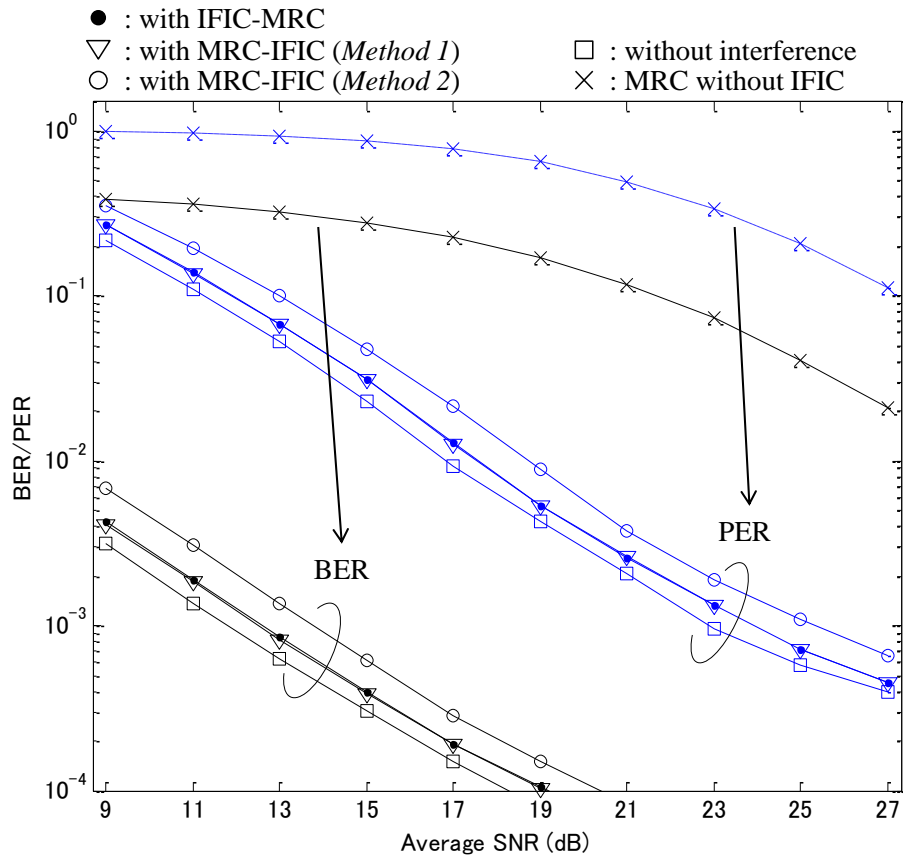


Fig. 4-17. BER/PER performances of different combinations of IFIC and MRC with 2-antenna receivers for single-hop scenario..

By comparing Figs. 4-16 and 4-17, it is found that the BER/PER of IFIC-MRC is lower than the corresponding BER/PER of IFIC without MRC, and IFIC-MRC can accept lower SNR. For instance, IFIC needs 19dB SNR for 10% PER, whereas 12dB (-11dB SIR) is enough if cooperating with MRC. The SNR-PER relationship when no interference presents can be interpreted as the metric indicating the lowest SNR required for achieving a specific PER value. Fig. 4-16 and Fig. 4-17 show that using IFIC or IFIC-MRC demands only 1 dB additional SNR to cancel the interference.

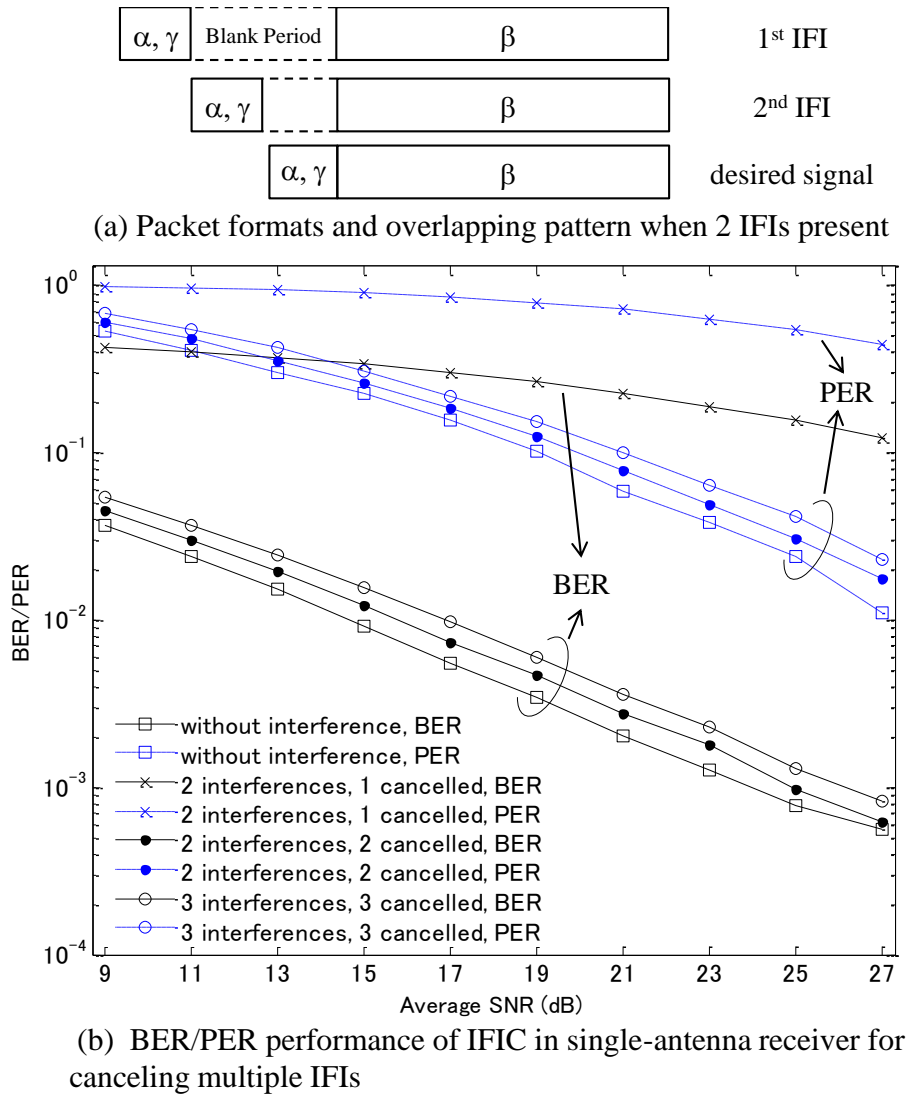


Fig. 4-18. BER/PER performance of IFIC with single antenna for canceling multiple IFIs.

Figure 4-18 gives the BER/PER performances when 2 or 3 interference signals appear simultaneously. The SNR for both IFIs are 23dB. Fig. 4-18 (a) provides an example of assigning packet formats when 2 IFIs present. Fig. 4-18 (b) proves that IFIC is capable of canceling multiple interference signals with small performance loss. In Section 4-7, the scenario that requires canceling multiple known interferences will be introduced.

Since the proposed IC process is independent of the modulation scheme and is carried out before demodulation, it is predicable that more complex modulation schemes

such as QAM and OFDM can also be used for β and γ parts. Fig. 4-19 proves this predication by plotting the BER/PER performance of IFIC when 16QAM or 64QAM is employed. It also implies that higher order modulation requires extra SNR for performing IC.

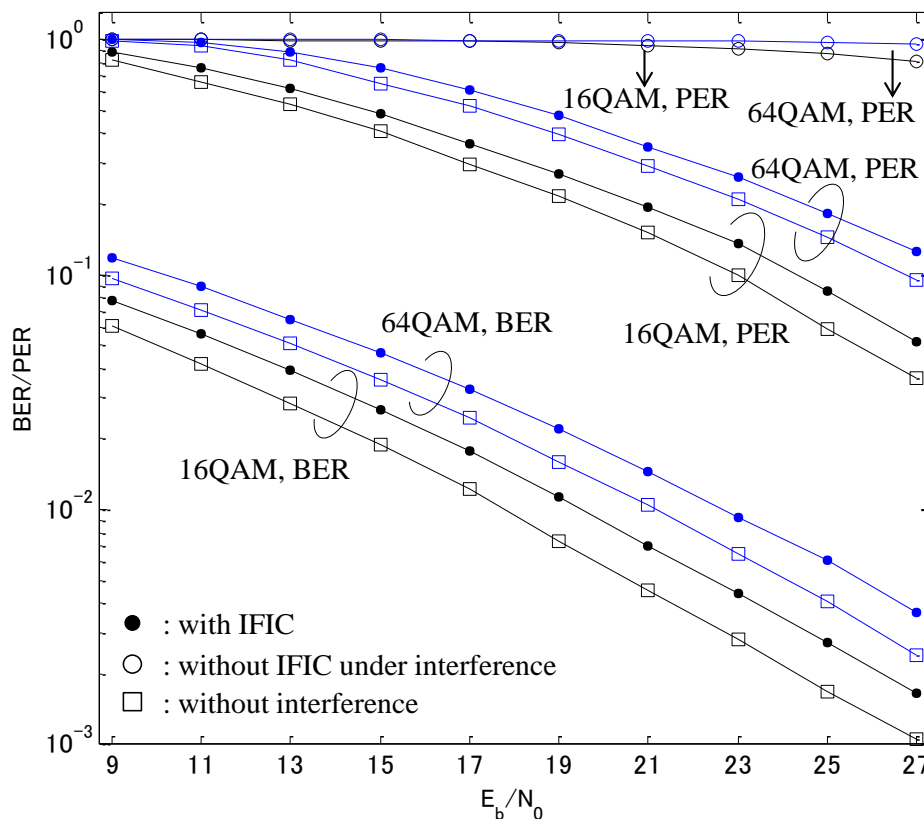


Fig. 4-19. BER/PER performance of IFIC for QAM signals.

For OFDM signal employed in IEEE 802.11series, its waveform varies according to the protocols (i.e., 802.11a, 802.11g etc.) as well as the operation mode [53]. For instance, 802.11g can work at normal OFDM mode or CCK-OFDM hybrid mode. CCK-OFDM is designed to make 802.11g compatible with 802.11b (which is referred in the simulation of this chapter). For CCK-OFDM mode, the PLCP (physical layer convergence protocol) preamble and PLCP header (i.e., in α part) are modulated by DBPSK at 1Mbps (single carrier) and the payload part (i.e., β and γ parts) is modulated by OFDM (multicarrier).

A simulation is conducted to implement IFIC with OFDM referring IEEE 802.11g CCK-OFDM operation mode. The block diagram for transmitting and receiving is

shown in Fig. 4-20. As shown in this figure, IC is performed transparently to the OFDM modulation/demodulation. The propagation channel is set as 2-path Rayleigh fading channel so that the performance at frequency selective channel is verified. The constellation diagrams for a 16QAM signal at a subcarrier are shown in Fig.4-21. The results prove that IFIC is able to cancel interference in OFDM system and improve the reception performance. (The equalization performed at each subcarrier in frequency domain is not implemented.)

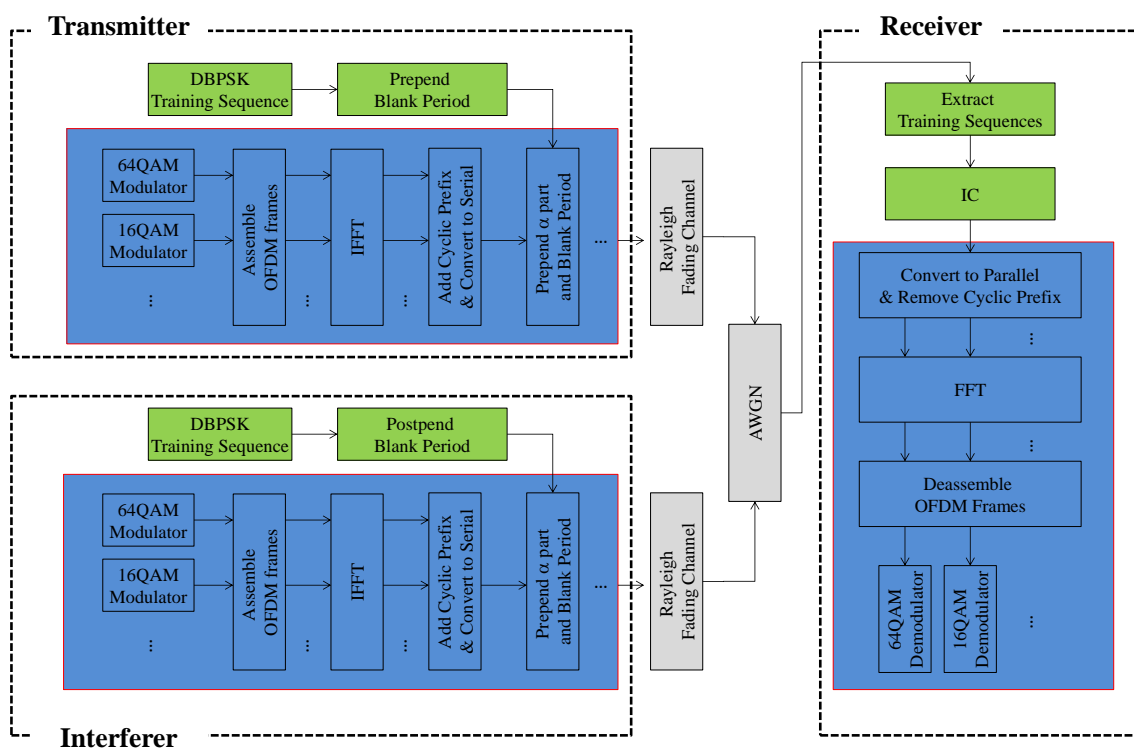
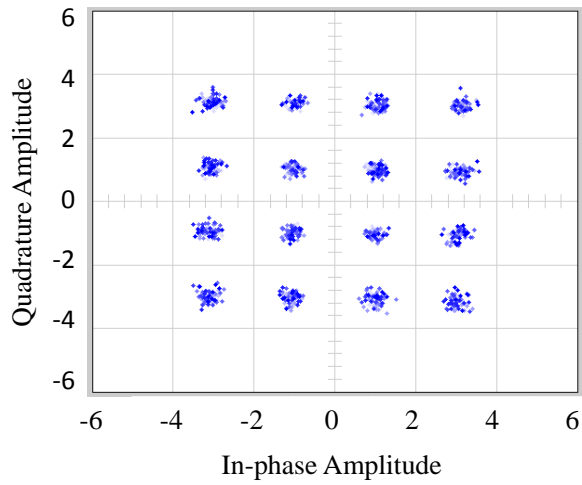
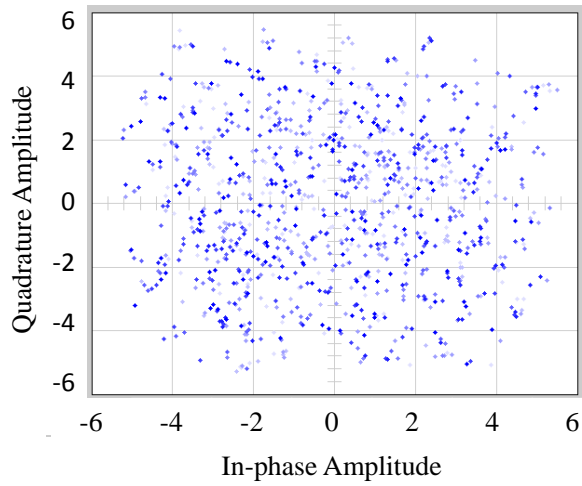


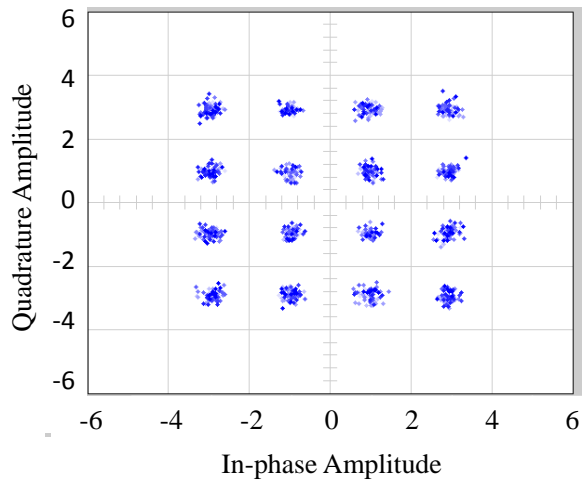
Fig. 4-20. Block diagram of OFDM transmitters and receiver with IFIC.



(a) Desired signal received without interference



(b) Desired signal received without IFIC under interference



(c) Desired signal received with IFIC under interference

Fig. 4-21. A group of snapshots that record the constellations of desired signal at receiver. (16QAM in OFDM subcarrier)

4.6.4 Performance of 5-Hop IFIC-MHT without Retransmission

To evaluate the multi-hop transmission performance of IFIC-MHT, another scenario where packets are delivered via 5 hop links is assumed. The 6 nodes are one-dimensionally arranged with constant interval of 100 m, therefore average SNR and SIR for each link are 23 dB and 0 dB, respectively. The arrival probabilities and PDR

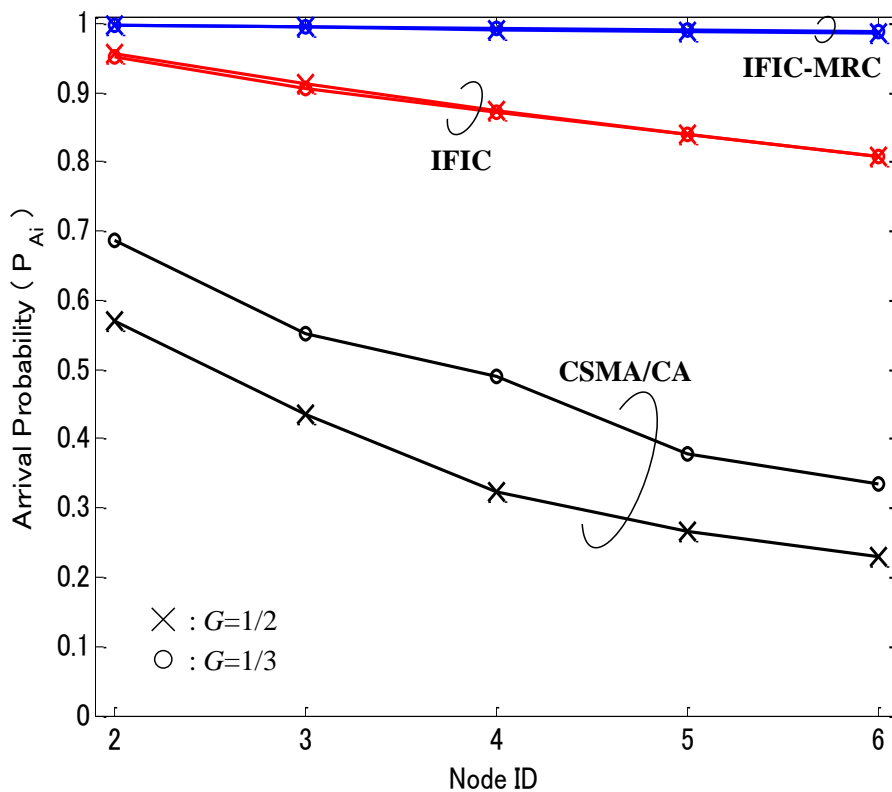


Fig. 4-22. Arrival probabilities of IFIC-MHT and CSMA/CA for 5-hop network.

when G is 1/2 or 1/3 are shown in Fig. 4-22. For comparison, the results of IEEE 802.11b CSMA/CA simulated under the same condition are included. Obviously, IFIC-MHT has superior performance compared to CSMA/CA. For the case of CSMA/CA and G is 1/2, 43% of packets are dropped before they reach the first relay node (Node 2) due to IFI caused by hidden terminal. For IFIC-MHT, the probability of successful transmission of each hop, p_H , stays at 95% with IFIC and even higher if MRC is combined. Thus, packets can be delivered with high probability to the end node. The IFIC-MHT network can deliver 60% more packets with IFIC and 75% more

packets with IFIC-MRC than CSMA/CA. Fig. 4-23 gives the occurrence ratio of each demodulation mode (introduced in Section IV-C) to the arrival probability. It clearly proves that IFI cancellation greatly improves the arrival probabilities

at Nodes 2, 3, and 4 which suffer most from IFI in a 5-hop network because 70% of the successfully arrived packets are received under Demodulation Mode 3 (i.e. by IFIC).

In Fig.4-22, arrival probabilities and PDR for CSMA/CA increase when G is lowered to $1/3$. This is because signal power of IFI becomes weaker due larger path loss (as shown in Fig. 4-1). Nevertheless, they are still much lower than that of the proposed scheme. Meanwhile, the results for IFIC-MHT indicate that IFIC-MHT has steady packet transmission performance for variable traffic loads.

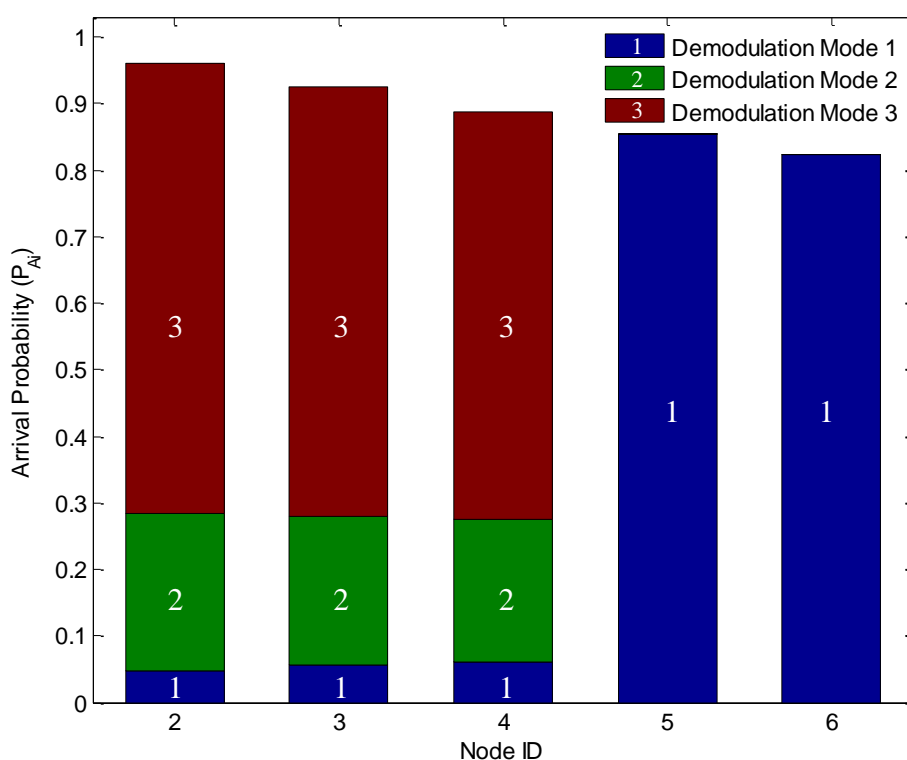


Fig. 4-23. Occurrence ratios of three demodulation modes to Arrival probabilities.

In Fig. 4-24, the simulation results of throughputs S defined by Eq. 4-15 for the two schemes are compared under different traffic load conditions. IFIC-MHT has superior throughput compared with CSMA/CA regardless of G . Specifically:

- The theoretically maximum throughput is obtained if all packets are delivered to the end node without retransmission. As shown in the figure, if the radio environment is fading-free (only thermal noise exists), IFIC achieves this upper bound. When fading is present, IFIC with MRC approaches this maximum.
- IFIC-MHT and CSMA/CA have comparable performance when G is lower than $1/5$ regardless of the fading condition. As G increases, CSMA/CA suffers from IFI and throughput decreases. The highest throughput that CSMA/CA can achieve is around 200 kbps at $G=1/5$. On the other hand, the throughput of IFIC-MHT increases linearly with G . When G is $1/2$, IFIC-MHT provides throughput of 554 kbps without MRC and 665 kbps with MRC. They are 82% and 98% of the theoretical maximum, respectively, whereas CSMA/CA offers only 23%.

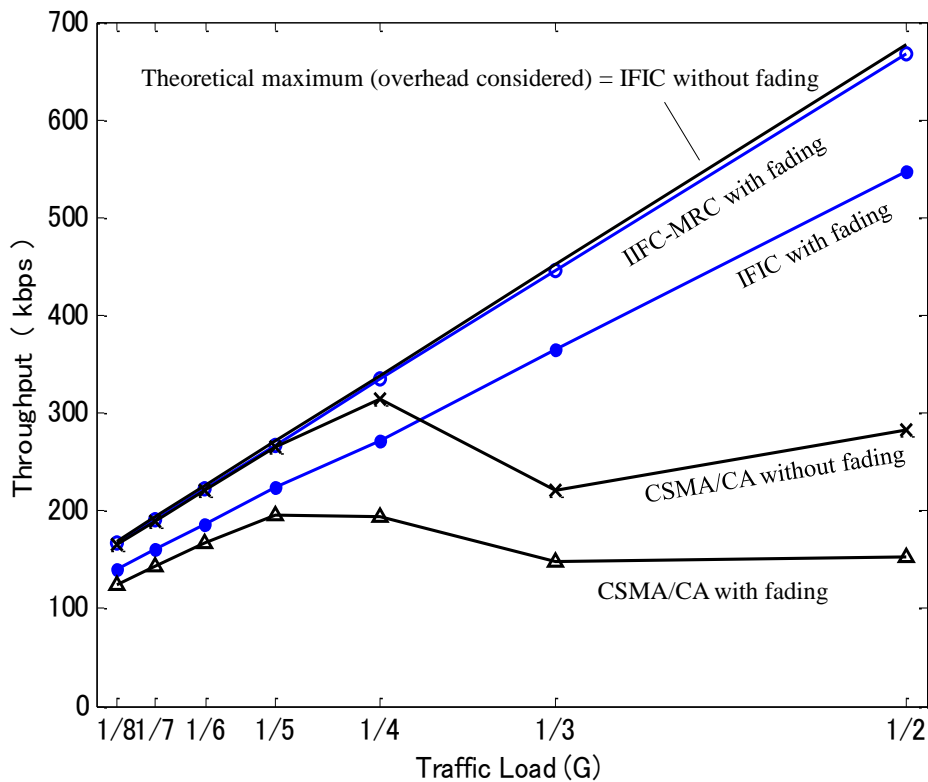


Fig. 4-24. Throughput for 5-hop IFIC-MHT and CSMA /CA under different traffic loads G .

4.6.5 Performance of 5-Hop IFIC-MHT with Retransmission

4.6.5.1 Relationship between Arrival Probability and Retransmission

The arrival probabilities calculated by using the analysis mode created in Section V are shown in Fig. 4-25. The basic interference cancellation performance of IFIC: p_{int} , p_{nor} and p_{can} presented in Section VII-C are referred for the calculation. For validation, the results obtained by Monte-Carlo simulations are also plotted. As shown by this figure, the analysis model can well describe the arrival probabilities. The probability of successful transmission in each hop, p_H , is around 95% without retransmission while using single retransmission gains an additional 3%. This 3% gain accumulates hop by hop, so that PDR at the end node can be improved by 10%.

By using the analysis model, The ideal single-retransmission performance can be estimated by simply letting \tilde{q}_{nor} as well as \tilde{p}_{nor} equal p_{nor} , that is, the success/failure states of the receptions of successive packets are uncorrelated. The result is also plotted in this figure.

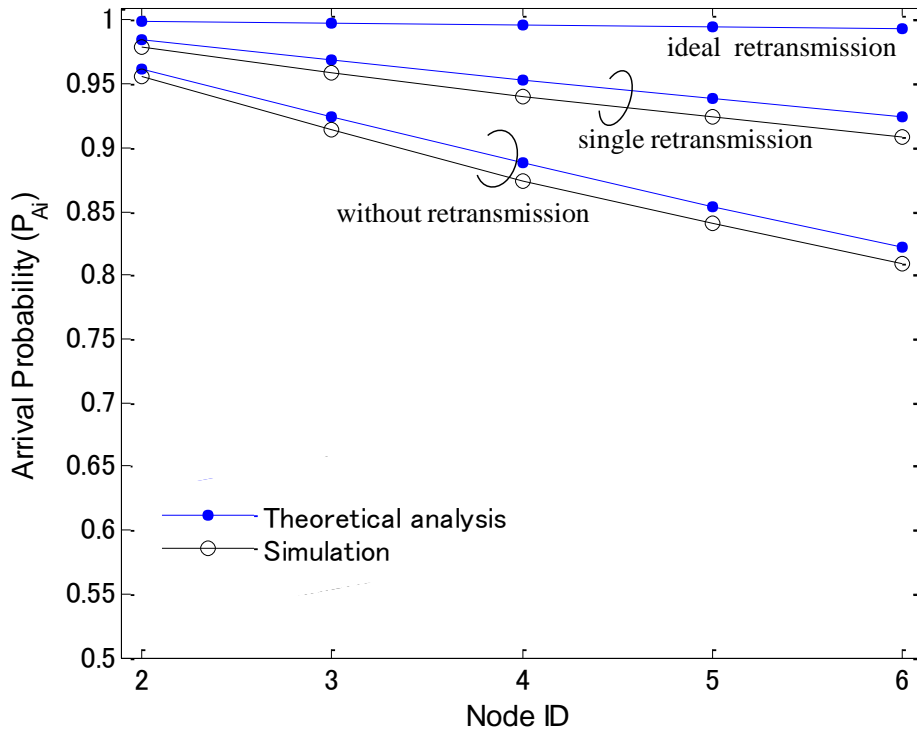


Fig. 4-25. Arrival probabilities of 5-hop IFIC-MHT with or without retransmission (SNR=23 dB, SIR=0 dB, $G=1/2$).

4.6.5.2 Relationship between Throughput, Doppler Frequency and Number of Retransmissions

The relationship between throughput, Doppler frequency f_D and number of retransmissions is important but also complex. Fig. 4-26 shows the simulated throughputs for different combinations of Doppler frequency and maximum number of retransmissions. The normalized traffic load is 1/2 and the retransmission interval is 6.164ms. When Doppler frequency increases, it becomes difficult for the equalizer to track the channel and large estimation errors will occur more frequently, resulting in packet transmission error and decrease of throughput. On the other hand, the retransmitted signals on the same channel become decorrelated with the initial transmission, yielding time diversity gain. Then packet error is recovered and the throughput can be improved by retransmission. In other words, retransmission is effective in improving the throughput of channels whose state varies faster. For instance, the throughput increases 40% with single retransmission when f_D is 25Hz while the

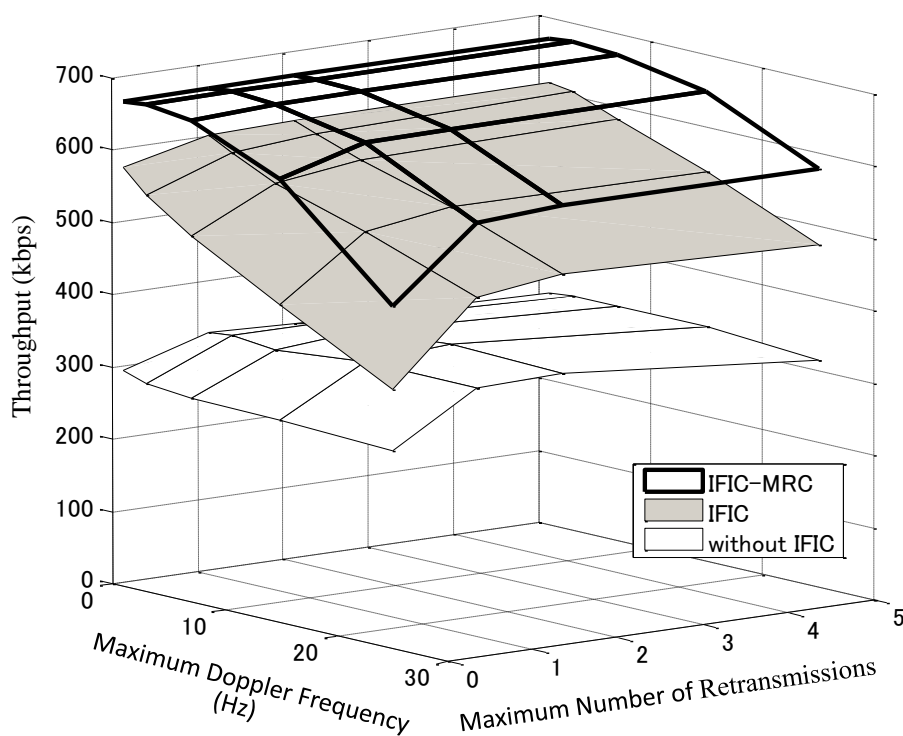


Fig. 4-26. Throughput of 5-hop IFIC-MHT with a variety of maximum Doppler frequencies and maximum number of retransmissions (SNR=23 dB, SIR=0 dB, $G=1/2$).

improvement is about 5% when f_D is 1Hz. The performance can be further improved by adding MRC. For comparison, throughputs without IFIC are also shown in Fig. 4-26. The results prove that IFIC-MHT is always effective to improve the system performance in slow fading environment.

4.7 Consideration for Multiple IFIs

In many scenarios, there are multiple interferences that take place simultaneously. Therefore, a natural question comes: how does IFIC-MHT perform with multiple IFIs. Depending on node layout or node topology, IFIC-MHT uses different strategies. In Section 4.7.1, Zigzag Node layout is considered where IFIs have different signal power and only one of them is influential that should be cancelled. In section 4.7.1, branch topologies are assumed where the interferences have comparable signal power.

4.7.1 Zigzag Node Layout

Linear (one-dimensional) node layout in the previous sections has been the focus of discussion because it is a basic example in which IFI most seriously restricts the performance of multi-hop transmission. In addition, the IFIC-MHT scheme can adapt to other node layouts and topologies and effectively improve the performance.

Figure 4-27 shows the zigzag multi-hop transmission scenario where G is equal to $1/2$. As shown in this figure, Node $i-3$, Node $i-1$ and Node $i+1$ are transmitting during the same time slot. Let Link $i-3$ from Node $i-3$ to Node $i-2$ be the concerned link. Different from the linear node layout, the signal from Node $i+1$ has considerable average power at the receiver, Node $i-2$, because the distance between Node $i+1$ and Node $i-2$ is shorter than that in the linear node layout. The backward interferences from Node $i-1$ and Node $i+1$ are known IFIs that can be cancelled by IFIC if the INR at the receiver is strong enough. In order to cancel the two backward interferences,

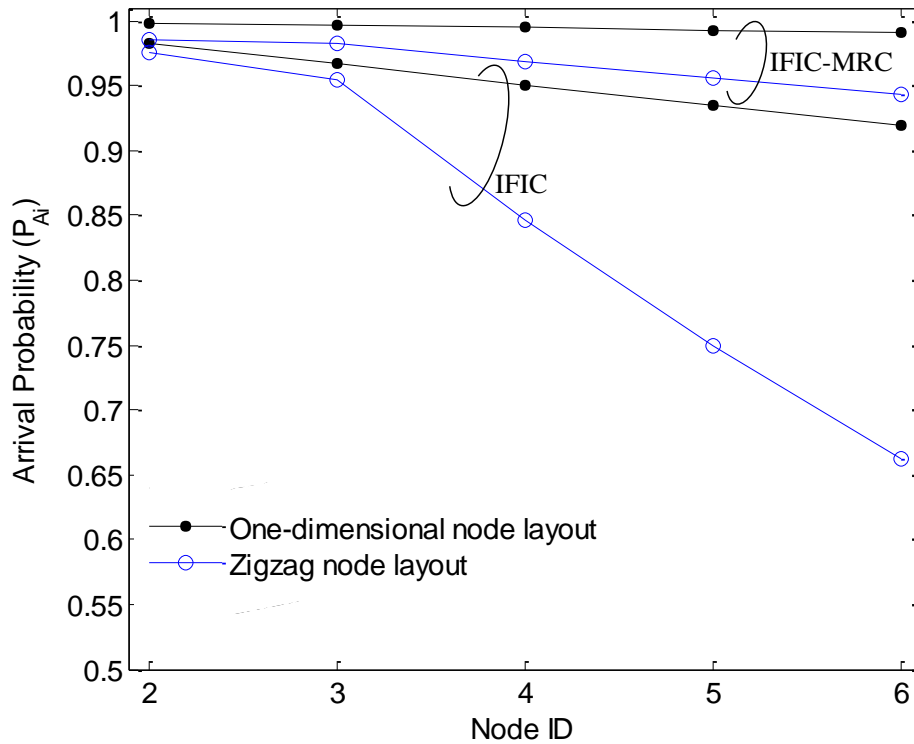


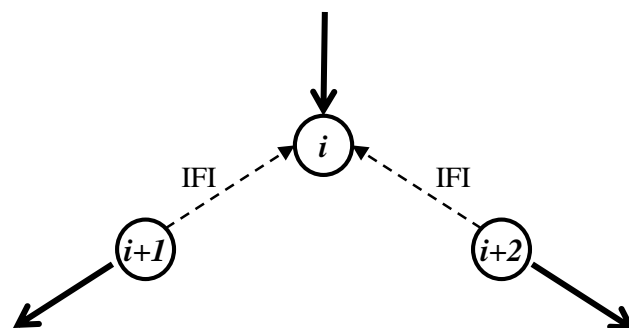
Fig. 4-28. Arrival probabilities of 5-hop IFIC-MHT with zigzag node layout (single retransmission).

1/2 and single retransmission is performed. Angle θ of Fig. 4-28 is set to 90° . It can be found that the third and further hops degrade more rapidly than the first two hops for zigzag node layout. This is because that these hops may be simultaneously interfered not only by known IFI but also by unknown IFI generated by the upstream node. However, by combining IFIC with MRC, the hops still have more than 95% link STP even under this severe condition. Although the first hop may be affected by two known interference signals with high possibility, STP of this hop is still higher than 95% because IFIC is able to cancel multiple IFIs.

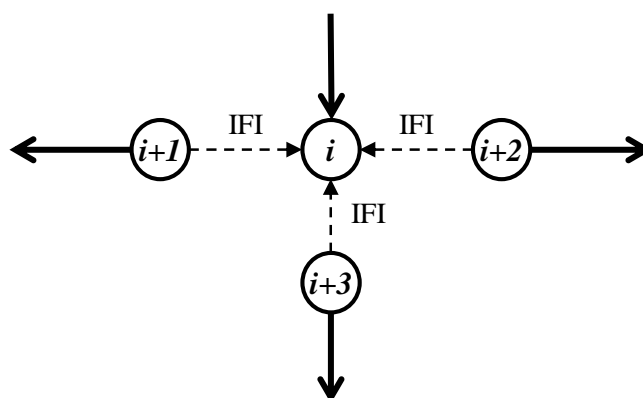
4.7.2 Branch Topologies

Branch topologies are other examples that require multiple IFIs. As shown in Fig. 4-29(a), the data packet transmitted to Node i will be further forwarded to Node $i+1$ and Node $i+2$. Then it is possible that Node $i+1$ and Node $i+2$ will simultaneously cause known IFIs at Node i . In Fig. 4-29(b), the reception is interfered by 3 IFIs. In contrast to zigzag node layout, the signal power every IFI is comparable to that of desired signal.

Therefore, cancelling multiple IFIs is necessary. Fig. 4-18 has proved that IFIC is capable of canceling multiple IFIs.



(a) 2-Branch Topology



(b) 3-Branch Topology

Fig. 4-29. IFIs in Branch Topology

4.8 Intra-Flow Interference Cancellation in Large-Scale Ad Hoc Network

For the case of multi-hop ad hoc network where numbers of nodes are two-dimensionally distributed and packets flow along multiple routes, the network performance will be affected not only by intra-flow interference but also by inter-flow interference. In most scenarios where node or traffic density is not high, the influence of intra-flow interference is dominant compared with that of inter-flow interference. This is because the former always takes place near the receiver as long as multi-hop transmission is being conducted, while the latter occurs farther, occasionally and temporally. Therefore, using IFIC-MHT to eliminate the effect of intra-flow interference

will be still an effective approach for such scenarios. To further alleviate the effect made by inter-flow interference, CSMA/CA is combined with IFIC in this section.

4.8.1 Modeling for Large-Scale Ad Hoc Network

4.8.1.1 Node Layout and Traffic Generation Model

Consider a large-scale network where node distribution obeys Poisson Point Process (PPP) as illustrated in Fig. 4-30, if carrier sense media access control is used, as shown in this figure, the distribution of transmitting nodes can be described as Matérn hard-core process [54]. In this model, no other transmitter can exist within a range defined by carrier sense range. If network becomes dense, the layout of transmitters becomes a lattice due to the sphere packing and thus the distance between neighboring nodes approaches to the same. Therefore, it is possible to use the model in Fig. 4-31 to study on the large-scale ad hoc network.

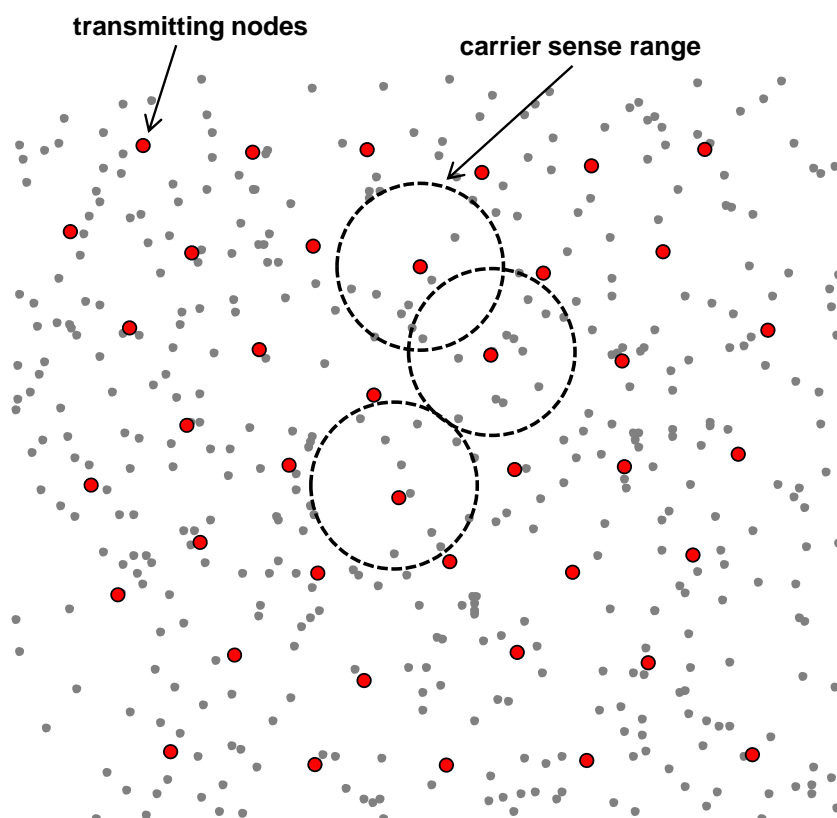


Fig. 4-30. Ad hoc network with nodes (grey and red dots) follow Poisson Point Process. The transmitting nodes (red dots) obey hard-core process.

As shown in Fig. 4-31 N nodes are uniformly distributed in an area where the distance between neighboring nodes is D m. All of the nodes can generate packets as source nodes, pass on packets as relay nodes and receive packets as end nodes. A node generates bit data with the generation interval t_G satisfies exponential distribution with mean of T_G (i.e. the number of generations satisfies Poisson Distribution.). The generated bit data needs to be packaged in M packets and the latter will be sent relayed over K hops with fixed transmission time interval T_{int} . The transmission time interval T_{int} is expressed as

$$T_{int} = 2(T_{DP} + SIFS + T_{ACK} + DIFS + T_{BO}) \quad (4-34)$$

where T_{DP} and T_{ACK} respectively represent the time for transmitting a data packet and an ACK packet. T_{BO} is the average time for performing initial backoff. The multiplier 2 in this equation guarantees that nodes have enough time to receive and then forward one packet (in multi-hop transmission with nodes working at half-duplex mode). The relationship between t_G , T_G and T_{int} is illustrated in Fig.4-32. In order to quantify the overall density of generated traffic, traffic load H is defined by the following equation:

$$H = \frac{NMKT_{int}}{T_G} \quad (4-35)$$

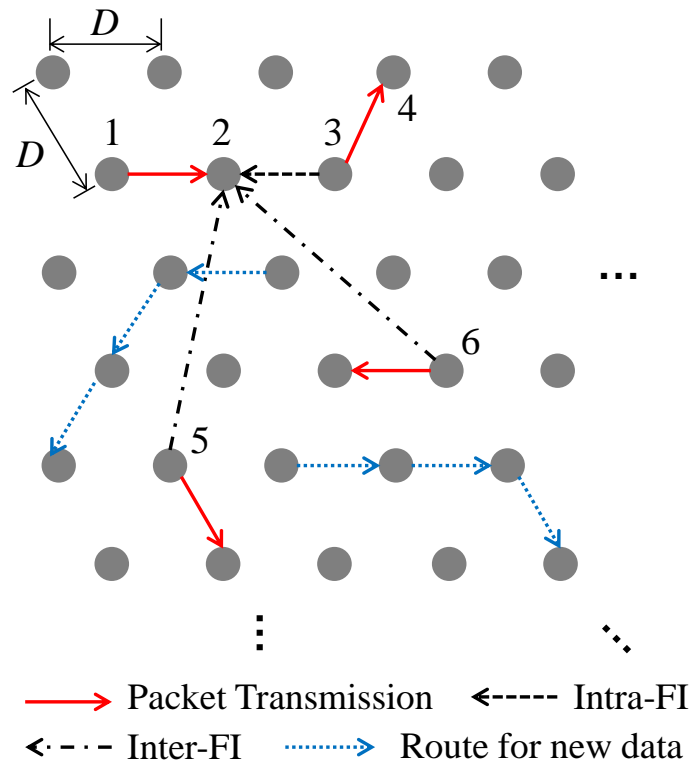


Fig. 4-31. Node layout, routes and interferences at Node 2.

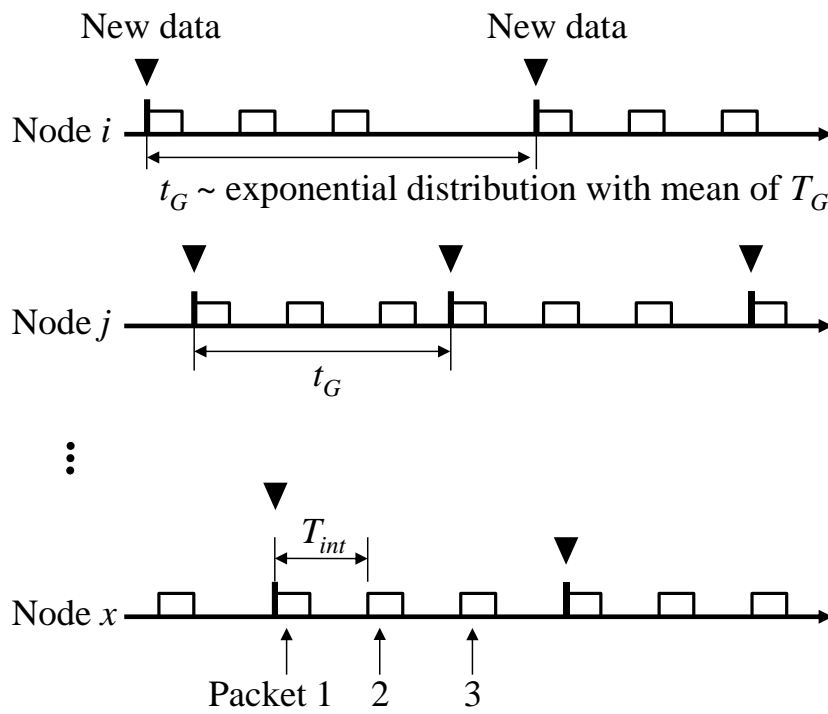


Fig. 4-32. Data traffic model. ($M=3$)

4.8.1.2 Topology: Random Pair Model

Random pair is a classical analysis model used for studying the behavior of ad hoc network. In this model, the pair of sources node and end node, as well as the corresponding route, is created temporarily and randomly. It can be used to describe the scenario where a source node has multiple possible destination nodes. In order to avoid introducing too many elements and to accurately measure the multi-hop packet delivery ratio, route tables are predefined in simulation (multiple candidates routes are available and one will be randomly chosen) and the destination node is always K hops away from the corresponding source node. The dashed lines (blue) shown in Fig. 4-31 illustrate the route that is chosen when new data is generated so that M packets will be continuously forwarded over this route. This figure also gives a snapshot that shows the communication between Node 1 and Node 2 is being interfered by intra-flow interference and inter-flow interferences. Node 3, 5 and 6 are transmitting simultaneously because they are mutually out of their carrier sense areas. Meanwhile, at Node2, the intra-flow interference from Node 3 is much stronger compared with the inter-flow interferences from Node 5 and 6. Furthermore, because multiple packets will be relayed over the same route, the reception at Node 2 will be continuously affected by the same intra-flow interference that contains the packet that Node 2 previously transmitted. In other words, intra-flow interference is influential, known and predictable.

4.8.2 Implementation of IFIC-MHT for Large-Scale Ad-Hoc Network

With small modification, the proposed IFIC-MHT scheme can be used in large-scale ad hoc network without the need of additional packet formats or global synchronization. Specifically, the modification is to let the transmitting node perform carrier sense (CS) to avoid collision with the inter-flow interferences that takes place near the receiver. If interference is detected, the transmission will be delayed to the next corresponding transmission time slot. The transmitting/receiving process and backoff process are respectively shown in Fig. 4-33 and Fig. 4-34.

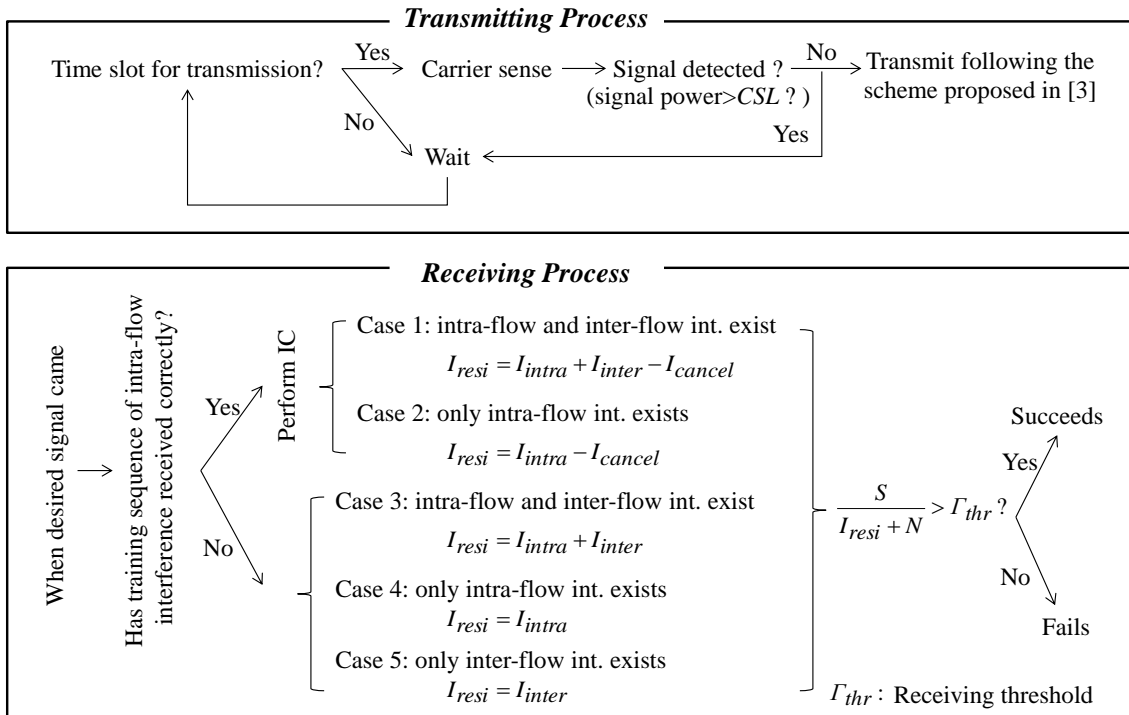


Fig. 4-33. Transmitting and receiving process for implementing intra-flow IC in ad hoc network.

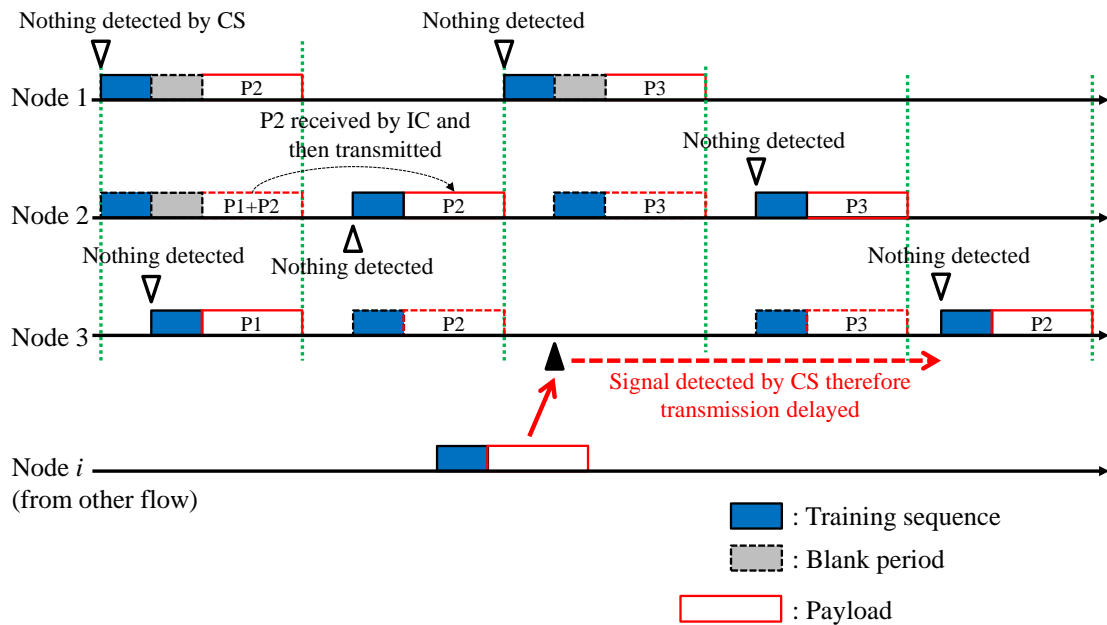


Fig. 4-34. IFIC-MHT with CSMA/CA backoff mechanism.

4.8.3 Simulation and Discussion

In this section, the global PDR that indicates the reliability of multi-hop transmission is obtained. It is defined as the proportion of received packets at end nodes to the total transmitted packets at source nodes. The PDRs corresponding to the simulations of CSMA/CA ad hoc network with and without intra-flow IC are compared for revealing the effect of intra-flow IC. In the simulation where intra-flow IC is implemented, when intra-flow interference occurs due to HT, the power of intra-flow interference will not be counted into the calculation of SINR. This approach avoids introducing influential factors that highly depend on the settings of interference canceller. The simulation parameters are shown in Table 4-2.

TABLE 4-2 Simulation Parameters

Number of Nodes in Ad hoc Network, N	100						
Node Interval, D	100 m						
Number of Hops, K	3			5			
Payload Size	1500 byte						
Data Rate	1M bps for header, 11M bps for payload						
Time for Transmitting Data Packet, T_{DP}	1324 μ s						
Time for Transmitting ACK Packet, T_{ACK}	202 μ s						
SIFS ,DIFS	10 μ s for SIFS, 50 μ s for DIFS						
Average Time of Initial Backoff, T_{BO}	310 μ s						
Number of Data Packets for Each Data, M	10						
Traffic Load, H	0.25	1	4	16	64	128	256
Carrier Sense Level, CSL	-87dBm		-77dBm		-67dBm		
Transmission Power	15 dBm						
Path Loss Model	ITU-R p.1411-6, LOS, lower bound [5]						
Fading model	Flat Rayleigh						
Maximum Doppler Frequency	3 Hz						
Receiving SINR Threshold	3 dB						
Thermal Noise Power	-91 dBm						

The global PDRs for CSMA/CA and CSMA/CA-IC networks with a variety of carrier sense levels and numbers of hops are shown in Fig. 4-35. Since the performance

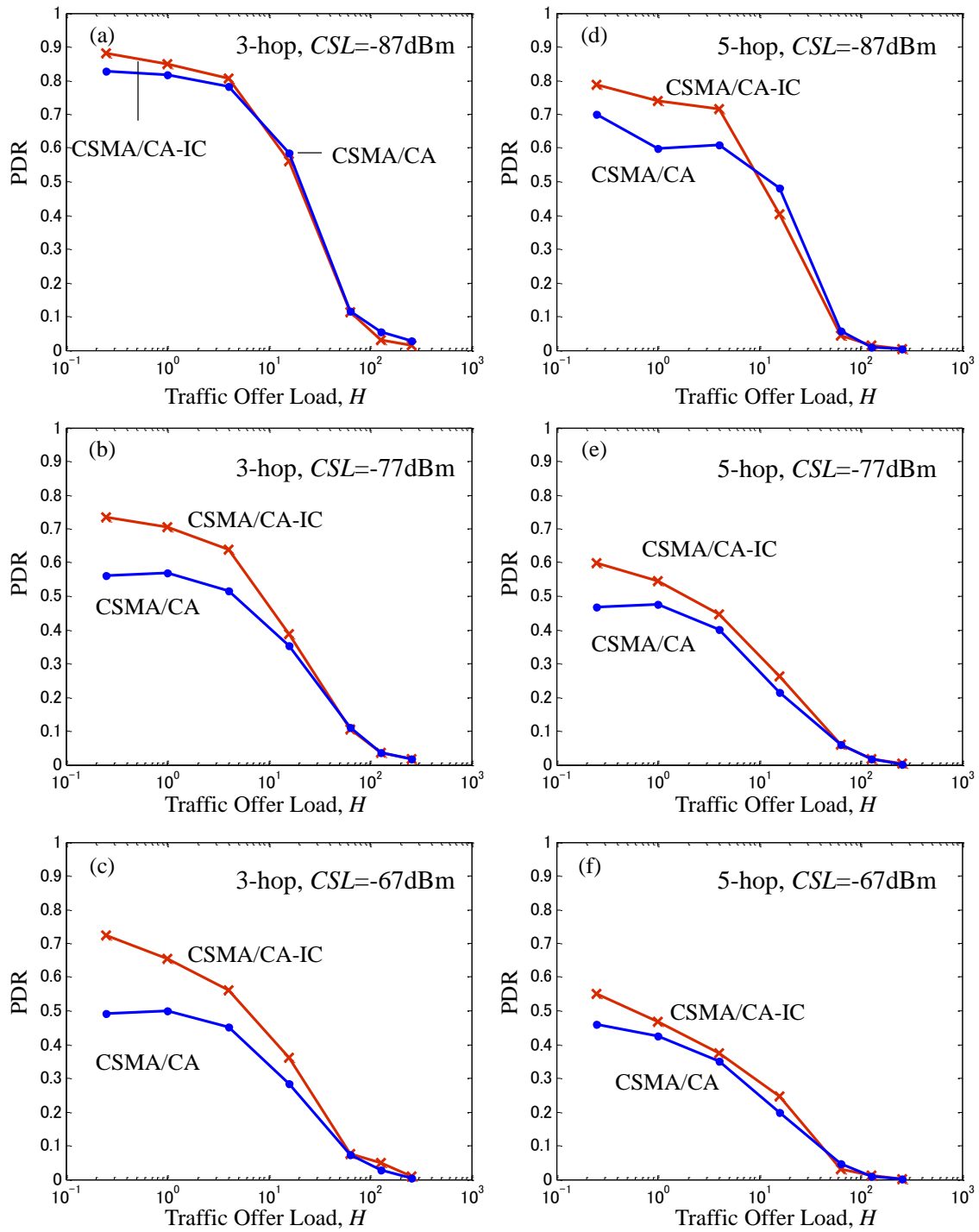


Fig. 4-35. PDRs vs. traffic load with different CSLs and numbers of hops.

improvements made by introducing intra-flow IC represents the effect of intra-flow interference, the results can be concluded as:

1. With the increase of traffic load, it is more likely that multiple packets over

different flows will be being transmitting at the same time, so that the power of inter-flow interferences becomes dominant at the receiver and hence yields the degradation of the effect of intra-flow IC.

2. PDR decreases if carrier sensitivity is lowered because inter-flow interference and intra-flow interference are more likely to take place;

3. PDR can be significantly improved by canceling intra-flow interference especially with lower CSL and H (from 0.25 to 16). For instance, when CSL is -67dBm, PDR of 3-hop ad hoc network is increased by 47% (23 percentage point) with intra-flow IC at traffic load of 0.25, which corresponds to 14% improvement of each hop. Intra-flow IC is still effective when the number of hops increases.

In ad hoc sensor networks that require high reliability such as factory automation and process control, the average data generation interval T_G is long (i.e. traffic load H is low) while the data is important that needs to be safely relayed to the end node in time. For this case, introducing intra-flow IC will be an effective approach to improve the link reliability and reduce the number of retransmissions.

Inter-flow interference can be avoided by interference alignment with multiple input multiple output (MIMO) Recently, many studies focus on achieving high degree of freedom gain with space-time code [49][50]. Reference [50] proposed an inter-flow interference alignment technique with MIMO that enables two multi-hop flows work simultaneously. Combining intra-flow IC with inter-flow IC will further improve the performance of multi-hop ad hoc network in high traffic load scenario.

4.9 Conclusion of Chapter 4

In order to improve the multi-hop transmission performance, in this chapter, a new intra-flow interference canceling multi-hop transmission (IFIC-MHT) scheme is proposed for achieving more efficient multi-hop packet transmission. The interference cancellation is based on the NLMS algorithm and can cooperate with MRC reception to reduce the packet error rate and enhance throughput. The results show that the throughput of IFIC-MHT under fading increases linearly with traffic load up to its maximum, and it has significantly higher performance than CSMA/CA multi-hop transmission. An analysis model is also created that can accurately predict the multi-hop transmission performance of IFIC-MHT.

The effect of the proposed IC on large-scale multi-hop ad hoc network is also investigated through simulation by combining IFIC with conventional CSMA/CA to mitigate both intra- and inter-flow interferences. The results indicated that the improvement of packet delivery ratio achieved by IFIC in large-scale multi-hop ad hoc network is remarkable when the traffic density is low because intra-flow interference is dominant.

Chapter 5

Conclusion

The thesis has studied the performance improvement of wireless ad hoc networks suffering from hidden terminal (HT) problem. The effects of HT problem on single-hop and multi-hop network performance have been carefully studied. An interference canceling solution that removes HT-caused IFI has been proposed. It significantly improves the performance of multi-hop ad hoc networks.

In Chapter 2, a new mathematical analysis is created considering fading and capture effect, which has more generality and reveals the mathematical relationship between the HT position and HT effect. It is found that CSMA/CA multi-hop is vulnerable to HT problem due to the mutual-position of transmitting nodes. Therefore, in Chapter 3, a case study method for analyzing IFI effect is proposed. This method can be used to precisely calculate the packet delivery ratio for CSMA/CA multi-hop network. With the method, it is proved that the capability of CSMA/CA multi-hop transmission is limited due to HT problem thus high traffic load cannot be supported. In order to improve the multi-hop transmission performance, in Chapter 4, a new IFI canceling multi-hop transmission (IFIC-MHT) scheme is proposed for achieving more efficient multi-hop packet transmission. It is shown that the scheme provides significantly higher performance than CSMA/CA multi-hop transmission. Then in the later part of Chapter 4, the effect of IFIC-MHT on large-scale multi-hop ad hoc networks is also investigated by simulation. Modification of IFIC-MHT is made to adapt itself to large-scale ad hoc networks. The results indicated that IFIC effectively improves the reliability of multi-hop transmission in the scenario where IFI dominates.

The most important conclusions are listed below:

- In fading environments, the effect of HT on unicast communication cannot be eliminated by optimizing carrier sense level or receiving threshold with the conventional CSMA/CA scheme;
- In multi-hop communication, end-to-end performance of CSMA/CA is severely affected by IFI. Improving carrier sensitivity can suppress the occurrence of HT

but also increases the transmission latency. Therefore the end-to-end throughput decreases when the traffic load is high;

- Canceling IFI allows neighboring nodes to use the same radio resources. Therefore, the proposed IFIC multi-hop transmission scheme is able to improve the end-to-end throughput even in high traffic load;
- Improvement of packet delivery ratio achieved by IFIC in large-scale multi-hop ad hoc network is remarkable when the traffic density is low and IFI is dominant.

The rapid development of M2M and IoT (Internet of Things) communications brings the stage for multi-hop ad hoc networks. Video streaming [55] and real-time monitoring/control [56] over multi-hop ad hoc networks attract considerable attention. For example, they are considered in vehicular ad hoc network (VANET) for safety and non-safety purposes [57]. Another example is in Access Point networks such as mobile network and WLAN. It is widely considered that the next-generation mobile network will support M2M/IoT communications. Assuming battery-driven devices far from base station, multi-hop transmission to base station will be much power efficient rather than single hop transmission. Instead, multi-hop transmission can be used to expand the coverage area for low power devices. Furthermore, multi-hop ad hoc networks (e.g., sensor networks) can also be used in factory for transmitting real-time command and data for factory automation and process control [58]. For all applications above, network suffers from IFIs. Therefore, the proposed IFIC is good solution for such kind of applications.

Optimizing IC algorithm that considers multiple antennas is an important study item in the future. Since MIMO technologies have been widely used and many devices have multiple antennas, realizing intra-flow, inter-flow and self-interference cancellation by IC and MIMO is an important topic.

References

- [1] C. Siva Ram Murthy and B. S. Manoj, "Ad hoc wireless networks architectures and protocols," Prentice Hall, 2004.
- [2] J. Holler, V. Tsiatsis, C. Mulligan, S. Karnouskos, S. Avesand, and D. Boyle, "From machine-to-machine to the internet of things: introduction to a new age of intelligence," Elsevier, 2014.
- [3] Cisco, "10th annual VNI Global IP Traffic and Service Adoption Forecasts for 2014-2019," May 2015.
- [4] E. Setton, T. Yoo, X. Zhu, and A. Goldsmith, and B. Girod, "Cross-layer design of ad hoc networks for real-time video streaming," *Wireless Communications, IEEE*, vol.12, no.4, pp.59-65, Aug. 2005.
- [5] M. Van der Schaar and N. Sai Shankar, "Cross-layer wireless multimedia transmission: challenges, principles, and new paradigms," *Wireless Communications, IEEE* , vol.12, no.4, pp.50-58, Aug. 2005.
- [6] D. Li and J. Pan, "Performance evaluation of video streaming over multi-hop wireless local area networks," *IEEE Transactions on Wireless Communications*, vol.9, no.1, pp.338-347, Jan. 2010.
- [7] L. Thanayankizil and M.A. Ingram, "Reactive routing for multi-hop dynamic ad hoc networks based on opportunistic large arrays," in *Proc. IEEE GLOBECOM 2008*, pp. 1-6, Nov. 4 2008.
- [8] R. Patil and V. Kerji, "SINR based routing for mobile ad-hoc networks," in *Proc. ICECT 2011*, pp. 369-372, Apr. 2011.
- [9] S. Mao, S. Lin, S.S. Panwar, Y. Wang and E. Celebi, "Video transport over ad hoc networks: multistream coding with multipath transport," *IEEE Journal on Selected Areas in Communications*, vol. 21, no. 10, pp.1721-1737, Dec. 2003.
- [10] K. Nagao, Y. Kadowaki and Y. Yamao, "Multi-hop transmission performance of cognitive temporary bypassing for wireless ad hoc networks," in *Proc. IEEE CCNC 2009*, pp.1-5, Jan. 2009.
- [11] P. Di Marco, P. Pangun, C. Fischione and K.H. Johansson, "Analytical modelling of IEEE 802.15.4 for multi-hop networks with heterogeneous traffic and hidden terminals," in *Proc. IEEE GLOBECOM 2010*, pp.1-6, Dec. 2010.
- [12] A. Gkelias, M. Dohler, V. Friderikos and A.H. Aghvami, "Wireless multi-hop CSMA/CA with cross-optimised PHY/MAC," in *Proc. IEEE GLOBECOM 2004*, pp.39-43, Nov. 2004.

- [13] A. Colvin, "CSMA with collision avoidance," *Computer Communications*, vol. 6, pp. 227–235, 1983.
- [14] D. Jiang and L. Delgrossi, "IEEE 802.11p: Towards an International Standard for Wireless Access in Vehicular Environments," in *Proc. IEEE VTS 2008 spring*, pp. 2036-2040, May 2008.
- [15] S. Pollin, M. Ergen, S. Ergen, B. Bougard, L. Der Perre, I. Moerman, A. Bahai, P. Varaiya and F. Catthoor, "Performance Analysis of Slotted Carrier Sense IEEE 802.15.4 Medium Access Layer," *IEEE Transactions on Wireless Communications*, pp. 3359 – 3371, Sept. 2008.
- [16] F. A. Tobagi and L. Kleinrock, "Packet Switching in Radio Channels: Part II the Hidden Terminal Problem in Carrier Sense Multiple-Access and the Busy-Tone Solution," *IEEE Transactions on Communications*, vol. 23, pp. 1417-1433, 1975.
- [17] A. Zahedi, K. Pahlavan, "Natural hidden terminal and the performance of the wireless LANs," in *Proc. IEEE ICUPC 1997*, vol.2, pp.929-933, Oct. 1997.
- [18] G. Anastasi, E. Borgia, M. Conti, and E. Gregori, "IEEE 802.11b Ad Hoc Networks: Performance Measurements," *Cluster Computing*, vol. 8, no. 2-3, pp. 135-145, Jul. 2005.
- [19] T. C. Hou, L. F. Tsao, and H. C. Liu, "Analyzing the throughput of IEEE 802.11 DCF scheme with hidden nodes," in *Proc. IEEE VTC 2003 Fall*, vol. 5, pp. 2870–2874.
- [20] A. Tsertou and D. I. Laurenson, "Revisiting the hidden terminal problem in a CSMA/CA wireless network," *IEEE Transactions on Mobile Computing*, vol. 7, no. 7, pp. 817–831, Jul. 2008.
- [21] M. N. Krishnan, S. Pollin and A. Zakhori, "Local Estimation of Probabilities of Direct and Staggered Collisions in 802.11 WLANs," in *Proc. IEEE GLOBECOM 2009*, pp. 1-8, Nov. 2009.
- [22] C. Huang, C. Lea and K. Albert, "Rate matching: a new approach to hidden terminal problem in ad hoc networks," *Wireless Networks*, vol. 16, issue 8, pp. 2139- 2150, Nov. 2010.
- [23] H. Zhao, E. Garcia-Palacios, J. Wei and A. Song, "Calculating End-to-End Throughput Capacity in Wireless Networks with Consideration of Hidden Nodes and Multi-Rate Terminals," in *Proc. VTC 2011 Spring*, pp. 1-5, May 2011.
- [24] C. Cano, B. Bellalta, A. Cisneros and M. Olive, "Quantitative analysis of the hidden terminal problem in preamble sampling WSNs," *Ad Hoc Networks*, vol. 10, issue 1, pp. 19–36, Jan. 2012.
- [25] Z. Hadzi-Velkov and B. Spasenovski, "The influence of flat Rayleigh fading channel with hidden terminals and capture over the IEEE 802.11 WLANs," in *Proc. VTC 2001 Fall*, pp. 972-976, vol. 2, Oct. 2001.

- [26] Part II; Wireless LAN Medium Access Control (MAC) and Physical Layer Specifications, IEEE Std. 802.11 a/b/g, 1999/1999/2003.
- [27] J. Li, Charles Blake, Douglas S.J. De Couto, Hu Imm Lee and Robert Morris. "Capacity of ad hoc wireless networks," in Proc. ACM MobiCom 2001, pp. 61-69, 2001
- [28] P. C. Ng and S. C. Liew, "Throughput Analysis of IEEE802.11 Multi-Hop Ad Hoc Networks," IEEE/ACM Transactions on Networking, vol.15, no.2, pp.309-322, Apr. 2007.
- [29] S. Razak and Nael B. Abu-Ghazaleh. "Self-interference in Multi-hop Wireless Chains: Geometric Analysis and Performance Study," in Proc. ADHOC-NOW 2008, pp. 58-71, 2008.
- [30] H. Zhao, S. Wang, Y. Xi and J. Wei, "Modeling intra-flow contention problem in IEEE 802.11 wireless multi-hop networks," IEEE Communications Letters, vol.14, no.1, pp.18-20, Jan. 2010.
- [31] J. Yoo and J. Won Kim, "Maximum End-to-End Throughput of Chain-Topology Wireless Multi-Hop Networks," in Proc. IEEE WCNC 2007, pp.4279-4283, Mar. 2007.
- [32] P. Sondi, D. Gantsoy, "Improving real-time video streaming delivery over dense multi-hop wireless ad hoc networks," Wireless Days, 2014 IFIP, pp.1-4, Nov. 2014
- [33] H. Suzuki, "Interference canceling characteristics of diversity reception with least-squares combining — MMSE characteristics and BER performance," IEICE Transactions on Communications, vol. J 74-B, no. 12, pp. 637-645, Dec. 1991.
- [34] D. Halperin, T. Anderson and D. Andwetherall, "Taking the sting out of carrier sense: Interference cancellation for wireless LANs," in Proc. ACM MobiCom 2008, pp. 339-350, Sept. 2008.
- [35] S. Zhang, S. C. Liew and H. Wang, "Blind Known-Interference Cancellation," IEEE Journal on Selected Areas in Communications, vol.31, no.8, pp.1572-1582, Aug. 2013
- [36] S. Katti, S. Gollakota, and D. Katabi, "Embracing wireless interference: Analog network coding," in Proc. ACM SIGCOMM 2007, pp. 397-408, Aug. 2007.
- [37] S. Gollakota and D. Katabi, "ZigZag decoding: Combating hidden terminals in wireless networks," in Proc. ACM SIGCOM 2008, pp. 159-170, Aug. 2008.
- [38] C. Qin, N. Santhapuri, S. Sen, and S. Nelakuditi, "Known interference cancellation: Resolving collisions due to repeated transmissions," in Proc. IEEE WIMESH 2010, pp.1-6, Jun. 2010.
- [39] J. H. Kim, and J. Pearl, "A computational model for combined causal and diagnostic reasoning in inference systems," in Proc. IJCAI-83, pp. 190-193, 1983.
- [40] ITU-R Recommendation P. 1411-6, "Propagation data and prediction methods for the planning of short-range outdoor radiocommunication systems and radio local area networks in the frequency range 300 MHz to 100 GHz," 2012.

- [41] V. Bharghavan, A. Demers, S. Shenker, and L. Zhang. MACAW, “A Media Access Protocol for Wireless LANs,” in Proc. ACM SIGCOMM 1994, pp. 212-225, Sept. 1994.
- [42] Andrea Goldsmith, “Wireless Communications,” pp.359-367, Cambridge University Press, 2005.
- [43] B. Widrow and M. E. Hoff, “Adaptive switching circuits,” in Proc. WESCON Conv. Rec., vol. 4, pp. 96-140, 1960.
- [44] S. Haykin, “Adaptive Filter Theory”, Prentice-Hall, 1986.
- [45] O. Wiener, “Extrapolation, Interpolation and Smoothing of Stationary Time Series,” The Technology Press of the Massachusetts Institute of Technology, and Wiley, 1949.
- [46] J. I. Nagumo and A. Noda, “A Learning Method for System Identification,” IEEE Transactions on Automatic Control, vol. AC-12, pp. 282-287, Jun. 1967.
- [47] P. R. Bit mead and B. D. O. Anderson, “Performance of Adaptive Estimation Algorithms in Dependent Random Environments,” IEEE Transactions on Automatic Control, vol. AC-25, pp. 788-794, Jun. 1980.
- [48] Jakes, W. C., Ed. “Microwave Mobile Communications,” pp. 39, Wiley, 1974.
- [49] L. Li and H. Jafarkhani, “Maximum-rate transmission with improved diversity gain for interference networks,” IEEE Transactions on Information Theory, vol.59, no.9, pp.5313 - 5330, Sept. 2013.
- [50] A. Zaki, C. Wang and L. K. Rasmussen, “Combining interference alignment and Alamouti codes for the 3-user MIMO interference channel,” in Proc. IEEE WCNC 2013, pp.3563 – 3567, Apr. 2013.
- [51] Y. Xu, C. Jiang, Y. Shi, Y.T. Hou, W. Lou and S. Kompella, “Beyond interference avoidance: On transparent coexistence for multi-hop secondary CR networks,” in Proc. IEEE SECON 2013, pp.398-405, Jun. 2013.
- [52] G. Shyamnath, S. David Perli and D. Katabi, “Interference alignment and cancellation,” in Proc. ACM SIGCOMM 2009, vol. 39, no. 4, pp. 159-170, Aug. 2009.
- [53] B. O'Hara and A. Petrick, “IEEE 802.11 Handbook, A Designers Companion 2nd Edition,” Chapter 14.
- [54] Martin Haenggi, “Stochastic Geometry for Wireless Networks,” pp.41, pp.59. Cambridge Press, Nov. 2012
- [55] T. Ramachandran, P. Rajamohan, and R. Leelavathi, “Video Streaming Application: Image Quality Analysis of Wireless Ad-hoc Network Routing Protocols,” International Journal of Scientific Engineering and Technology, vol. 3, no.12, pp. 1468-1471, Dec. 2014.
- [56] J. Chang, K. Sun, C. Chen, and A.A.-K. Jeng, “Distortion-based video streaming over Vehicular Ad Hoc Networks in highway,” in Proc. ITSC 2014, pp.2324-2329, Oct. 2014.

- [57] X. Jiang, X. Cao, and D.H.C. Du, "Multihop transmission and retransmission measurement of real-time video streaming over DSRC devices," in Proc. IEEE WoWMoM 2014, pp. 1-9, Jun. 2014.
- [58] L .Q. Zhuang, K. M. Goh, J.B. Zhang, "The wireless sensor networks for factory automation: Issues and challenges," in Proc. IEEE ETFA 2007, pp.141 - 148, Sept. 2007

Publications

Journal Papers:

1. Jingze Dai and Yasushi Yamao, "CSMA/CA Unicast Communication Performance under Fading Environment with Two-Dimensional Distribution of Hidden Terminal," *IEICE Transactions on Communications*, Vol.E95-B, No.09, pp. 2708-2717, Sept. 2012.
2. Jingze Dai, Koji Ishibashi and Yasushi Yamao, "Highly Efficient Multi-Hop Packet Transmission Using Intra-Flow Interference Cancellation and Maximal-Ratio Combining," *IEEE Transactions on Wireless Communications* (2015, Accepted, DOI: 10.1109/TWC.2015.2446978), Jun. 2015.

International Conference Papers:

1. Jingze Dai and Yasushi Yamao, "Highly Efficient Multi-Hop Transmission Using Intra-Flow Interference Cancellation and MRC," *Proc. IEEE International Conference on Communications (ICC 2014)*, pp. 5520 – 5525, Sydney, Australia, Jun. 2014.
2. Jingze Dai and Yasushi Yamao, "Performance of CSMA/CA Multi-Hop Network Considering Intra-Flow Interference under Fading Environment," *Proc. IEEE 77th Vehicular Technology Conference (VTC2013-Spring)*, pp. 1-5, Dresden, Germany, June. 2013.
3. Jingze Dai and Yasushi Yamao, "CSMA/CA Performance under Fading Environment with Two-Dimensional Distribution of Hidden Terminal," *Proc. IEEE 74th Vehicular Technology Conference (VTC2011-Fall)*, pp. 1-5, San Francisco, USA, Sept. 2011.
4. Jingze Dai and Yasushi Yamao, "Analysis of hidden terminal effect on a CSMA/CA network under fading environment," *Proc. IEEE 2009 International Conference on Wireless Communications and Signal Processing (WCSP 2009)*, pp. 1-5, Nanjing, China, Nov. 2009.
5. Kazuya Minato, Jingze Dai and Yasushi Yamao, "Theoretical Analysis of Broadcast Packet Delivery Rate in ITS V2V Communication with CSMA/CA," *Proc. 4th IEEE International Symposium on Wireless Vehicular Communications (WIVEC 2011)*, pp.1-5, San Francisco, USA, Sept. 2011

Domestic Workshop Papers:

1. 戴競擇, 山尾泰, “ホップ間干渉キャンセルおよび最大比合成を用いた高効率マルチホップ伝送,” 信学技報vol. 113, no. 456, RCS2013-347, pp. 247-252, 2014年3月, 東京.
2. 戴競擇, 山尾泰, “フェージング環境におけるホップ間干渉を考慮したCSMA/CAマルチホップネットワークの性能評価,” 信学技報vol. 112, no. 89, RCS2012-71, pp. 165-170, 2012年6月, 函館.
3. 戴競擇, 山尾泰, “隠れ端末が2次元配置するフェージング環境におけるCSMA/CAパケット伝送成功率の解析,” 信学技報Vol. 111 No. 94, RCS2011-36, pp. 7-12, 2011年6月, 沖縄.
4. 戴競擇, 山尾泰, “レイリーフェージング環境下のCSMA/CA分散ネットワークにおける隠れ端末の影響の解析,” 信学技報 Vol. 110 No. 340, RCS2010-170, pp. 67-72, 2010年12月, 岡山.
5. 湊和也, 戴競擇, 山尾泰, “CSMA/CAを用いた車車間通信環境におけるブロードキャストパケット伝送成功率の理論解析,” 信学技報 Vol. 110 No. 340, RCS2010-171, pp.73-78, 2010年12月, 岡山.